THE REPRESENTATION OF SPACE IN THE RAT HIPPOCAMPUS AS REVEALED USING NEW COMPUTER-BASED METHODS

Michael L. Recce

A thesis submitted for the degree of Doctor of Philosophy

Department of Anatomy and Developmental Biology,
University College London

March 1994

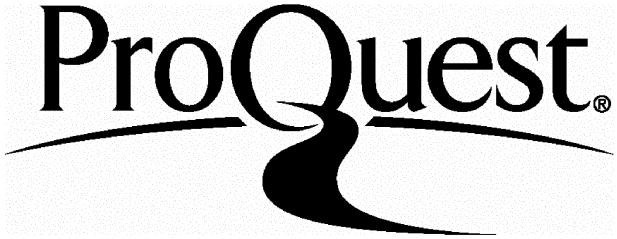

We shall not cease from exploration.
And the end of our exploring
will be to arrive where we started
And know the place for the first time.

T.S. Eliot

ABSTRACT

While there is agreement that the hippocampus plays an important role in brain function, the details are hotly debated. Extracellular recordings from freely moving rats have provided significant but not conclusive evidence that the rodent hippocampus is specific to map based spatial navigation. The spatial hypothesis is supported by a well developed theory, and can be readily tested. These experiments require methods for accurately and simultaneously measuring the activity patterns of multiple single hippocampal neurons with high resolution in both space (location of the animal) and time of spike firing.

Computer based methods are described which improve the accuracy of chronic hippocampal recording. Experiments using these methods reveal differences, from previous studies, in the characteristics of hippocampal single neurons and the relationship between extracellular electrical activity and the animal's spatial location. In particular, the receptive field of each putative hippocampal pyramidal cell (place cell) is smaller and more localised. Smaller firing regions improve the performance of an associative memory for places, perhaps located in the hippocampus (region CA3).

During displacement behaviours in the rat, hippocampal EEG has a striking sinusoidal activity pattern, the *theta rhythm.* In contrast to published data the frequency of the theta rhythm is shown to be correlated with the speed of locomotion of the rat. In addition the frequency of the theta rhythm is shown to predict the speed of the animal's movement. The correlation between speed and EEG frequency may explain how place cell firing maintains spatial specificity with changes in movement parameters.

Experiments were conducted to study the detailed firing relationship between the theta rhythm and the activity of single hippocampal neurons in the freely moving rat. The preferential firing phase of single place cells was found to shift systematically as the animal ran through the place field. This firing phase is shown to be spatially coded to the location in the place field. These results change the way in which place cell firing is interpreted.

CONTENTS

Acknowledgements

This research would not have been possible without valuable interaction with my research colleagues. In particular I would like to thank Andrew Speakman and Neil Burgess for many helpful discussions. I also received excellent technical support from Clive Parker, editorial and secretarial support from Maureen Cartwright, and administrative support from Barbara Pittam, for which I am very grateful. I would also like to thank many friends and colleagues who read drafts of this work and provided useful comments. My greatest debt, however, is to John O'Keefe, who provided tremendous inspiration and guidance throughout this research.

Chapter 1: Background

When first the shaft into his vision shone
Of light anatomized! Euclid alone
Has looked on Beauty bare. Fortunate they
Who, though once only and then but far away,
Have heard her massive sandal set on stone.

Edna St. Vincent Millay

1.1 The role of the hippocampus

The hippocampus is one of the most studied areas of the brain. Interest stems from: (1) its position deep in the brain, many synapses removed from transducers or motor-effectors, (2) its putative role in human memory, (3) the discovery of long term potentiation (LTP) , the most widely studied model of synaptic plasticity), and (4) the discovery that cells are spatially coded.

Structurally the hippocampus is the simplest form of cortex. It contains one major cell type, confined to a single layer (compared with the large number of cell types and six principal layers of the neocortex). This simplicity is in stark contrast with its role in processing information from sensory systems. Swanson (1983) grouped brain regions according to the level of sensory processing they perform. He proposed a sequence of hierarchically organised sensory areas in which later stages abstract and integrate information from earlier stages. Early stages (e.g. V1) are specialised for processing a single modality, whereas later stages handle polymodal and supramodal associations. The hippocampus is one of the most complex supramodal association areas, receiving inputs from other supramodal association areas and accumulating input from all sensory systems. The anatomy of the rat hippocampus and related brain structures is reviewed in Chapter 2.

Each of the brain areas upstream from the hippocampus can, and probably does, change the representation of the sensory information collected from the animal's environment. In a sensory area, the representation of information is strongly linked to the characteristics of the signals that are being transduced. For example, the auditory system must be arranged to manage the physical properties of sound just as a computer keyboard is arranged to fit the characteristics of our hands. If the electronic signals in a keyboard are examined, they reflect the key layout as much as any information managing process. The hippocampus is sufficiently far from the sensory transduction process that the representation of information can be assumed to be in a format independent of the peculiarities of any input modality. For this reason, among others, the representation of information in the hippocampus may reveal more clearly the nature of neuronal function.

As the sensory signals are transformed by the sequence of processing stages on the way to the hippocampus, the representation might be expected to reflect less

and less the characteristics of the animal's environment. With this view it is quite surprising that activity patterns of hippocampal neurons were found to correlate with observable behaviour (O'Keefe and Dostrovsky 1971). The firing properties of these putative pyramidal cells, called *place cells*, provided the first evidence that the hippocampus plays a role in spatial information processing. Place cells have a spatially specific and an environment specific firing pattern. The previously measured properties of these cells are explored in Chapter 3, and new measurements form a central part of this research (Chapter 5).

Place cells, along with three other lines of evidence, led O'Keefe and Nadel (1978) to propose that the hippocampus is a cognitive map. Cognitive maps were first introduced by Tolman (1932,1948) to explain place learning in rats. Use of maps provided an explanation for the rat's ability to find short-cuts, and to learn goal locations in the absence of behavioural drives, suchas hunger (latent learning). An alternative view, suggested by Hull (1932), is that navigation is achieved by following a sequence of stimulus-response-stimulus steps. O'Keefe and Nadel (1978) developed a more concrete and explicit distinction between these two paradigms for navigation, one based on routes and the other based on maps (for a current synopsis see O'Keefe 1991), and proposed that independent neural systems exist in the brain to support these two types of navigation. They called these systems the *taxon* system for route navigation, and the *locale* system for map-based navigation, and they proposed that the locale navigation system resides in the hippocampus.

The second form of evidence given for the cognitive map model was the behavioural correlations of the hippocampal electroencephalogram (EEG). The EEG recorded in the hippocampus is the largest electrical signal in the brain, and one form of the EEG, called the theta (θ) rhythm, is nearly a true sinusoidal oscillation (7-12 Hz). In rats, the θ rhythm was found to occur during voluntary movements (including walking, running and swimming) and rapid eye movement (r.e.m.) sleep, but not while the animal is stationary, performing more automatic movements (including eating and grooming) or in slow wave sleep (Vanderwolf 1969; Whishaw and Vanderwolf 1971). An alternative interpretation of these data, suggested by O'Keefe and Nadel (1978) to fit with the cognitive map theory, is that the θ rhythm

occurs during displacement movements, but not stationary movements. The published correlations between movement and the θ rhythm are reviewed in Chapter 3, and new results are described in Chapter 6.

The hippocampus has also been intensively studied for its role in neurological disorders including epilepsy, schizophrenia and Alzheimer's disease. Bilateral removal of the hippocampus (and nearby structures) in patient H.M., as treatment for epilepsy, produced a profound retrograde and anterograde amnesia (Scoville and Milner 1957). This finding has led to extensive lesion experiments on various species to uncover the specific memory deficit that results from hippocampal damage. It has also led to numerous functional block level models in which the hippocampus has a memory role. One partitioning of memory function, suggested by Olton et al. (1979), subdivides into reference memory (e.g. the rules for performing a task) and working memory (e.g. scratch pad for the current conditions in a task). In most cases these models do not predict the activity patterns of single neurons, and they are difficult to test with methods other than lesions.

Lesion experiments have played an essential role in the development of the current understanding of brain function, but the removal of one brain region can both affect overall behaviour and change the level and form of activity in another brain region. Other methods, which provide a means to observe normal brain function in natural circumstances, will be required to determine the function of the brain at the neuron level. Currently, extracellular recording in freely moving animals is as close as it is possible to get to the ideal method of observing brain function.

A memory system role for the hippocampus was given further impetus by the discovery of long term potentiation (LTP) (Bliss and Lømo 1973). From this finding the hippocampus has become the primary region in the mammalian brain for the study of the synaptic basis of memory and learning. This research has revealed in unprecedented detail the physiology and pharmacology of single hippocampal neurons and their synapses. In particular, the CA1 pyramidal cell is the most studied cell in the brain. LTP is also the best model for studying the basis for synaptic plasticity (Hebb 1949).

In 1971 Marr proposed a theory which describes how the hippocampus could provide a memory function. The strength of this theory is that it provides an explicit role for each type of neuron found in the hippocampus, and it provides a rationale for the numbers and connectivities of these neurons. However Marr's model does not describe how the proposed memory function of the hippocampus fits into the overall processing of information in the brain, which makes it difficult to test.

Extensions to this model have been proposed which either describe ways to make the memory function more explicit (Gardner-Medwin 1976; Willshaw and Buckingham 1990), or suggest how the putative memory role of the hippocampus fits into the overall function of the brain (McNaughton and Nadel 1990; Treves and Rolls 1992). In general this type of memory model proposes that the hippocampus is a short term memory store, which requires only a single presentation of the event to remember, and then plays an important role in constructing the longer term memory trace.

O'Keefe and Nadel re-interpreted the hippocampal lesion literature, and found further evidence for the hippocampal cognitive map. Following the theory, tasks were divided into those involving and those not involving the locale system, and predictions were made about the expected performance in each task following a hippocampal lesion. Spatial tasks including the Morris water maze and the Olton 8-arm maze show clear deficits in performance after hippocampal lesions (Morris et al. 1982; Olton et al. 1978; for review see Jarrard 1993).

Finally, the fourth piece of evidence was the interpretation of the amnesic syndrome as the loss of episodic memory (memory for specific events set in a spatio-temporal context). This hypothesis is supported by the finding that patients with hippocampal damage are impaired on spatial memory tasks (Milner 1965). More recently Pigott and Milner (1993) found that patients, following right anterior temporal lobectomy, were deficient in recognising changes in objects in a complex scene. However, only the subset of patients with hippocampal damage were unable to detect the case in which two objects were interchanged.

There is currently little agreement concerning the overall role played by the hippocampus in the brain (e.g. Sutherland and Rudy 1989; Zola-Morgan et al. 1989; Eichenbaum and Cohen 1988; Rawlins 1985; Gray 1982; see also *Hippocampus*

1991 vol. 1). As described above, there is empirical evidence and theoretical support for both the hypothesis that the hippocampus is a memory store and that it is important for processing spatial maps of environments. It could be argued that without the measurable correlate of neuronal activity, hippocampal function is too difficult to understand until the earlier stages of neuronal processing are better understood.

The cognitive map theory, and the navigation role that it proposes for the hippocampus, is a detailed functional level model that has not yet been tied to the function of single neurons. However, the place cell phenomenon brings the cognitive map model closer to a neuron level model than achieved by other function block level models. Out of the set of possible functions for the hippocampus, the spatial hypothesis is the most directly testable using extracellular recording.

The spatial function hypothesis also makes specific predictions about the neuron level representation of space. The cognitive map was taken to be an explicit Euclidean description of an environment in a coordinate system that was based on the world and not on some part of the animal's body or sensory surfaces. In addition, it was proposed that the map is a complete and homogeneous representation for an environment, rather than a collection of independent fragments or sets of associations between movements and local views. For example, this predicts that the place cell representation of an environment should change holistically rather than in parts.

The predictions of the cognitive map model have not yet been fully tested. From the literature review in Chapter 3, it is clear that there is wide variation in the published qualitative and quantitative properties of place cells. In part, this is due to limitations in the technology for extracellular recording. Higher resolution measurements of the representation of space in the activity of groups of hippocampal neurons should lead either to an extension of the hippocampal cognitive map theory to the neuronal level or to a revision of the hypothesised spatial role.

In addition, measurement of the detailed properties of *individual* hippocampal neurons is not sufficient. Most of the important characterictics of neuron level function involve the interaction between active cells during normal

function. The spatial coding could be present mostly in the dynamic interaction between active cells. This requires simultaneous recordings from as many single neurons as possible.

1.2 Outline of this research

The goal of the research described in this dissertation is to record accurately and simultaneously the extracellular firing properties of several single hippocampal place cells and the hippocampal EEG, and to correlate these electrical signals with the animal's location in an environment. The emphasis is on increasing the spatial and temporal resolution of these recordings and the number of simultaneously recorded single neurons.

In 1983 McNaughton, O'Keefe and Barnes proposed a method that uses two extracellular electrodes, called a *stereotrode*, to improve the chances for isolating the activity of the individual neurons and to increase the number of simultaneously recorded neurons. In the same paper they suggested that four electrodes could be used to improve the recording further. This suggestion has led to the development of the new apparatus, described in Chapter 4, based on a four electrode bundle, called the *tetrode*. The tetrode has the additional advantage that it may enable identification of the relative anatomical location of active cells. Chapter 4 includes a description of the computer based methods that are the heart of the new method, and presents the important design decisions.

Chapter 5 contains results from experiments that have been designed to measure the basic properties of place cells with the tetrode and the new apparatus. In these experiments, measurements of place cell receptive field size, shape and distribution were made in several different environments including an open field, a walled box, an open circular area, a plus maze and a linear track. Most of the data were collected while the animal searched for randomly scattered food (open field, walled box, and open circular area), but in other experiments the animal ran back and forth for a food reward on a linear track. Also, some of the data were collected while the animal performed a more complex arm selection task in a plus maze.

The new methods can also be applied to study the relationship between the animal's movements (speed and spatial location) and the characteristics of the

hippocampal EEG. The correlation between the θ rhythm and displacement movements was a key argument given in support of the cognitive map theory, but the published data are far from conclusive. As described above, the primary question is the relationship between the θ rhythm frequency and the animal's speed of movement. In these experiments (Chapter 6) the animal is run on a linear track or a plus maze.

Finally, the spatial and temporal relationship between the hippocampal θ rhythm and the activity of hippocampal place cells is examined. Prior published experimental results examined only the average phase relationship between the θ rhythm and the activity of single hippocampal neurons. The new methods make it possible to analyse the phase relationship independently for each cycle of the θ rhythm and for many cells in the same electrode placement. In these experiments (Chapter 7) the animal ran back and forth on a linear track for a food reward at both ends of the track.

In Chapter 8 the implications of the observed representation of space in the activity of single cells and EEG is presented. The size, shape and distribution of place cell receptive fields is important in the quest to understand the nature of a hippocampal map. The cognitive map theory makes the prediction that the spatial representation is uniformly distributed, explicitly Euclidean, and changes in a holistic manner. Also, the size of place fields and the number of multiple firing fields may determine the capacity of the hippocampus as a spatial memory system. The results from the analysis of the properties of the θ rhythm may resolve its suggested role in clocking the activity of place cells and maintaining spatially stable firing in the presence of changes in the way that the animal moves around in an environment. Also the timing properties of cell firing may constrain the times (and locations) at which synaptic change can occur.

Chapter 2: Hippocampal Anatomy

2.1 Gross anatomy of the hippocampus

In the rat, the three-dimensional structure of the hippocampus resembles two wings that bend from the midline to follow the contour of the brain surface. The shape of the rat hippocampus is shown with computer reconstruction in Figure 2.1. It is dorsal and lateral to the thalamus, and in its most dorsal and medial extent the hippocampus is just posterior to the septum at the midline of the brain. It extends caudally and laterally at about 45° to the midline, and curves vertically, stopping just posterior to the amygdala in the temporal lobe.

The anatomical location and relative size of the hippocampus has varied dramatically with phylogenetic development. It has migrated vertically down into the temporal region, and has shrunk in comparison with the neocortex.

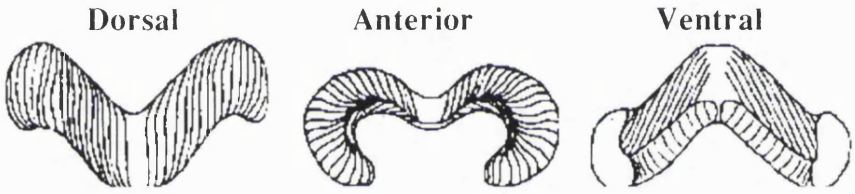

Figure 2.1 Three computer reconstructed views of the rat hippocampus. The lines show the path take by fibres in the alveus (modified from Tamamaki and Nojyo 1991).

Ramón y Cajal (1911) observed, based on connectivity patterns, that the hippocampus is highly associated with the adjoining cortical regions. These cortical areas, called the *parahippocampal region*, contain the transition from the six layers of neurons in neocortex to the single cell layer in the hippocampus. The *hippocampal formation* includes the hippocampus and the parahippocampal region. Most of the connections between the hippocampus and the rest of the neocortex are made through the parahippocampal region, which includes the *entorhinal cortex* and the *subicular complex*. As suggested above, the functional characteristics of the hippocampus can probably not be fully separated from those of the parahippocampal region. Therefore, the anatomy of the entire hippocampal formation is examined in this dissertation.

The coordinate system used to describe the detailed structure of the hippocampus includes a *longitudinal axis* that begins at the septal pole and follows

the curve of the hippocampus to the temporal pole. Along this axis, each perpendicular slice defines a *transverse plane,* which is shown unrolled into an axis in Figure 2.2B.

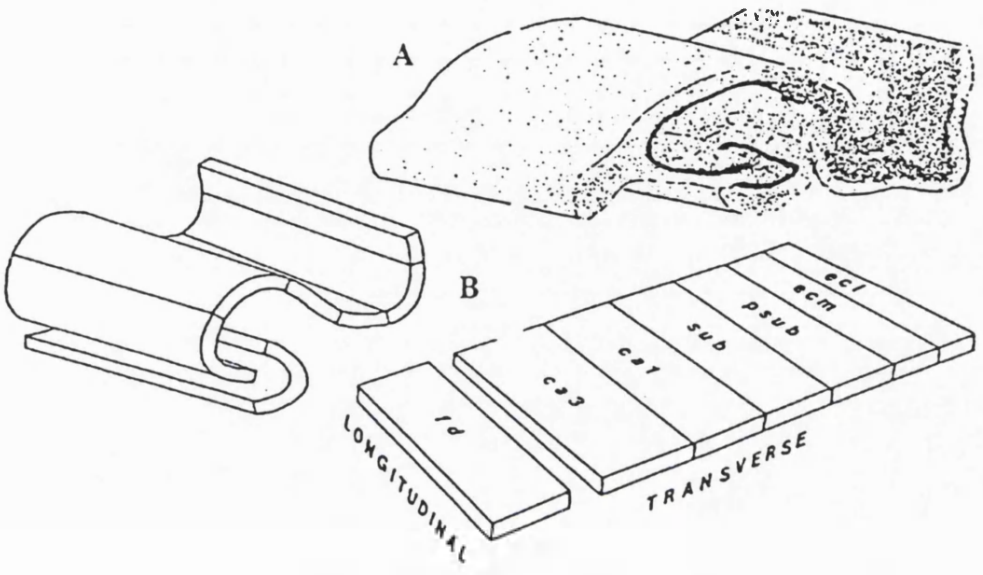

Figure 2.2 The hippocampal formation and the primary subregions are shown unrolled. Part A is a Nissl stained longitudinal segment of the hippocampus. Part B shows relative anatomical location of the subregions [fd (fascia dentata), sub (subiculum), psub (parasubiculum), ecm (medial entorhinal cortex), ecl (lateral entorhinal cortex)] (reprinted from McNaughton 1989).

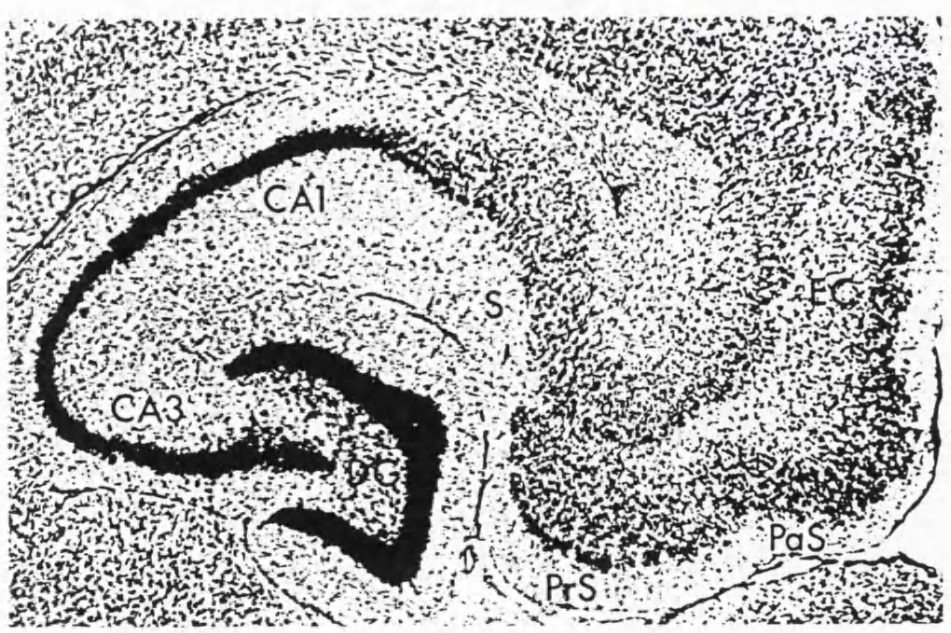

Figure 2.3 Photomicrograph of a Thionin-stained horizontal section through the rat hippocampal formation. The subregions are labelled and the interaction between the regions are described in the text (Subiculum(S), presubiculum(PrS), parasubiculum (PaS), entorhinal cortex (EC), and dentate gyrus (DG). (reprinted from Amaral and Witter 1989)

In the transverse plane, the hippocampus is defined by the two interlocking C-shaped layers of cells and the surrounding white matter. The shorter, thicker C shape with a smaller radius of curvature is the *dentate gyrus* (also called the *fascia dentata*), and the larger C shape is the *hippocampus proper* (also called the *cornu ammonis*). These layers, are visible as bands in the transverse section, that is shown in Figure 2.2 and 2.3. These layers are extend to form sheets of cells in Figure 2.2B.

2.2 Hippocampus proper

Based on morphological criteria, from the Golgi studies of Ramón y Cajal (1911) and Lorente de Nó (1934), and the degeneration studies by Blackstad (1956), the hippocampus proper is most often divided into three subregions, CA1-CA3. In the transverse plane, the subregions, or fields, are in numerical sequence with the CA1 field bordering on the subicular complex, where the cell layer broadens. The CA3 field is partly contained within the bend of the dentate gyrus, and the border between field CA3 and field CA2 (Lorente de Nó 1934) is defined by the projection to the CA3 field from the dentate gyrus, called the *mossy fibres*. Blackstad (1956) found no difference between the comparatively small CA2 field and the CA3 field, but more recent data (Ishizuka et al. 1990) provide evidence that it should be considered as a separate region. The cell bodies in field CA2 are most similar to those of field CA1, but the pattern of connections is more like those in field CA3. For the most part, CA2 will be treated as part of CA3 in the remainder of this dissertation.

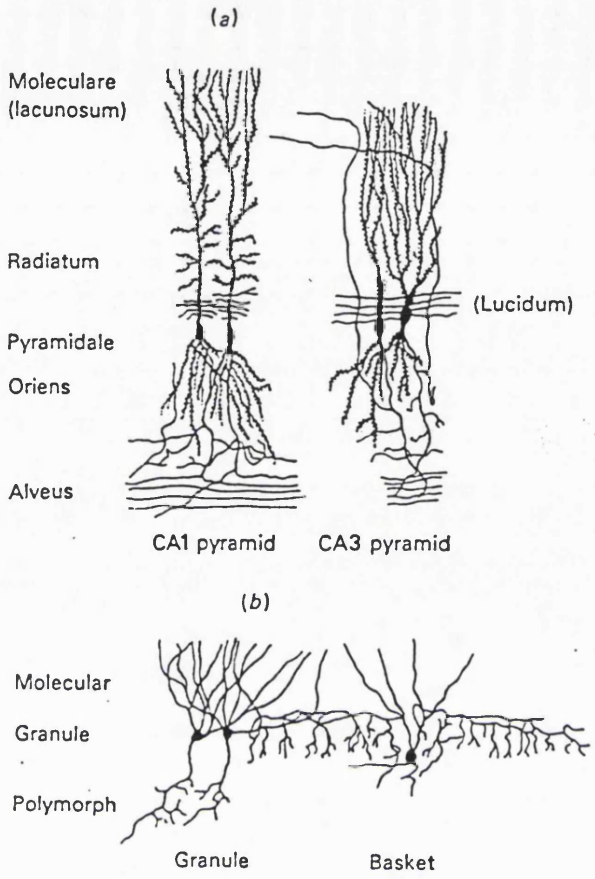

Figure 2.4 (a) Examples of CA1 and CA3 pyramidal cells. (b) Examples of dentate granule cells and a basket cell. (Reprinted from O'Keefe and Nadel 1978 p.110)

All of the subregions of the hippocampus proper contain roughly the same cell types and anatomical layers. Over 99% of the neurons are pyramidal cells, and the cell bodies are in a single cell layer. Pyramidal cells have both apical and basal dendrites, which are oriented nearly parallel to each other. In addition to the cell body layer, the *stratum pyramidale*, four to five additional layers are distinguished (see Figure 2.4), which contain the axons and dendrites of the pyramidal cells and a small number of interneurons. The basal dendrites divide into many branches just below the cell soma in the *stratum oriens*, but the apical dendrites extend for several hundred microns through the *stratum radiatum* before dividing into many sub-branches in the *stratum moleculare*. In the CA3 field there is an additional layer, called the *stratum*

lucidum, between the stratum pyramidale and the stratum radiatum, which is the termination region for the mossy fibres. Axons arising from hippocampal pyramidal cells divide into branches in the *alveus* and usually travel perpendicular to the orientation of the dendrites (Ishizuka et al. 1990). These cells make excitatory (Gray's type I) connections, and glutamate is the putative neurotransmitter.

In addition to the pyramidal cells, several interneurons have been identified in the hippocampus proper (Ramón y Cajal 1911; Lorente de Nó 1934). The most abundant interneurons are called *basket cells*, and have cell bodies either in the stratum pyramidale or just below in the stratum oriens. Like pyramidal cells, basket cells have both apical and basal dendrites, and are oriented in the same direction as pyramidal cells. However, unlike pyramidal cells, basket cell dendrites have no spines and their axons form a dense plexus extending for several hundred microns in the stratum pyramidale. There is approximately one basket cell for every 200 pyramidal cells in the hippocampus proper, and GABA is the putative neurotransmitter.

Other interneurons are present in the stratum oriens, stratum radiatum and stratum moleculare, but their role is less well understood. It has been suggested that one group of interneurons in the stratum oriens may provide a second inhibitory control system (Lacaille et al. 1987).

Numbers of neurons and synapses

There is considerable variation in the number and distribution of neurons among strains of rats, and unfortunately the available data cross both strains and species. In each of the two hippocampi of a Sprague-Dawley rat there are 420,000 pyramidal neurons in the CA1 field, 26,000 in the CA2 field and 304,000 in the CA3 field (Amaral et al. 1990). The size of the cell bodies decreases from CA3 to CA1, and the density of cells roughly doubles (Boss et al. 1985). Even within a region of the hippocampus the pyramidal cells are not uniformly distributed. The density of CA3 pyramidal cells increases three to four times from the septal to the temporal pole (Gaarskjaer 1978).

The number of synapses innervating a neuron is usually estimated from measurements of the dendritic length and the density of spines or synapses along

dendritic branches. Accurate quantitative measurements have only recently become possible with the development of new methods in intracellular labelling and computer reconstruction. These methods have been used (Ishizuka et al. 1990, Tamamaki and Nojyo 1991, Amaral et al. 1990) to re-examine the shape and extent of neuronal processes within the hippocampus. The dendritic length in the CA1 field is largely uniform throughout the region, with approximately one third of the dendritic length in the basal dendrites, and two thirds in the apical dendrites (mostly concentrated in the stratum radiatum). It is estimated that these cells receive 11,000 synapses from CA3 pyramidal cells and 2500 from the entorhinal cortex. In contrast, the length and distribution of the dendrites of CA3 neurons varies with their position in the transverse plane. The largest dendritic arbors are located close to the CA2 field. CA3 cells are estimated to receive 12,000 synapses from other CA3 pyramidal cells and as many as 3500 inputs from the entorhinal cortex. The axons of pyramidal cells in the hippocampus proper branch into several intrinsic and extrinsic projections, which are described in more detail below.

The distribution of interneurons within the hippocampus proper is not known in detail, but it is often assumed to be uniform. However the structure of the axons and dendrites of basket cells suggests that they correlate activity across large regions of the hippocampus. Basket cell axons make strong inhibitory connections with the soma of approximately 3000 pyramidal cells (estimated from Schwartzkroin and Kunkel 1985 and Boss et al. 1985). One method for analysing the anatomical evidence for the influence of inhibitory interneurons is to examine the relative spread of their axons and dendrites in the two-dimensional surface defined by the cell body layer. Along this surface the basket cell dendrites have much less spread than their axons. This implies that the group of pyramidal cells influenced by basket cells is more widespread than, and somewhat different from, the set that provides their inputs. Of course, this influence also depends on the distribution of pyramidal cell axons and dendrites.

Intrinsic projections within the hippocampus proper

Within the hippocampus proper there are several important intrinsic projections, including forms of feed-forward and feedback excitatory connections, and

feed-forward and feedback inhibitory connections. Some of these projections are included in the description of the cells above. They are summarised in Figure 2.5 which contains a block diagram of principal projections between regions of the hippocampal formation.

The axons of the CA3 and CA2 pyramidal cells provide a feed-forward excitatory pathway to CA1 which innervates both ipsilateral and contralateral regions. The ipsilateral projection is called the *Schaffer collaterals*, and the contralateral fibres form the *commissural projection.* Each CA1 pyramidal cell receives approximately 5500 synapses from the collaterals originating in each hemisphere, which course through the stratum radiatum. Assuming one contact per neuron, each CA3 pyramidal cell randomly contacts 1.8% of the CA1 pyramidal neurons (Amaral et al. 1990). However, the axonal plexus of pyramidal cells does not extend over the entire region and therefore the synaptic contact is not randomly distributed. From data on the size of the axonal plexus (Tamamaki and Nojyo 1991) the probability of contact is six to eight times higher, or about 15%, within the projection zone.

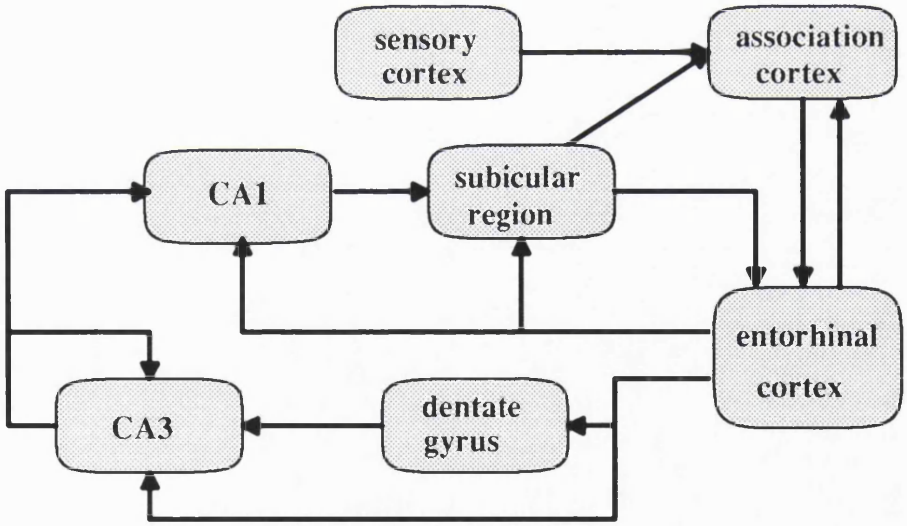

Figure 2.5 Block diagram of the principal projections between regions of the hippocampal formation.

In addition to the Schaffer collaterals, axons from CA3 pyramidal cells branch to produce direct excitatory feedback to ipsilateral and contralateral CA3 pyramidal cells, called the *association projection.* As with the feed-forward projections, the association fibres are presumed to produce equal numbers of synapses in both CA3 fields. In comparison with other brain regions, the density of excitatory feedback in CA3 is high; each pyramidal cell innervates the dendrites of approximately 6000 others in each hemisphere, which terminate in the stratum radiatum, on dendritic spines. As with the Schaffer collaterals, the probability of contact is higher than expected by random contact, since the axonal plexus of each neuron reaches only part of the hippocampus. Random contact would result in each pyramidal cell projecting to 1.9% of the others. However constraints on the area covered by the branching of pyramidal cell axons (Tamamaki and Nojyo 1991) may increase the probability of contact to over 6%.

The organisation of the Schaffer collateral and association fibre projections has been the focus of considerable recent study. However these studies have not produced completely consistent results. Using extracellular labelling and the extended hippocampus, Ishizuka et al. (1990) and Chan et al. (1992) agreed on the organisation in the termination zones of Schaffer collaterals, in which a band of CA3 cells projects to a band of CA1 cells. In three dimensions the two bands correspond to a single slice of the hippocampus. This slice is not perpendicular to the longitudinal axis, but is tilted towards the temporal pole as if it were hinged at the fimbria. Unfortunately this view is not consistent with complete cells reconstructed from intracellular injection of HRP (Tamamaki and Nojyo 1991).

The same studies also examined the structure of the association projection. Using intracellular injection of HRP in 400 μm slices, Ishizuka et al. (1990) proposed that the feedback projections within the CA3 field are largely contained within the same slanted slice described above. In contrast, both Tamamaki and Nojyo (1991) and Chan et al. (1992) suggest that the association projections are oriented parallel to the longitudinal axis, and extend for approximately two thirds of the length of the hippocampus. These two possible patterns for the association projection have very different implications for the function of the region. If the association projection and

the Schaffer collaterals are largely within the same slice, then there is considerably more modularity in the function of the hippocampus.

This level of structural detail is very important in guiding the construction of neuron level models for hippocampal function, but is very difficult to obtain. In the first place, the axes used to described the gross anatomy are not sufficient for analysing the low level structure of the projections. To improve the definition of axes, some researchers are using the mossy fibres as an axis (Andersen et al. 1971), while others propose using the alvear fibres (Tamamaki and Nojyo 1991) or the CA3-CA2 border (Ishizuka et al. 1990). Secondly, unlike projections in the neocortex, the collaterals of hippocampal pyramidal cells are not restricted to the vicinity of the cell body. The functional implications of this fact are discussed in the next chapter, but from the anatomical point of view the fact makes measurements of the axonal branching patterns more difficult. Currently there are either detailed data for a small number of cells or less precise data from extracellular dye injection or degeneration studies.

Within a transverse slice there is an ordering in the termination pattern of the association projection and the Schaffer collaterals along the dendrites of hippocampal pyramidal cells (reviewed in Ishizuka et al. 1990). In general it is not clear how much of this structure is associated with variation in function. Some of the structure results from the sites available during the development of the fibre projections, and may not have a functional role.

There is considerable anatomical and physiological evidence that basket cells in the hippocampus perform feed-forward (Andersen et al. 1971) and feedback (Kandel and Spencer 1961; Andersen et al. 1964; Knowles and Schwartzkroin 1981) inhibition. They receive excitatory feedback from pyramidal cells, which produces feedback inhibition to the surrounding pyramidal cells. The feed-forward inhibition is produced by excitatory inputs to the basket cells from the afferents reaching each of the regions of the hippocampus (Frotscher et al. 1984). In the CA3 field, the basket cells receive synapses from the mossy fibres (Frotscher 1985), and in the CA1 field they receive inputs from the Schaffer collaterals. Basket cells also receive afferents from outside the hippocampus, and some project outside the hippocampus. Both of these projections are discussed below.

Recently feedback connections with much lower density have been demonstrated both anatomically (Chan 1992) and physiologically (Christian and Dudek 1988) between CA1 pyramidal cells.

2.3 Dentate gyrus

In transverse section, the dentate gyrus is divided into three principal layers. One of these, the *granule layer*, stands out as a C shape in a Nissl stain, and is densely packed (>75k per mm^3, four times the density of CA3) with the soma of the principal projection cells, the *granule cells*. These small cells (<10 μm soma) have only apical dendrites, which are directed outward from the bend of the granule layer and arborize in the *molecular layer*. Within the concave bend of the granule layer there is a second cell-rich layer called the *polymorph layer* or the *dentate hilus*. The granule layer bends around the proximal part of the CA3 field. It is often divided into the *suprapyramidal blade* between CA1 and CA3, and the *infrapyramidal blade* below the CA3 pyramidal layer. Among strains of rat there is variation in the number of granule cells (Boss et al. 1985), but on average there are approximately one million. This accounts for 97% of the neurons in the dentate gyrus, and over 99% of the granule layer neurons. The axons of the granule cells make excitatory synapses in the dentate hilus and project to the CA3 field. The projection to CA3, called the mossy fibres, is described in detail below.

The remainder of the neurons in the cell body layer are interneurons (approx. 4500), which receive excitatory projections from the granule cells and provide inhibitory feedback. Most of the interneurons are basket cells and their cell bodies lie just below the granule layer. Basket cells have both apical and basal dendrites, and their axons extend over one third of the longitudinal and transverse extent of the granule layer (Struble et al. 1978), forming inhibitory synapses on approximately 1000 granule cells (McNaughton 1989). There are on average 180 granule cells for every basket cell, and each receives about 10 basket cell synapses.

The distribution of interneurons in the granule layer is not uniform. There are 50% more basket cells near the septal pole of the hippocampus, as compared to the temporal poles, and there are consistently twice as many basket cells in the infrapyramidal blade as in the suprapyramidal blade.

The dentate hilus contains a large number (>21) of morphologically distinct types of neuron (Amaral 1978). The most abundant type of neuron, called the *mossy cell*, is a large spiny multipolar cell that makes extensive excitatory synapses along the longitudinal axis of the hippocampus. There are approximately 32,500 neurons in the polymorph layer, out of which 10,000 are immunoreactive for somatostatin and GAD, and 20,000 are presumed to be mossy cells (Amaral et al. 1990). The hilus receives extensive inputs from the brain stem, which are discussed below.

As in the hippocampus proper, there are many important neuronal projections within the dentate gyrus. Unlike the hippocampal pyramidal cells, there is no direct excitatory feedback connection between granule cells (Claiborne et al. 1986), but there is an excitatory feedback pathway in the interaction between mossy cells and granule cells. Each granule cell receives approximately 2000 contacts from mossy cells. There is also a suggestion of an excitatory feed-forward pathway, as the mossy cell dendrites extend into the molecular layer and may receive direct entorhinal input. Inhibitory feedback exists between basket cells and granule cells, and between mossy cells and interneurons in the hilus. There is also evidence for inhibitory feed-forward connections in a direct projection from the entorhinal cortex to the granule cell layer basket cells.

The dentate gyrus is the primary target for projections from the upper layers of the entorhinal cortex. The afferent fibres terminate in the outer two thirds of the molecular layer in a highly ordered manner, and each granule cell receives about 6000 synapses. The inner third receives synapses from the ipsilateral and the contralateral mossy cells. The projection from the entorhinal cortex is discussed in more detail below. The dentate gyrus also receives substantial projections from sub-cortical regions.

Mossy fibres

The primary dentate gyrus efferent is the mossy fibre system, which projects in a highly organised fashion along the entire extent of the CA3 field. These thin (0.1 to 0.7 μm; Laatsch and Cowan 1966; Amaral and Dent 1981) unmyelinated fibres ramify in a dense plexus in the dentate hilus (Golgi 1886), where they make *en passage* synapses on mossy cells and interneurons, before projecting in a narrow

transverse band (<400μm; Gaarskjaer 1981) into the CA3 region. When the mossy fibres reach the CA2-CA3 border they turn sharply towards the temporal pole of the hippocampus, where there is a larger density of CA3 pyramidal cells. Each mossy fibre contacts a very small fraction of the population of CA3 pyramidal cells (4.6 x 10^{-5}), with one synapse for every 135 μm of length (Claiborne et al. 1986), resulting in contact with 14 pyramidal cells along its approximately 2mm projection in the CA3 field.

These synapses are unique in the brain, with a large size (up to 10 μm) that envelops complex spines of CA3 pyramidal cells (Kjaerheim and Blackstad 1961). Each mossy fibre bouton synapses on four or five dendritic spines, but they are all from the same pyramidal cell (Frotscher et al. 1991). The mossy fibres are well known to exert an excitatory influence on CA3 pyramidal cells, and there is evidence that the neurotransmitter used is glutamate (Crawford and Connor 1972; Storm-Mathisen et al. 1983). However there is also evidence from histochemical staining that the terminals contain the inhibitory neurotransmitter GABA (Ottersen and Storm-Mathisen 1985) and that it coexists in the same terminals with glutamate (Sandler and Smith 1991). In addition the terminals contain several neuropeptides and unusual quantities of zinc (Stengaard-Pedersen et al. 1983).

There is considerable structure in the mossy fibre projection. Claiborne et al. (1986) found that portions of the CA3 field nearest the dentate hilus are preferentially reached by fibres in the infrapyramidal blade, while the parts of field CA3 farthest from the dentate hilus are reached by mossy fibres from the granule cells in the tip of the suprapyramidal blade. Again it is not clear how much of this is due to the availability of connection sites and how much has a direct effect on the function of the mossy fibre projection.

The striking organisation in the mossy fibre projection has inspired several interpretations of its role in hippocampal function. Andersen et al. (1971) proposed that the entire hippocampus is organised in a series of transverse slices that are largely functionally independent. This suggestion, called the *lamella hypothesis*, implies that an *in vitro* slice contains all the essential circuitry for studying hippocampal function. While physiological evidence supports the lamella hypothesis the anatomical support is not yet fully resolved (Amaral and Witter 1989). A second

role for this projection, proposed also in 1971 by Marr, is described in detail at the end of this chapter.

2.4 Entorhinal cortex

The entorhinal cortex, which is part of the parahippocampal gyrus, receives and integrates projections from large parts of the cortical mantle (Insausti et al. 1987a) and relays the input into the hippocampus. It is the principal source of neocortical information for the hippocampus, and from the connectivity patterns its role must be functionally linked with the hippocampus. The output from the entorhinal area is distributed to all the major regions of the hippocampus, but the majority of the entorhinal projections to the hippocampus terminate on the dendrites of neurons in the dentate gyrus. This important fibre tract is called the *perforant path* (Ramón y Cajal 1911).

The entorhinal cortex is divided into the *medial entorhinal* (MEA) and the *lateral entorhinal areas* (LEA) (Lorente de Nó 1933), based on morphological differences (Steward and Scoville 1976) and on their projection patterns (Haug 1973). The anatomy and connection patterns of the entorhinal cortex have recently been reviewed (Witter et al. 1989) and are only summarised here. It has six cell layers, of which layers I-III are called *superficial* and IV-VI are called *deep*. The cortex differs from neocortical regions in that the deep and superficial layers are separated by a cell-sparse layer called the *lamina dessicans*, which disappears at the distal extent of the entorhinal cortex. There are numerous morphologically distinct cell types in the entorhinal cortex. Their structure and distribution were recently re-examined by Germroth et al. (1991).

The perforant path, which arises from the superficial layers of the entorhinal cortex, contains approximately 100,000 projection neurons, and provides the major input to the dentate gyrus. Mathews et al. (1976) found that unilateral removal of the entorhinal cortex resulted in loss of at least 86% of the synapses in the outer two thirds of the molecular layer of the dentate gyrus. The MEA projects to the middle third of the molecular layer and the LEA projects to the outer third. The projection from the MEA is highly topographic and is directed at a narrow segment of the transverse extent of the hippocampus (Wyss 1981), whereas the LEA projection is

more widespread over the longitudinal axis. McNaughton et al. (1981) showed that 2-3% of the perforant path synapses generated an activation which was greater by a factor of 10 to 20 than that caused by other synapses. It has been suggested (McNaughton 1989) that these synapses have an important role in constructing memory traces. In 1973, Bliss and Lømo discovered that tetanic stimulation of this pathway caused a long lasting potentiation of the synapses, called *LTP*.

The entorhinal cortex also projects to the CA1 and CA3 fields. The projection to the CA3 field is similar to the projection to the dentate gyrus. There is a clear proximal to distal gradient along the apical dendrites, and they both arise from layer II neurons in the entorhinal cortex (Steward and Scoville 1976). The more distal synapses in the dendritic arborisations are from the most distal region of the LEA.

The projection to the CA1 field is quite different, however, and originates from a separate group of neurons in layer III of the entorhinal cortex. The region of the CA1 field nearest to the subicular border receives an input from the LEA only, and the part of the CA1 field nearest to the CA3 field receives input from the MEA only (Witter et al. 1989). A few neurons in layer V of the entorhinal cortex also send axons to the hippocampus (Kohler 1985a).

The major input to the entorhinal cortex is from the perirhinal area, which in turn makes reciprocal connections with sensory and parasensory areas of the cortex. The only direct sensory input to the entorhinal area is from the olfactory bulb (Heimer 1968; Kosel et al. 1981), which projects to the LEA. The inputs from the perirhinal cortex project to the lateral aspects of the LEA and MEA. The inputs to the more medial aspects of the LEA and MEA are not known, but it is suspected that they get inputs primarily from the aforementioned lateral aspects. The pattern of termination of the inputs to the entorhinal cortex is highly topographic.

There is also a projection to the entorhinal cortex from the CA1 field and the subiculum. In most cases, the same CA1 pyramidal cell projects to the subiculum, the medial septum and the entorhinal cortex (Swanson et al. 1981).

2.5 Subicular complex

The subicular complex is subdivided into the *subiculum*, the *presubiculum* and the *parasubiculum* (Ramón y Cajal 1911; Brodmann 1909; Lorente de Nó 1934). There

is disagreement among researchers about further subdivision of the subicular complex. However, based on differences in connectivity, van Groen and Wyss (1990) suggest that the *postsubiculum* is distinct from other subicular regions. The postsubiculum has attracted significant recent attention due to the discovery of head direction cells (Taube et al. 1990a,b) in that area. The subiculum is closest to the CA1 field and resembles most closely the layered structure of the hippocampus proper. It is a five-layered cortex, and layer II is similar in structure to CA1 (Lorente de Nó 1934). Presubiculum and parasubiculum more closely resemble the structure of the neocortex.

Comparatively little is known about the subicular complex, perhaps because the cortical fields are small in the rodent brain and they have a high degree of diversity and complexity. There are approximately 128,000 pyramidal cells in the subiculum (Amaral et al. 1990), but no numbers of cells are available for the other areas of the subicular complex.

This area has an important role in hippocampal function, as it receives a massive projection from the CA1 and relays the information to the entorhinal cortex. CA1 pyramidal neurons project principally to the ipsilateral subiculum (Finch and Babb 1980,1981; Finch et al. 1983). The projection forms a column that is 250-300 μm wide, 550 μm high, and 2 mm long, and parallel to the border between the CA1 and the subiculum (Tamamaki et al. 1987; Tamamaki and Nojyo 1990). The subicular complex completes a loop in an information pathway that leads from the entorhinal cortex to the dentate gyrus, on to the CA3, then to the CA1 and the subiculum, and back to the entorhinal cortex. However, this is not the only pathway for information to return to the entorhinal cortex (reviewed in Witter et al. 1989). The projections from the subiculum are solely ipsilateral (Kohler 1985b) and reach all layers of the entorhinal cortex. The subiculum also projects to the retrosplenial cortex, and to sub-cortical regions including the thalamus and nucleus accumbens.

2.6 Projections to and from the septum

The functions of the hippocampus and the septal complex are highly interrelated. All subdivisions of the hippocampal formation receive input from the medial septum and nucleus of the diagonal band (Swanson and Cowan 1976; Alonso and Kohler 1984).

The projections are concentrated in the dentate gyrus and the CA3 region, but are comparatively sparse in the CA1 region (Swanson and Cowan 1979). In return, there is a projection back to the septum from all parts of the hippocampal formation (in particular from CA1) (Raisman et al. 1966), but these fibres largely terminate in the lateral septum. A surprising recent finding is that there are very few projections between the lateral and the medial septum (Leranth et al. 1992).

The densest termination of the input from the medial septum is in the dentate gyrus polymorph layer. A substantial projection also exists to the subiculum and to the entorhinal cortex (Milner and Amaral 1984). This projection is mostly to the MEA, and terminates in the lamina desiccans and in layer II.

The projection from the medial septum is topographic. The cells near the midline project to MEA and to septal parts of the remainder of the hippocampal formation, but more lateral parts project to lateral parts of the entorhinal cortex and to temporal parts of the hippocampal formation (Meibach and Siegel 1977; Monmaur and Thomson 1983; Saper 1984). Input from the septum is more dense in more temporal hippocampal regions (Milner et al. 1983). Fibres from the medial septum terminate on both pyramidal cells and basket cells in the hippocampus proper. The projection has been thought to be entirely cholinergic (Lewis and Shute 1967), but more recently it has been shown that at least 30% of the projection cells are GABAergic (Kohler et al. 1984) and form an independent group from the cholinergic cells (Brashear et al. 1986).

The return projection from the hippocampal formation to the lateral septum is also topographic. In the entorhinal cortex, layer IV and part of layer II project to the lateral septum (Alonso and Kohler 1984; Witter and Groenewegen 1986). There is also a significant projection from the CA3 field to all parts of the lateral septum, which includes the ipsilateral and the contralateral regions. In addition there is a projection from the subiculum and non-pyramidal hippocampal cells (Schwerdtfeger and Buhl 1986) to the septum, which includes basket cells in the hippocampus proper and interneurons in the dentate hilus.

2.7 Additional hippocampal efferents/afferents

The primary projections to and from the hippocampus pass through either the parahippocampal region or the septum, and have been discussed above. There are however several projections from brainstem areas, which primarily innervate the dentate hilus. These include a noradrenergic input from the locus coeruleus (Fuxe 1965) and a serotonergic input from the median and dorsal raphe (Kohler and Steinbusch 1982). From the hypothalamus there is a cholinergic projection to the hippocampal formation (Wyss et al. 1979), and a histaminergic input from the supramammillary region (Segal 1979) which terminates in the hilus.

In addition to the hippocampal efferents discussed above there is a projection from the CA1 and the subiculum to the nucleus accumbens (Phillipson and Griffiths 1985) and a projection from the CA3 to the hypothalamus (Swanson and Cowan 1977).

2.8 Summary

This presentation of the anatomy of the hippocampal formation is necessarily incomplete for several reasons. Firstly, it is impossible in a short space to include all the detail that is available. Secondly, some of this detail has a less significant impact on the function of the region. Most importantly, only a small part of the anatomical detail is known.

A neuron-level model of hippocampal function will not require a complete wiring diagram for all the neurons. Some of the processes guiding development of the region must be random and therefore independent of specific contact between particular neurons. However, it is clear that much more quantitative information is needed. There is no dispute that one part of this useful anatomical information is the number, distribution and type of synaptic contacts that are typical for each class of neuron in each region of the hippocampus (Amaral et al. 1990; McNaughton 1989). Secondly, there are systematic patterns of connectivity within regions of the hippocampus which are not sufficient to warrant further parcellation, as proposed (for example) in the lamella hypothesis, but which are sufficient to alter dramatically the function of the region. Finally, there is insufficient information on the distribution of cell types within a region of the hippocampus.

For example, it would be very useful to know the distribution of basket cells, which may help to explain how groups of neurons interact. One possible distribution would predict independent control of cell assemblies; another would predict a mechanism for integrating activity levels over a large region.

The second difficulty with anatomical detail is how to manage so large a body of information. As the quantitative information becomes available, a better way must be found to communicate the detail unambiguously. The important information spans several scales, from the high-level convergence and divergence characteristics to low-level synaptic contact for individual neurons. An efficient communication mechanism for anatomical details should incorporate all the scales, and it should be unambiguous where a new piece of information fits in. Other fields of scientific research, such as molecular biology, have developed this kind of common communication scheme.

One scheme that could be used to manage and communicate the anatomical characteristics of the hippocampus is a connectivity matrix. If all the neurons, grouped by region, are arranged along a line at the top and left side of the matrix, the matrix shows the type and level of connections between neurons and regions. The columns of the matrix are the output projections of each neuron, and the rows are the inputs.

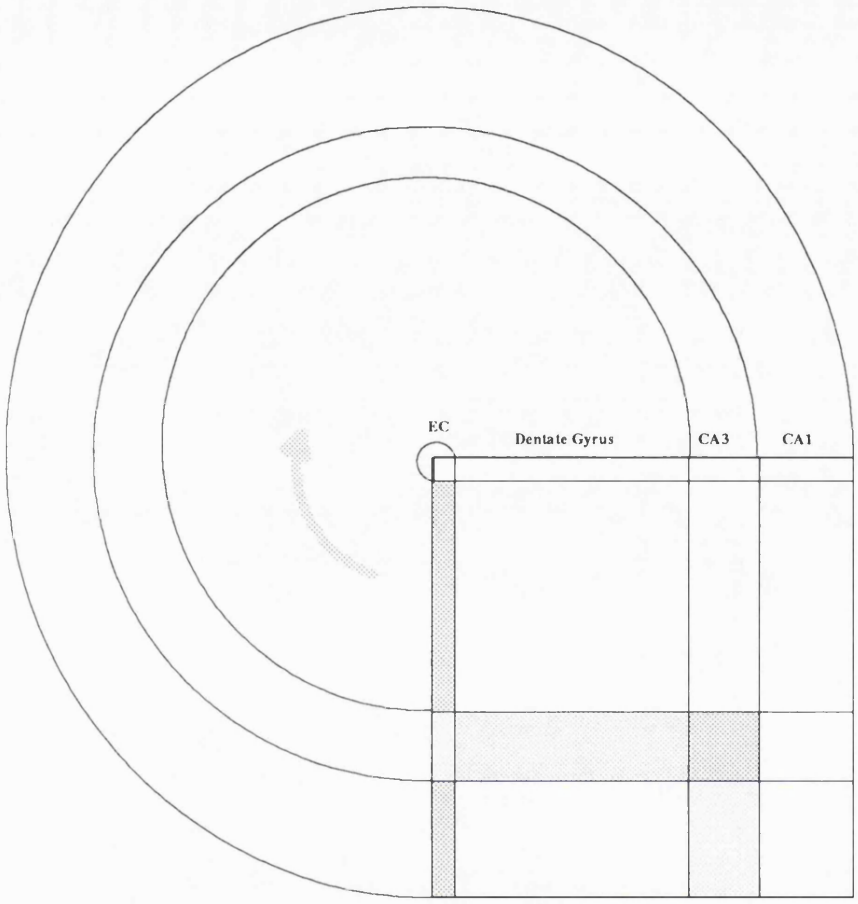

Figure 2.6 Connectivity matrix suggested for describing the functional characteristics of hippocampal anatomy. The neurons are aligned along the rows and columns of the matrix (box) , and they are divided into the regions of the hippocampus proper, dentate gyrus and entorhinal cortex. The size of boxes is in proportion to the number of neurons in the region. Each row can be considered the dendrite of a single neuron, and then the axon follows the curve around to synapse on other neurons. The shading is intended to represent symbolically the structure and density of connectivity between regions. The diagram also represents the time sequence of the information flow.

The connectivity matrix can be treated as a larger number of submatrices, each of which contains the connections from the column region to the row region. As an example an approximate connectivity matrix is presented in Figure 2.6. When examined at the high level, each submatrix appears shaded if there are synaptic connections, but at finer scales the pattern of connections can be seen. The ratio of the height to the width of a submatrix clearly presents the amount of convergence or

divergence. If this ratio is large there is divergence, and if it is small there is convergence. Information flow is indicated by the stippled arrow in the figure. The input arrives at the top of the connection matrix and is projected through the connections to a second region. It then follows the arrow to become an input to the next region. In this way the diagram can incorporate both the connectivity and the time of occurrence for events. The propagation delays in the neuronal circuits correspond to the time to flow from one region to another.

For example, it is very easy with this diagram to show both the divergence between the entorhinal cortex and the dentate gyrus, and the specific nature of the mossy fibre projection to the CA3. Using this kind of diagram it is possible to test the impact of different connection patterns. For example, using the CA3 association projection in one configuration (Tamamaki and Nojyo 1991), the activation of synapses from one mossy fibre can reach all CA3 pyramidal cells by the second cycle around the diagram. At this same point in time, the activation will have reached only a fraction of the CA1 pyramidal cells.

This kind of diagram is very useful for presenting the detailed anatomy of a region. Firstly, it clearly shows the convergence and divergence from one region to another. Secondly, it illustrates the extent to which regions are interconnected (number of shaded submatrices). Finally, it contains a mechanism for representing the temporal properties. All these properties can be examined at many different scales within the same diagram.

The connectivity diagram has two major problems. Firstly, it will be large and difficult to manage for a realistic representation of the anatomy. However it is no more difficult in this regard than the genetic map for a chromosome. Secondly, it is not clear how to map the three-dimensional position of each of the neurons in the hippocampus onto a one-dimensional line along the top edge of the connectivity matrix. One solution to this problem is to enumerate the cells using a fixed sequence like the raster pattern used to convert two-dimensional data on a screen into a single list. A more reasonable approach to this problem is to use a higher dimension connectivity matrix.

Chapter 3: Hippocampal Physiology

3.1 Introduction

The discovery of place cells (O'Keefe and Dostrovsky 1971) and the cognitive map model (O'Keefe and Nadel 1978) have provided a major new inroad into the study of hippocampal function. However, after two decades of active research there is not yet general agreement that hippocampal pyramidal cell activity is primarily correlated with spatial position (e.g. Eichenbaum et al. 1992). This chapter reviews the properties of place cells, which are divided into: (1) a set of "static" properties in unchanging environments, (2) the effect of sensory input and memory on cell activity patterns, and (3) the changes in activity between environments.

A large part of the variation in the published properties of place cells is a direct result of variation in methods and the design of experiments. For this reason, the place cell characteristics must be reviewed in the context of methodological issues.

Most of the research on place cells does not distinguish between cells in the CA1-3 fields, and in this review they are discussed together. Spatially biased firing patterns have also been seen in some of the neurons that project to, or receive inputs from, place cells. These results are summarised in Section 3.8.

In addition, this chapter briefly reviews the characteristics of the hippocampal EEG. In most of the literature the hippocampal EEG is classified into two forms: the theta rhythm, and large irregular activity (LIA). In this review particular attention is paid to the theta rhythm, and the evidence for its part in the hippocampal navigation system.

3.2 Neuronal firing patterns

Based on physiological properties, the activity pattern of hippocampal neurons in the freely moving rat divides into two distinct classes (Ranck 1973; Fox and Ranck 1975). The largest group of these neurons are called *complex spike cells* due to their characteristic bursting pattern. These cells are normally silent but produce a vigorous phasic firing pattern when strongly activated. A complex spike is a series of 2 to 11 spikes with 1.6 to 6 msec interspike intervals (Ranck 1973), in which the amplitude of the extracellularly recorded spike changes during the series, usually monotonically

decreasing. Firing of complex spikes was found to have no simple relation to presence or absence of a slow wave θ rhythm.

Figure 3.1 Complex-spike recorded in the CA1 region. (reprinted from Fox and Ranck 1981)

The second type of neurons is more tonic, has a more uniform and higher frequency firing rate, and never produces complex spike bursts. Ranck called these neurons *theta cells*, due to the correlation between their activity and the presence of the hippocampal θ rhythm. Theta cells and complex spike cells are also identified by the shape of their extracellular action potentials. Theta cells produce shorter duration and smaller amplitude spikes compared with complex spike cells (Ranck 1973; Fox and Ranck 1975).

Fox and Ranck (1975) also demonstrated that theta cells and complex spike cells have different anatomical distributions. These data led them to suggest that theta cells are interneurons, and that complex spike cells correspond to pyramidal neurons (Fox and Ranck 1975).

There is some controversy about this simple anatomical classification. Bland et al. (1980) found evidence, in the rabbit, that some CA1 pyramidal cells fire with the pattern attributed to theta cells, and there is evidence that interneurons in the pyramidal layer project out of the hippocampus (Alonso and Kohler 1982). There is also evidence for an additional group of cells called *theta-off* cells, which fire during LIA but are mostly silent during the θ rhythm (Colom and Bland 1987). Bland and Colom have suggested that these cells are inhibitory interneurons which receive inhibitory input from the medial septum (Bland and Colom 1989).

Place cells

In 1971, O'Keefe and Dostrovsky demonstrated that some of the cells recorded from CA1 in a freely moving rat code for the animal's spatial location. Place cells have a low overall firing rate, which is significantly higher in the active region (place field) than in the remainder of the environment. In another study (O'Keefe 1976), place cells in the dorsal CA1 field were found to be a subset of the complex spike cells, and therefore putative pyramidal cells. In agreement with Ranck, O'Keefe (1976) identified a physiologically separate group of cells, correlated with the θ rhythm and movements, which he called *displace cells*. In the recent literature, and this dissertation, displace cells are called *theta cells*.

The data from several research groups are consistent in the report of spatial firing in hippocampal complex spike cells (see Table 3.1, p.50). However, there is much less agreement on the qualitative and quantitative details of the firing pattern of these cells. The variations in properties include: (1) the size and shape of the place field of a cell, (2) the extent to which spatial location alone controls the firing of the cells, and (3) the persistence of the firing pattern over time. Differences in observed properties result from the structure of the environment and the design of the experiments, and these differences are compounded by the difficulty in isolating the activity of single neurons with extracellular electrodes.

3.3 Methodological issues

Tasks and environments

One of the key characteristics of place cells, demonstrated in all of the initial studies, is that their firing pattern is largely independent of specific behaviour patterns or the task that the animal is performing. In spite of this evidence, the design of hippocampal recording experiments can affect the characteristics of the recorded place cells. In this section these design issues are discussed, in order to provide the context for a review of the published properties of place cells.

Two competing demands influence the design of hippocampal recording experiments in freely moving rats. One objective in these tasks is to achieve

reasonably balanced coverage of the environment, and the second is for the animal to display a set of behaviours (e.g. selecting a turn in a maze) to indicate that it knows its spatial location. The defining characteristic of a place cell is comparatively higher firing in one part of an environment, which can be reliably measured only if the animal's behaviour is almost uniformly distributed in space. In many of the initial studies there was no measurement of the time that the rat spent in parts of the environment. In the extreme, if the rat has occupied only one place, then any active cell could be interpreted as a place cell. Some of the place cell data have been recorded during stereotyped movements that do not cover the environment, and to this extent the degree of spatial preference cannot really be determined. In a recent quantitative study (Muller and Kubie 1987) the task was designed to optimise coverage of the environment. In this task the animal searches for randomly placed food in a walled cylinder.

There are two problems with this type of task. The first problem is that there is no guarantee that the hippocampus is being used at any particular point in time. This issue is difficult to separate from a discussion of the investigator's model of hippocampal function. In models favouring a simple sensory correlate of hippocampal activity the issue is less critical. However if the cognitive map model is correct then there will be a useful hippocampal firing pattern only if the animal has an active mental map of the current environment and knows its location. The solution to this problem (O'Keefe and Conway 1978; Olton et al. 1978) is to record from place cells, while challenging the animal with a task that is known, from lesion studies, to require the hippocampus. During these tasks the animal demonstrates through its behaviour that it knows its spatial location.

One of the first tasks that both achieved nearly uniform coverage of the environment and is known to require the hippocampus (Olton et al. 1977) was developed by Olton et al. (1978). In this task the animal visits, in an arbitrary sequence, all of the arms in an eight-arm radial maze. Since each arm is baited once, the rat must keep track of the set of previously visited arms. However, in this task the behaviour is only really distributed in a set of one-dimensional environments (maze arms), and there is evidence, discussed below, that linear environments result in different place cell properties.

The requirement for a behavioural measure of the rat's awareness of location is even greater in changing environments. In the reviewed literature changing environments are often used. This type of experiment is, of course, the only means for determining the inputs that are driving place cell activity. If there is no method for testing the animal's use of the hippocampus then the activity patterns recorded from the place cells could be inaccurate. O'Keefe and Conway (1978, 198) pioneered a cue-controlled task in which the environment could be manipulate , while maintaining a behavioural test of hippocampal function. However, mo t experiments that require choice on the part of the animal have difficulty in achievi g a uniform behaviour pattern over the environment. This problem is addressed in tl e cue-controlled task, since there is largely uniform coverage in the start arr . However, a second problem is that even in a cue-controlled task the hippocampi s may be used for spatial processing during only part of the time (i.e. when the rat s making the choice).

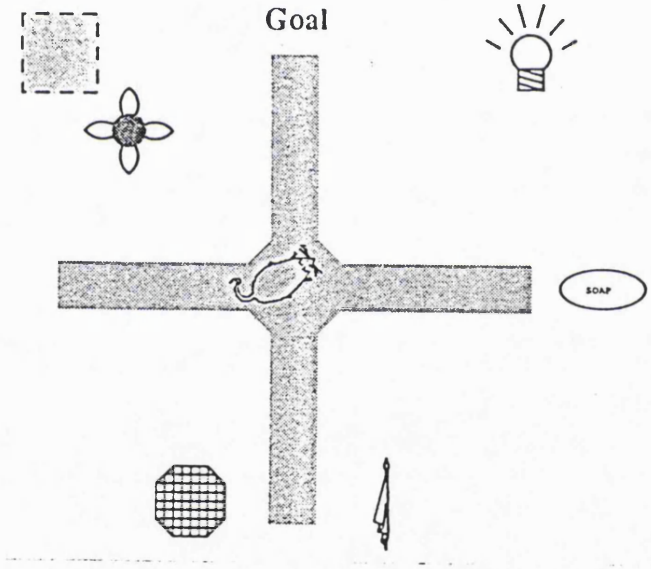

Figure 3.2 Cue-controlled recording environment. The animal is trained to obtain a food reward in the arm located between two extramaze cues. The maze was centred within an enclosure consisting of a set of black floor length curtains suspended from a false ceiling. The diameter of the curtains was 2.5m. The maze consisted of a circlar central platform (34.5 cm diameter) and 4 arms (15 cm wide x 38 cm long). Only the control cues, which are rotated, and not the background cues, which are stationary, can be used to perform the task. In this example the cues are (in clockwise order from the top): a light, a bar of scented soap, a white towel, a small cage, a fan and a white card (modified from Speakman and O'Keefe 1990).

Some of the published properties of place cells have been collected in tasks that have neither uniform coverage of the environment nor any indication of the concurrent use of the hippocampus. For example, Breese et al. (1989) recorded from thirsty rats while they ran in stereotyped movements between identical water dishes, which were placed in four corners and the centre of a platform. Initially the water dishes contained a drop of water in a random pattern, and during this period the firing of place cells was recorded. Following this period only one of the dishes was baited and the change in place cell firing was measured. Unfortunately, this task does not provide coverage of the entire environment, and since there is no measure of the rat's awareness of location the place cell firing could be very difficult to interpret.

In some of the published data the rat is coaxed or pushed around the environment. This is a less controlled form of the randomly distributed food task (Muller and Kubie 1987) discussed above, but since the behaviour is being disturbed, then the spatial representation could be disturbed as well.

Data on hippocampal single units have been collected using a range of different rewards and penalties to shape the rat's behaviour. Given the general plasticity of the nervous system, there is a risk that artificial and repetitive behavioural paradigms will lead to artificial representations in the neuronal activity patterns. For this reason, less credence is given to data collected during extreme food deprivation, water deprivation or shock penalties. Secondly, although useful data can result from lesion studies, recordings from cells in these circumstances must be treated differently.

From the original studies of complex spike cells (Ranck 1973) it was established that they fire at a low rate during periods of non-movement, including during periods of LIA (Ranck 1973; Olmstead et al. 1973; Suzuki and Smith 1985a,b). Most of the tasks used during hippocampal recording have periods during which the rat is non-moving, which are long enough to result in LIA firing of place cells. This contributes to the variation in the background, or out of field, rates reported in the literature.

Extracellular recording

All of the known properties of place cells have been found by recording the firing patterns of putative single neurons using extracellular electrodes, as the animal moves within an environment. There is great variation in the recording methods, which have produced corresponding variation in results. The important issues leading to this variation are briefly described here. Again, this analysis is used as context for the literature review that follows.

All membrane potential changes of neurons are in principle observable with an electrode outside the cell membrane. When the internal potential changes, one part of the cell is depolarised more than the adjacent areas and a current flows; an extracellular field is generated as a result of this current. The amplitude of the voltage outside the cell is significantly attenuated by the membrane resistance, and it decreases at least as fast as the inverse square of the distance from the cell membrane. The wave shape of action potentials is determined by several factors, including the type and distribution of the electrical sources and sinks present in the cellular membrane and the morphology of the cell's dendritic arborisation. If the extracellular medium behaves as a perfect ohmic resistor (i.e. no change in this resistance with current flow), with an isotropic impedance (i.e. no variation of the current flow with direction), then the extracellular wave shape at a point near the cell body is roughly the derivative with respect to time of the internal potential (Hubbard et al. 1969).

In the extracellular space, each action potential is superimposed on the background voltage, which results from the cumulation of many dendritic spikes, synaptic potentials and the firing of nearby neurons. The wave shape of a single unit, recorded from the hippocampus of a freely moving rat, is a small (10-20%) fluctuation superimposed on the accumulated electrical activity (EEG). If two or more neurons near the recording electrode are active at the same time, then the extracellular spikes can be distorted beyond recognition. In fact, it would be essentially impossible to record the activity of individual hippocampal neurons if there was a higher incidence of simultaneous activity.

All methods for extracellular recording of action potentials need to cope with the problem of separating the electrical activity of one cell from the background activity. In the hippocampus this is particularly difficult since the somata are packed

into a single cell layer, have similar morphology and orientation (see Chapter 2), and therefore produce similarly shaped action potentials. The lower frequency EEG and high frequency background are filtered out of the recorded signal. The design of the filters can dramatically affect the performance of the algorithm used to separate out single unit activity (see Chapter 4).

Of course, the properties of the electrode also affect the shape of the recorded extracellular spikes. The signals will vary with the size of the electrodes, their orientation with respect to the cell, and their chemical composition. In addition, the electrode can damage the cell, and chemically interact with it. All of these phenomena significantly affect the recorded signal. One important effect, which may be a result of damage, is that the activity level of cells greatly increases when an electrode is advanced into the cell layer. The delay between advancing the electrode and recording from the cells is a significant variable between reported data.

An ideal electrode would have a very small tip and a low impedance and would not interact chemically with the brain. Electrodes with smaller diameter tips have a higher resolution (i.e. they measure the voltage in a smaller region), but they also have a higher impedance. The minimum value for electrode impedance is determined by the conductor area of the tip. With fixed diameter electrode tips the surface area can be increased through electro-plating. Unfortunately small tipped electrodes reduce the stability of the recording. The loss of stability occurs both from small movements of the electrode, and from reported loss of cells during violent head shakes (O'Keefe 1976).

Single electrode methods

A wide spectrum of methods has been used to separate the extracellular activity of a single neuron from the background signal. These methods range from single voltage thresholds, to off-line analysis of recorded waveforms (summarised in Table 3.1, p.50). More recently simultaneous recording of neuronal activity with two electrodes has been used to improve these methods (McNaughton et al. 1983a). In a large fraction of the published research, place cells were recorded using single electrodes, and often using a single voltage threshold as a trigger (Table 3.1, p.50). The idea is that one neuron (because it is nearest, or generates larger voltage swings) will

produce the largest spikes. In this view an appropriately set threshold will be crossed by each spike produced by the neuron, and only by the spikes from a single neuron.

It is clear that the single threshold technique is highly inadequate for any quantitative analysis. One flawed assumption, with this method, is that all the neurons within recording distance of the electrode are active during the time period in which the threshold is set. Once the threshold has been set, a second neuron with a larger extracellular spike will cause false triggers. Since most neurons in the hippocampus have a very low firing rate, a long time interval is required to ensure that each has fired. In the hippocampus of the freely moving rat, this is further complicated by the fact that in any particular environment only a small fraction of the cells are active. Single threshold recording is also susceptible to false triggers from electrical artifacts (e.g. caused by scratching, chewing or loose contacts).

This problem can be partly overcome by adding a second threshold setting that defines the maximum signal. These two thresholds define a voltage window that brackets the spike peak. This window method greatly reduces the chance that activity from a previously silent neuron or noise will be mistaken for a spike, but in reducing the first problem it makes a second problem more severe.

The second problem with the single threshold method is the assumption that a threshold *exists* that separates the activity of one neuron from the background. Implicit is the expectation that the amplitude of spikes from one neuron varies less than the amplitude difference between spikes from two different neurons. This should not be expected from the neurons in the hippocampus. As discussed above, complex spike cells produce bursts with a monotonically decreasing amplitude. There is generally no single threshold that separates the activity of one neuron from the background without producing many false positives and false negatives.

The systematic nature of the wave shape can be taken advantage of by adding further threshold settings to the spike detector. The simplest extension is to place two window discriminators at the points of greatest variation between spikes from one neuron to another (i.e. the peak and the minima of the signal). With this method a waveform is selected based on its bracketed height at two points in time and its width, or equivalently a time window (Figure 3.3).

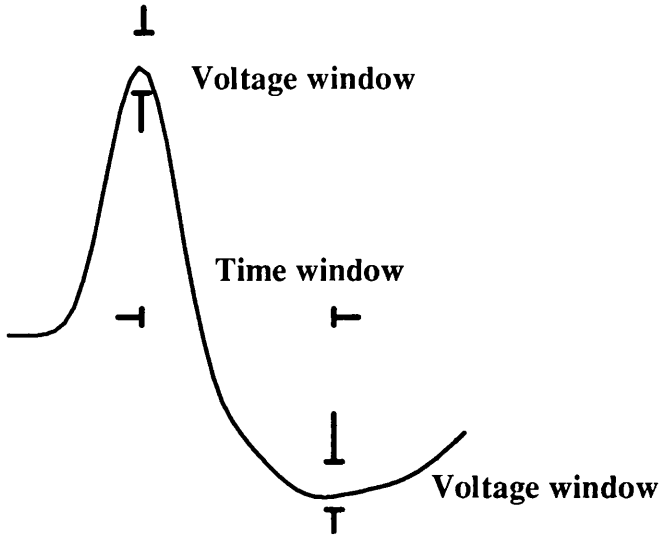

Figure 3.3 Threshold settings required to select an action potential waveform with bracketed levels at the peak and minimum.

It would be more difficult for a spurious waveform to meet these criteria, but there are still two problems. One problem is that five constants now have to be set correctly, and the second is that these five constants must have values that separate the activity of the neuron from the background. In spite of the difficulties, this method has been used during recording from the hippocampus.

It is very difficult to find values for these constants without recording the data and testing the threshold settings many times. This can only convincingly be accomplished by digitising and storing the waveforms. When digitised, the spikes' waveforms can be aligned and the variance can be computed as a function of time along the waveform. The peaks in the variance define the best time points for placing bracketed thresholds.

It should be pointed out that separation of extracellular neuronal activity is easier in the neocortex due to the looser packing of neurons and the greater variety of wave shapes, which result from the variations in cell type and morphology.

Multiple electrodes

The problem of isolating the activity of single hippocampal neurons can be solved by simultaneously recording the potentials with multiple electrodes (McNaughton et al. 1983a). McNaughton and co-workers developed a method in which an action

potential is recorded with different amplitudes on two adjacent electrodes, called a *stereotrode*. If the source of the signal is nearer to one of the electrodes, then it is larger on that electrode. An example of data recorded in this manner is shown in Figure 3.4.

This figure is a scatter plot of the peak-to-peak amplitude for each digitised spike on the two electrodes of the stereotrode. The y-axis is the amplitude on one electrode and the x-axis is the amplitude on the second electrode. Each cluster represents the activity of a putative single neuron. In the absence of noise, all of the action potentials from one neuron would be plotted on top of each other. Additive noise produces a spread uniformly in the x and y directions, and multiplicative noise (proportional to amplitude) produces a larger spread with distance from the origin. The figure contains several clearly distinguishable clusters and background noise near the origin.

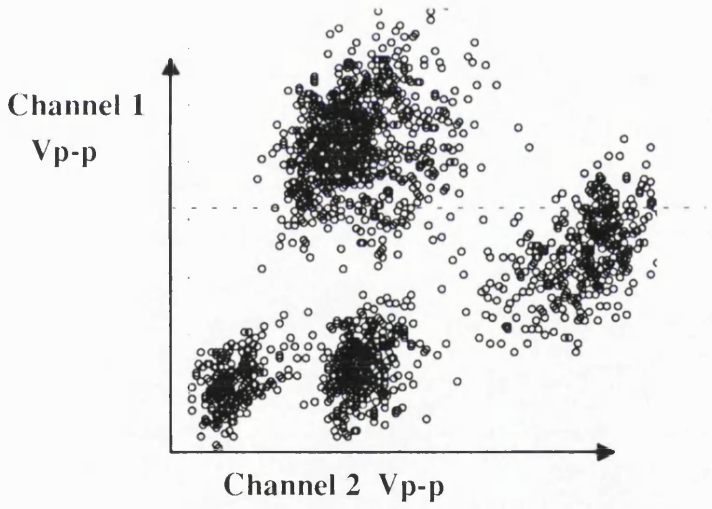

Figure 3.4 Stereotrode plot showing the activity of several hippocampal neurons. In the plot the peak to peak voltage on one channel is plotted against the peak to peak voltage on a second channel.

It is clear from the data that the clusters are oblong rather than circular and symmetrical, and their long axis is diagonal with a positive slope. As McNaughton et al. (1983a) pointed out, this structure is due to the complex spike firing pattern of the cells. Since the true amplitude of the spikes monotonically decreases, the recorded signal decreases proportionally on both electrodes.

If only one electrode had been used to collect these data, none of the separation between these clusters would be evident. Using a single threshold on one of the electrodes would be equivalent to drawing a dividing line perpendicular to the chosen axis. It is clear that the best dividing line perpendicular to the axis contains many false positives and false negatives (dotted line in figure).

Measuring spatial firing patterns

Place cells are characterised by a spatially specific firing pattern, but how spatial is it? Barnes and co-workers (1983) were the first to propose a quantitative measure of the spatial specificity of place cell firing. This measure was computed for each arm of an elevated eight-arm maze by dividing the rate on the peak arm by the average rate on the other arms. As they pointed out in a later paper (Barnes et al. 1990), a cell with a place field at one end of an arm will be considered less spatially specific, using this measure, than a place field occupying the entire arm. The specificity measure is accurate only if the place fields occupy exactly one arm of the maze. A second problem is that this measure confounds the place field size and the cell firing rate. For example, if one neuron had twice the ratio of place field to background firing rate and half the place field size in comparison with another neuron, then by this measure, they would have the same spatial specificity.

In 1987 Muller et al. applied a spatial autocorrelation function to quantify the degree of spatial firing in their data. This measure is equivalent to computing the total deformation of a sheet pulled over the environment. The environment is tessellated into 4096 bins, and the measure is computed by summing the differences in firing rate between all neighbouring bins. If the firing rate function has a single peak and is smooth, then the deformation is smaller than if the firing is consistent but scattered throughout the environment. With this measure, if the firing rate is not normalised, then higher firing rate cells are incorrectly found to be less spatial. One problem with this method is that it is dependent on having large amounts of data, since the measure improves as the noise is reduced. Also this measure cannot distinguish between large smoothly increasing place fields and small sharply peaked place fields.

An interesting new approach to this problem was recently suggested by Skaggs et al. (1993). They computed the information content of a pulse train of hippocampal spikes. This method has several advantages. One improvement is that it is based on the raw data, rather than time averages. It uses both the spatial region of cell firing and the firing rate. However it still does not test if the place field is a single contiguous region. For example, with this measure, a place field with a flat firing rate that covers exactly one half of a cylindrical environment provides one bit of information. The same amount of information is produced by the cell independent of which half of the environment is covered. In particular this half of the environment could be a random patchwork of "places".

The measures introduced in these two papers (Muller et al. 1987; Skaggs et al. 1993) are complementary. A place field that provides several bits of spatial information is specific to a small number of regions in the environment. If it also has a high spatial autocorrelation then it is confined to a single region in the environment. The problem is simpler if the well isolated firing of single hippocampal neurons can be characterised by a family of functions, such as (for example) two-dimensional gaussians.

3.4 Properties of place fields in static environments

The primary available means for studying the function of the hippocampus is through an analysis of the receptive field properties of its constituent neurons. If the hippocampus is a cognitive map, then the properties of the map are determined by the characteristics of place cell firing. Before considering changes in environments and the development of place cell firing over time, many useful measurements can be made of a cell's "static" place field. The most basic properties of place cells include: (1) the shape of the place field, or alternatively the fraction of the environment in which the place cell fires, (2) the relative firing rate over the area of activity of the place cell, (3) the persistence of the firing over time, (4) the consistency of the firing pattern with repeated entries of the rat into the cell's place field, (5) the number of connected regions in the environment in which the cell is active, and (6) the variation of these properties from one cell to another, and from one environment to another.

Study	Place Cells	Environment	Field size (cm^2)	Multiple fields	comments
O'Keefe & Dostrovsky 1971	8 /76 (3,5)	small box	NA	NA	glass insl.ulated tungsten (place , place+sensory)
O'Keefe 1976	26/34 (20,6)	3 arm maze	10-1350	NA	< 1sp./sec background, sharp tungsten, plated; single threshold
Hill 1978	12/14	shuttle box T maze	NA	NA	significant variation in place field firing rate 3-13.5 sp./s ; 62μm blunt tungsten; single threshold
O'Keefe & Conway 1978	32/34	T maze small box	NA	5 maze 0 box	10 on T maze; 7 on box; 15 both; 2 neither; window discriminators
Olton et al. 1978	28/31	8 arm maze	1-7 arms of maze	11/28	2-5μm tungsten; very high background rates some > in field of others; single threshold
Hill & Best 1981	15/15 (4,11)	8 arm maze	"	3/15	same as Olton et al .1978 (place, place+movement);
Best & Ranck 1982	9 /14 (4,5)	platform	NA	0	same as Olton et al. 1978 (place, place+movement)
Barnes et al.1983	54/54	8 arm maze	NA	NA	same as McNaughton et al. 1983b
Kubie & Ranck 1983	28/28	radial maze:23 operant box:15 home cage:17	50-900	NA	24% in only one env.; 25 μm nichrome; single threshold high background rates
McNaughton et al. 1983b	40/42	8 arm maze	900	13/25	25 μm plat-irid; sp. height & width;
Christian & Deadwyler 1986	38/36	platform	NA	NA	etched tungsten 1-3μm tip ; single threshold
Muller et al. 1987	34/40	cylinder	196 - 2842 mean 785	9/34	10 x 25μm nichrome; window discriminators
O'Keefe & Speakman 1987	42/55	plus maze	1,045	13/30	stereotrodes
Breese et al. 1989	47/47	open platform	1,500	NA	sharp tungsten
Mizumori et al. 1989b	95/95	8 arm maze	NA	NA	stereotrode
Pavlides & Winson 1989	13/13	box 8 arm maze	NA	>.5	10 x 22.5μm electroloy
Thompson & Best 1989	91/99	6 arm maze drum walled box	NA	NA	10 x 32μm nichrome; window discriminators
Wiener et al. 1989	311/415	metal platform	19 - 481 mean 94	169/311	10 x 25μm nichrome; window discriminators; only 179 cells analysed;101 double fields,47 triple, 18 quad., 3 quintuple.
Barnes et al. 1990	340/340	8 arm maze	NA	NA	stereotrode
Quirk et al. 1990	28/28	16 cylinder 5 box; 7 both	NA	NA	10 x 25μm nichrome; 3 window discriminators
Sharp et al. 1990	18/18	cylinder	NA	3/18	same as Quirk et al. 1990
Speakman & O'Keefe 1990	19/22	plus maze	NA	1 example	25 μm plat.-irid. tetrodes; peak height
Thompson & Best 1990	61/61	8 arm maze	NA	NA	10 x 32μm nichrome; window disriminators
Bostock et al. 1991	36/36	cylinder	NA	NA	10 x 25μm nichrome; window discriminator

Table 3.1: Properties of place cells. This table does not include data from papers that did not classify complex spike firing as place cells (e.g. Ranck 1973; Berger et al. 1983; Wible et al. 1986; Eichenbaum et al. 1987; Foster et al. 1987; Otto and Eichenbaum 1992). Also, where possible, second papers based on the same set of cells (e.g. Muller and Kubie 1987; Eichenbaum et al. 1989; Muller and Kubie 1989) are left out. The parentheses in the second column refer to the breakdown of cell types in the sixth column. The table includes papers published through 1991. Subsequent references are described in the text.

Some of these base-line properties of place cells have been measured, but a thorough analysis of the properties has not been performed. Most of the published research on place cells gives no detailed measurements of the static properties.

Firing rate of place cells

Several measurements have been reported of the firing rates of place cells inside and outside the place field. O'Keefe (1976) found that the cells fire at less than 1 spike/second outside the place field. Further analysis of the background firing rates (Kubie and Ranck 1983) revealed that the rate was sometimes more than 20 times smaller than in the place field. They suggested that consistent variations in the background firing in different environments were encoding context information.

In the first reports of place cell properties the methods for measuring the extent of spatial firing were inadequate. In 1978, Olton and his colleagues published a quantitative analysis of place cell firing. They defined the spatial firing by accumulating the firing on each of the eight arms in a radial arm maze. If the firing on an arm was significantly different from the grand mean of all the arms, then they defined the arm as either an *on-field* or an *off-field.* They found a wide range of firing rates among complex spike cells. The background firing of some cells exceeding the "on-field" firing of other cells.

In the first description of hippocampal complex spike cells, Ranck (1973) described their firing as *phasic.* During bursts the firing rate is high, but averaged over a longer period the rates are lower. It is therefore not surprising to find some variation in the firing rate of place cells in the place field. The reported values range from less than one per second to over 20 per second.

There have been several studies in which large numbers of place cells have been recorded (Table 3.1, p.50). Thompson and Best (1989) found very little variation in the firing rates of the large number of places cells (99) included in their study. In contrast, Wiener et al. (1989) found a wide variation in place cell firing rate in 311 place cells. Barnes and co-workers (1990) also recorded from a large number of place cells, but the paper does not include raw data, only the results of statistical analysis of spatial specificity and consistency.

Size and shape of place fields

In one of the first papers on place cells (O'Keefe 1976) the size of place fields was found to vary by over two orders of magnitude (10 cm^2 to 1350 cm^2 ,"half of the maze"). These cells, which were recorded on an elevated T maze, had rectangular or elongated place fields that followed the shape of the environment. Detailed firing rate maps were not computed for these cells.

Muller et al. (1987) found less variation in the size of the place fields in the cylinder. They classified the shape into crescent-like, elliptical or circular. As mentioned above, they analysed the size of place fields as a function of the cut-off firing rate. The firing fields had an average size of 785 cm^2. Breese et al. (1989) also found that the firing rate function of place fields has a single peak. In their recording environment the average size of place fields was 484 cm^2, and the range of place field size was not described. Much smaller firing fields were found by Wiener et al. (1989). They found place fields that ranged in size from 19 to 481 cm^2, with an average size of 94 cm^2 for each place that the cell fired. In the latter study, 57% of the cells fired in more than one place.

O'Keefe and Nadel (1978) postulated that the firing rate of a place cell should be a single peaked function of two-dimensional space. The first quantitative measurements of place fields supported this view (McNaughton et al. 1983b; Muller et al. 1987). Muller and co-workers (1987) found that the size and peak firing rates of place cells could vary independently, and that place fields have a firing rate function with a long gradual tail. Therefore the size of a place field can be determined only by specifying a minimum cut-off firing rate.

In most of the published data the firing pattern of place cells is not a single peaked spatial function (e.g. O'Keefe and Speakman 1987; Wiener et al. 1989; Barnes et al. 1990; Quirk et al. 1990; Thompson and Best 1990). Some of these studies describe the spatial firing pattern as multiple place fields (discussed below), but more often the spatial firing pattern is treated as an arbitrary function that has a defined value at several points in the environment.

Multiple place fields

From a review of the place literature, it is quite likely that some place cells have double or multiple place fields. Multiple place fields are independent regions in the environment in which a place cell is active. O'Keefe (1976) found that less than 10% of the place cells had more than one region in which the cell fired, but other groups (Pavlides and Winson 1989) found that over half of the place cells have multiple fields. In one paper, Wiener and co-workers (1989) report data from 311 place cells, in which 54% have multiple fields. This includes 101 with two fields, 47 with three fields, 18 with four fields and 3 with five fields.

Of course some of the reported double fields could be the superposition of the activity patterns from two or more neurons that have not been isolated. None of the published papers has included an analysis of the relative amplitude or firing rates of cells that have double fields. If double fields occur from poor single unit isolation, then the units might be expected to have, on average, a lower spike amplitude or a higher firing rate. Muller et al. (1987) recorded from the same cell following two 15μm advancements of the electrode, and demonstrated that the action potential had changed and that the cell still had a double field.

One of the complications with multi-arm mazes is that multiple fields can be recorded by finding place fields on adjacent arms. These fields could equally be single larger place fields, which are not measured because the animal cannot visit the area between the arms. The type III place cells from Olton et al. (1978) are the first published example of this type of firing. They have a high rate on a single arm, but significant firing on an adjacent arm.

Topographic coding: correlates of anatomically nearby cells

In contrast with most sensory and motor areas of the brain, no simple relationship has been found between the firing properties of anatomically nearby place cells in regions CA1-3 of the hippocampus. This was first suggested from recordings in which neurons were isolated sequentially in a single electrode penetration (0'Keefe 1976), and is supported by more recent data from simultaneously recorded neurons.

However, the distribution of the firing fields of anatomically nearby place cells does not appear to be completely random. O'Keefe (1976) found that place cells sometimes have spatially neighbouring place fields. Eichenbaum and his colleagues (1989) compared the location of place fields from 311 place cells to the distribution expected from random placement. The cells used in this study were recorded in 62 sets, in which there were on average 5.2 simultaneously recorded neurons. They found several place cells with overlapping firing fields, in which the second firing field of the two cells also overlapped. In addition, place fields which they simultaneously recorded from anatomically nearby cells were found to occur near one another in the environment.

In most of the published data the place fields of nearby place cells are distributed throughout the environment. This leads to a related question: how evenly are place fields distributed over an environment? O'Keefe (1976) found that there were more place fields on the arm of the maze nearest to the experimenter. In a comparison of place cell firing in two environments, O'Keefe and Conway (1978) found that on a small platform the cells were mostly near the edge, while they were more uniformly distributed on an elevated T maze. In a later study, O'Keefe and Speakman (1987) found that it requires a surprisingly small number of cells to cover the environment. Muller and co-workers also measured the distribution of place fields (Muller et al. 1987). In their high walled cylindrical environment they found no angular or radial bias in the location of place field centres.

Very recently it was demonstrated that a sufficient set of place cells can be used by a downstream system to determine the animal's location in an environment to an arbitrary accuracy (Wilson and McNaughton 1993). The number of cells required to locate the animal to within 1 cm on a 0.1 second time scale in a walled box was computed to be approximately 380.

Homogeneity of place cells

One of the most inconsistent issues in the literature on place cells is the extent to which they are a homogeneous group. This divides into two questions: (1) What fraction of hippocampal complex spike (putative pyramidal) cells are place cells?;

and (2) Do place cells have a homogeneous set of properties, or is there evidence for subdivision?

O'Keefe (1976) subdivided place cells into two groups. The firing pattern of one group of place cells depends only on the animal's location. The second group, called *misplace cells*, fire maximally in a part of the environment if either something is missing or there is a new object in the place. Olton et al. (1978) grouped cell firing patterns into three classes, based on the size of place fields. Their third class consisted of cells with an *off* place field, corresponding to the condition that the rat was *not* in a particular place. Off place fields were also reported in later publications by the same authors (Hill and Best 1981; Thompson and Best 1989) but have not been replicated by other laboratories. Best and Ranck (1982) proposed that place cells be divided into two groups: one that is purely spatial and a second group that depends on location and on movement.

In a review of place cells, O'Keefe (1979) claimed that place cells constitute the majority of the cells in the hippocampus. More recently, Thompson and Best (1989) recorded from 273 complex spike cells during anaesthesia, and in three different environments. They found that only 99 of these cells were active in at least one of the environments. However, even the "silent cells" that were not active in any of the environments had the same firing rates and characteristics during anaesthesia. Based on these data, they suggested that place cells form a homogeneous group. They did not report the size and shape of the place fields, but they found little variation in the average firing rates of place cells.

In the study published by Thompson and Best (1989) 92% of complex spike cells had place fields. In contrast, Wiener et al. (1989) found that only 75% of complex spike cells had spatially specific activity patterns. More recently Wilson and McNaughton (1993) recorded simultaneously from 73 to 148 cells, and found that 34% of the cells were active in the initial environment, which is consistent with the results described by Thompson and Best (1989). In the more recent study (Wilson and McNaughton 1993) 100% of the active complex spike cells had place fields.

3.5 Sensory control and memory in place cells

The claim that complex spike cells are mostly place cells is still contested (eg. Cohen and Eichenbaum 1991). The other possible correlates for hippocampal complex spike cell firing are described in Section 3.8. In this section the different mechanisms for producing spatially specific firing are described, and the evidence for the sensory control and memory properties of place cells is presented.

The cognitive map model proposes that the firing pattern of each place cell is constructed from a combination of sensory inputs and movement derived information, and that the activity pattern of place cells constructs a holistic world centred map of the animal's current environment. A holistic map is one in which the places in the map are mutually reinforcing, or equivalently that the co-active cells form a cell assembly (Hebb 1949). In a holistic map, part of the representation of an environment would not change independently from the overall representation. This is a useful property for a cognitive map, in that it makes the map more robust. Other schemes could be imagined in which each neuron fires if a particular combination of sensory stimuli occurs. In this latter case, if the activating combination of stimuli for one cell is removed, then only that single cell would stop firing in the environment. One implication of this view is that the place cells that fire in an environment, but not in the animal's current location are closer to firing than the place cells that are not active within the environment.

In contrast to neocortical sensory neurons, place cells were suggested to form part of a map of the environment, which was defined by the external world (allocentric) rather than by the space surrounding the animal and centred on the animal (egocentric).

The representation for a particular environment should be consistent and repeatable. Therefore the representation should return when the animal is reintroduced to an environment that has been explored before.

Spatial firing

In a review of the properties of place cells, O'Keefe (1979) discussed several other possible mechanisms that could produce neurons with spatial firing patterns. The cognitive map model is not the simplest mechanism that could produce spatial firing,

and some of the first experiments have compared the predictions of the model against simpler hypotheses.

For example, hippocampal complex spike cells could be coding for particular motor behaviours (e.g. turning right) that the rat is producing in only one part of an environment. The evidence against the simple motor hypothesis is that the cells fire independently of the behaviour that the rat performs in a place, and do not fire when those behaviours occur in other parts of the environment (O'Keefe and Conway 1978). Also the behaviour can be spatially homogeneous while maintaining a stable spatial firing pattern (Muller and Kubie 1987). An important part of the evidence supporting the sensory drive of place fields is that significant alterations of an environment (O'Keefe and Conway 1978; O'Keefe 1979) or disorienting the animal (Hill and Best 1981) bring about significant change in the place fields.

Another simpler hypothesis is that place cells are firing to a single sensory input (e.g. the size of a known object on the retina, or the texture of a part of the maze). This would make several predictions about the shape of place fields, since the quantity of a distal input (e.g. object on the retina, olfactory input) would be constant at all points on an arc equidistant from the source. On the other hand, proximal cues such as the texture of a part of the maze could result in multiple place fields with arbitrary shape. An argument against this hypothesis is that place cells can fire without the cues present (O'Keefe and Speakman 1987). This memory component of place cells is discussed below. The single cue hypothesis cannot explain the increase in the size of place fields found when the walled cylinder environment was increased in size (Muller and Kubie 1987). In the simplest interpretation of the single cue hypothesis, a place field that is constructed from a single distal cue (e.g. the size of an object on the retina) would move away from the cue in a scaled up environment. This change in field size also suggests that vestibular information is not being used, since the size of the place field does not depend on the number of steps taken by the rat.

One form of the simple sensory input hypothesis suggests that the activity of place cells is controlled by the location of the goal in a task. In the previously described experiment, Breese et al. (1989) changed the goal location and found a shift in the place fields towards the goal. They argued that the location of place fields

is determined by the significance of cues. However, as stated earlier, they had no measure of the animal's concurrent knowledge of spatial location. Speakman and O'Keefe (1990) found opposite results in the cue-controlled task. In this task, the animals learned to run towards a new goal location without changing the firing field of place cells.

A third view is that, rather than a simple sensory or motor correlate, the cells are firing to the time before or after a particular motor behaviour or sensory input. Evidence against this view has been found by changing the time taken by the animal to reach the goal location (detours) and by using distributed behaviour problems (e.g. O'Keefe and Conway 1978; O'Keefe and Speakman 1987).

Spatial memory

In a cue-controlled experiment, O'Keefe and Conway (1978) found that the place cell firing persisted following removal of several of the cues. Earlier, O'Keefe (1976) found that place cell firing persisted if the lights were turned off. These experiments suggested that place cell firing was the result of a complex set of stimuli, and that there was memory for the cues in the system. Quirk et al. (1990) repeated the lights-out experiments and found that if the animal was in the environment when the lights were turned off, then the place cells persisted. However, if the animal was brought into a dark environment, then the place cells fired in a different location, which persisted after the lights were turned back on. Hill and Best (1981) found that deafened and masked rats also develop place cells.

The conclusive demonstration of memory in the spatial system was published by O'Keefe and Speakman (1987). They used a cue-controlled task in which the cues were removed after the rat was put onto the maze, but before it was allowed to run to the goal. In order to perform this task the animal must either remember cue locations, or build short term associations with the background cues. Over many trials the remaining cues, including background auditory and olfactory inputs, and tactile inputs from the maze, give it spurious information. Only the memory of the removed cues (or information derived from the cues) tells it the correct turn. In this task the place cells still remain in the same orientation to the (removed) cues, which clearly demonstrates memory in the system, or upstream from the system.

A second significant result from this study was found during incorrect choices during the memory task. The data show that during an incorrect choice the cells fire to the maze orientation consistent with the choice. This demonstrates that the animal's behaviour is consistent with the spatial firing and more convincingly ties the animal's knowledge of spatial location with place cell activity.

Holistic firing in place cells

The prediction of holistic firing of a set of place cells is readily tested. For this to be true, any change in the environment must result in changes in all of the place cells. The simple sensory hypothesis, in contrast, would predict that each change in the environment would bring about a change in only the place cells associated with the cues that are changed.

One part of the evidence for the holistic nature of the place cell spatial representation is that rotation of the cues in a cue-controlled environment results in rotation of all the place cells (O'Keefe and Conway 1978; Muller and Kubie 1987). Most of these initial data were limited by the fact that only one cell was recorded from at any point in time; but more recent data with simultaneous recordings of multiple units have supported this hypothesis (O'Keefe and Speakman 1987).

The holistic activity hypothesis is more effectively tested by exposing the rat to a new environment or by making changes to an environment that are sufficient to change the place cell firing pattern (O'Keefe and Conway 1978). This hypothesis predicts that all of the place cells change away from one representation and stabilise onto a new firing field at the same time.

The first measurements of the set-up of place fields were published by Hill (1978). He found that the place fields fired on the first exposure to the environment. However, this experiment was carried out in a T maze that was very similar to a shuttle box in which the rat had extensive experience. Hill also recorded in the shuttle box, and found that half of the cells fired in the same place in the two environments. Most of the data recorded in multiple environments show no predictable relationship between the firing location in the two environments (discussed in Section 3.6). One interpretation of Hill's data is that the animal could not distinguish between the two environments.

Two studies have looked at this phenomenon more recently (Bostock et al. 1991; Wilson and McNaughton 1993). In the first of these (Bostock et al. 1991), change in the environment was produced by changing a cue card in the walled cylinder from white to black. They found that it took 12-30 minutes of exposure to a new environment for the cells to change to their final firing pattern, and that all of the cells recorded from one animal changed simultaneously. Wilson and McNaughton measured the activity of over 40 neurons and mapped out the change in firing pattern as the rat was exposed to a previously unseen second half of a walled box. They found that activity of place cells was much less spatially specific during the first 10 minutes in an environment than in the second 10 minutes.

There is evidence against the holistic representation hypothesis. One part of this evidence is the change in spatial firing seen when a barrier is put into the place field (Hill 1978; Muller et al. 1987; Breese et al. 1989). All three studies found that the place cell firing could be stopped by introducing a barrier into the place field. In the first study, Hill found that if the rat crossed the barrier the cell did not fire, but if the animal sniffed the base of the barrier the cell fired. Muller and his colleagues found consistent results. The barrier stopped the cell firing, but if the lead base of the barrier only was put into the place field then the cell continued to fire in the same location.

In many studies a small fraction of the recorded cells did not change with the others. It is therefore possible that there are spatially selective cells in the hippocampus in addition to the holistic cell assembly that seems to represent the animal's environment.

3.6 Environment dependent firing

Empirical evidence has clearly demonstrated that only a subset of place cells is active in any particular environment. This property was first reported by O'Keefe and Conway (1978). Place cells were recorded on both a small platform (holding box) and an elevated T maze. Some of the cells fired in both of the environments, but the majority were active in only one of the environments. Kubie and Ranck (1983) replicated this finding, using three different tasks and recording chambers. The tasks were: (1) retrieving food from the end of the arms in an eight-arm radial maze, (2) an

operant chamber with a differential reinforcement for low bar-press rate schedule, and (3) a large home box containing the rat's pups. Unlike the prior study, all three environments were located in the same part of the laboratory. This removes any doubt, in the prior study, that the two environments are treated as parts of one environment. They found that 24% of the cells fired in only one environment, 33% in two situations, and 43% in all three situations.

Muller et al. (1987) compared cell firing patterns in two similar environments in which the animal performed the same task. One environment was a walled cylinder, polarised by a white cue card. The second was a square walled environment, which also had a polarising white cue card. They found that half of the cells were active in one environment, and the other half were active in both environments.

All three papers describe place cells that were active in two (or more) different environments (see Table 3.1, p.50), but in all cases there was no predictable relationship between the locations and the size of the place fields in the two environments.

As part of the previously discussed study of "silent cells", Thompson and Best (1989) found that 14% of the place cells were active in two of three environments, and 1.4% in all three environments. However over two thirds of the cells recorded under anaesthesia either were silent or fired only with background rates in all three environments. The place cell data from multiple environments are consistent in finding more cells active on the radial arm maze (Thompson and Best 1989; Kubie and Ranck 1983), which Thompson and Best suggest is due to more complex sensory inputs.

The hypothesis that there are independent subsets of place cells active in each environment can be fully tested only if the place fields of the cells are measured both before and after the animal is introduced into a new environment. None of the studies discussed above performed this test, but two recent papers have addressed this point. Bostock et al. (1991) mapped out the changes in place field firing during a change in the animal's environment. In this case the data were recorded as the animal searched for food in a walled cylindrical environment, polarised by a white card. After the fields had been measured, the white card was exchanged with a black cue

card and the fields gradually changed. Naive observers were asked if the place fields of paired cells were rotated copies of each other, or if there was a more complex change. In most cases (10/19) the change was classified as "complex" because the cell stopped firing. After the change, the white cue card was replaced, and the place fields were measured again. More recently Wilson and McNaughton (1993) demonstrated the same effect. They recorded from 75-148 place cells while the rat explored one side of a walled rectangular box divided into two by a partition. After mapping the place fields on one side of the partition, they let the rat explore beyond the partition, and found that new place fields were established for the new part of the environment without disturbing the place fields for the first environment.

At one level, all of these studies are consistent: they all report evidence that different subsets of cells are active in each unique environment. However, very few of the details are consistent. One study found an increasing percentage of cells active in one, two and three environments (Kubie and Ranck 1983), while another study found exactly the opposite (Thompson and Best 1989). The fraction of cells active in two environments varies from 14% to over 50%.

3.7 Other properties of place cells

In addition to a correlation with spatial position the cells have also been shown to vary their rate with other movement parameters. In particular, from the first report of place cells it was shown that the firing rate of some of the cells was dependent on the direction of movement of the animal (O'Keefe and Dostrovsky 1971). Several recent papers report directional firing in place cells (McNaughton et al. 1983b; Breese et al. 1989; Wiener et al. 1989; Barnes et al. 1990). In many cases the cells are reported to have a direction bias, which is not exclusive for particular directions.

Other studies have found place cells with little or no direction specific firing (Muller et al. 1987; O'Keefe and Speakman 1987). Measurements of the directional bias in place cell activity suffer from the same problems as the previously discussed measurements of spatial firing. Several different directionality measures have been proposed, many of which are inadequate. Several labs are now employing tracking systems that use two lights to measure the animal's head direction.

A second movement parameter that has been correlated with changes in place cell firing rate is the animal's velocity. Both theta cells and complex spike cells are reported to increase their frequency with increased speed (McNaughton et al. 1983b). At higher speeds the animal moves more quickly through a place field, which could explain a higher firing rate. On the other hand, Wiener et al. (1989) found that complex spike cells, recorded in their task, fired at the highest rate for a particular speed, producing fewer spikes at both higher and lower speeds. The simplest hypothesis is that the total number of spikes on a pass through a place field is constant, but the data do not fit this hypothesis.

Another interesting property of place cells is that they seem to predict the animal's entry into the place field (Muller and Kubie 1989). Based on three different measures of spatial activity, they demonstrated that the firing fields become more "ideal" if the firing is predicting the field by 120 msec. However, Breese et al. (1989) performed the same time shift analysis on their place cell data and found no improvement in either the area of the place field or the spatial density of neuronal activity. They tested this hypothesis with a new measure of spatial firing, which is the total distance of each spike from the centre of the place field. The field centre was defined as the location with the highest firing rate.

3.8 Other correlates of hippocampal complex spike cells

In the first report of the characteristics of complex spike cells, Ranck (1973) proposed that the cells code for behaviour in relation to a specific goal. The classification scheme included four categories: (1) approach-consummate cells which had higher firing during eating, drinking and approach to these "objects"; (2) approach-consummate-mismatch cells which fired during the same behaviours as the prior category, but also fired during unsuccessful attempts; (3) appetitive cells which fired during orienting and approach behaviours but not during eating and drinking; and (4) motion punctate cells which are active at the end of orienting movements and occasionally during direction changes. In a later paper (Best and Ranck 1982) this classification was found less convincing than the spatial interpretation of the firing.

Eichenbaum and colleagues (Eichenbaum et al. 1987; review in Eichenbaum et al. 1992) proposed a classification similar to the one previously suggested by

Ranck. They designed an olfactory conditioning task that also has a large spatial component. In this task the animal learns to associate a water reward with particular olfactory cues. The beginning of each trial is signaled by a tone, at which time the animal goes to a sampling port, and if the cue is one of the set associated with a reward (S+) then the animal finds a drop of water in a cup on the opposite side of the environment. This task made it possible to test two alternative hypotheses: (1) that complex spike cells were best correlated with particular stimulus-response-reinforcement patterns (e.g. Berger et al. 1983; Segal and Olds 1972, 1973); or (2) with a spatial location within an environment. They divided complex spike cells into cue-sampling and goal-approach cells. Cue-sampling cells fired while the animal was sampling the odour, and their firing rate depended on the significance of the current and prior stimulus. An S- trial followed by an S+ trial resulted in the highest firing rate, while an S+ trial follwed by an S- resulted in the lowest rate. They do not discuss the possibility that the firing is spatially modulated by an attentional component. Goal-approach cells fired at a particular time (and distance from the goal). They did not necessarily fire if the animal moved through the place during times other than the part of the trial in which it was approaching the goal. In this study the possibility that this firing pattern was due to directionality in place cells was not considered. They concluded that their classification was better than the spatial hypothesis for explaining their results.

The activity of complex spike cells has been recorded during several "non-spatial" tasks. Several of these require the rat to discriminate between two cues. Various cues have been used in these tasks, including visual (Wible et al. 1986), olfactory (Eichenbaum et al. 1987; Wiener et al. 1989) and auditory (Foster et al. 1987) cues.

At one level it is difficult to distinguish between sensory related firing and spatial firing, as the particular sensory input may only be present in one place. In addition, from the first reports of place cells, some of the single units have been fire only if the animal was sniffing in a particular smell in a place. The spatial hypothesis proposes that the location is the primary stimulus for the majority of the cells, while the alternative is that it is just the combination of sensory inputs.

The apparent memory component of hippocampal complex spike activity makes it even more difficult to distinguish between the alternative hypotheses of sensory specific and spatial firing. If a single stimulus is removed from a place, the cell may be completing the pattern and reconstructing the stimulus, or may be coding for the location itself.

Ultimately new experiments will be required to distinguish between these two hypotheses. In particular the cognitive map model links the firing of different locations in space, while the alternatives are mostly concerned with the sensory conjunction at a single spatial location. In the spatial model the relative position, and distances between the place fields of the active subset of place cells is important. The spatial hypothesis would be disproven if, for example, a method is discovered to determine the cues that are driving each place cell and using this method the place field of individual cells is moved relative to others that are being simultaneously recorded. Alternatively, if new experiments lead to the discovery of additional properties of place cells, which have more relavance to the computation of distances or the use of Euclidean maps, then the spatial hypothesis will be strengthened.

The present research is directed at testing the cognitive map model of hippocampal function.

3.9 Spatial activity in other hippocampal cells

It is reasonable to expect spatially specific firing in some of the projections to or from the CA1-3 place cells. In a recent paper, Barnes and co-workers (1990) compared the spatial firing pattern of neurons upstream and downstream from CA1-3 pyramidal cells. Consistent with prior results (McNaughton et al. 1983b; Christian and Deadwyler 1986), Barnes et al. (1990) found no spatial specificity in 94 theta cells recorded in the CA1 and CA3 fields. This result is somewhat surprising, since theta cells are putative interneurons that receive mostly local afferents from place cells. Furthermore, while Kubie et al. (1990) found spatially preferential firing in hippocampal theta cells during random searching for food in a cylindrical environment, the spatial firing function did not have a single peak and did not have large regions with no firing. However, the spatial firing pattern was repeatable from trial to trial. It should be noted that in all of the published work except Kubie et al.

(1990), spatial firing was measured by taking the ratio of firing in pre-defined parts of the environment (eg. arms or quadrants) which may not find a broad spatially biased firing pattern.

The largest projection from CA1 place cells is to the subiculum. Barnes and co-workers found evidence for spatially consistent firing in the 194 neurons recorded in the subiculum. The firing rate of neurons in the subiculum is higher than in regions CA1-3, which increases the number of overlapping extracellular spikes, and makes it more difficult to isolate the activity of single cells (discussed above).

An important group of cells was recently found in another part of the subicular complex, the postsubiculum (Taube et al. 1990a,b). These cells fire only when the animal is pointing its head in a particular direction. Like place cells, direction cells do not appear to respond to simple sensory stimuli. The activity of direction cells does not depend on the animal's location in the environment, only on its orientation.

As discussed in Chapter 2, the mossy fibres are a direct and specific projection from the dentate gyrus to the CA3 region. In one of the early place cell papers, O'Keefe (1976) reported data from three neurons in the dentate gyrus that were maximally active when the rat sniffed in a particular place. Consistent with prior data (Ranck 1973), O'Keefe also found cells with firing correlates similar to region CA1-3 theta cells. Until recently, other investigations into the firing pattern of neurons in the dentate gyrus have found only cells with a high firing rate and correlates similar to theta cells (Rose et al. 1983; Buzsaki et al. 1983). These high firing rate neurons have been shown to be interneurons (Mizumori et al. 1989a), and Jung and McNaughton (1993) have reported spatial firing properties of low firing rate granule cells in freely moving rats.

The entorhinal cortex provides substantial projections to the hippocampus, and is the target of many projections from the hippocampus. In a recent study Quirk et al. (1992) found spatial firing patterns in some neurons in layers II and III of the entorhinal cortex. These cells also fire in a complex spike burst (Mitchell and Ranck 1977), but the spatial firing is far less spatially specific than that found in place cells in the CA1-3 fields. Quirk et al. (1992) found that, unlike place cells, entorhinal neurons were consistently active in both environments tested (square walled

environment and high walled cylinder), and there was more predictability in the location of the high firing region. This suggests that the entorhinal neurons are more sensitive to particular sensory input.

3.10 Hippocampal EEG

Extracellular electrical activity in the hippocampus of freely moving rats is dominated by a roughly 7-12 Hz pattern of rhythmical slow activity called the *theta* (θ) *rhythm*. This component of the hippocampal EEG, first described by Jung and Kornmüller in 1938, is constructed by summed intracellular potentials (Green et al. 1961), and must be present for the hippocampus to function. The θ rhythm is generated in the hippocampus (Green et al. 1960) from a pacemaker input located in the medial septum (Petsche et al. 1962). Lesions blocking the projection from the septum (Green and Arduini 1954; Becker et al. 1980) or reversible inactivation with local injections of procaine (Mizumori et al. 1989b) produce behavioural deficits akin to those resulting from full hippocampal lesions.

The striking transition to the sinusoidal θ rhythm from the form of EEG called *large irregular activity* (LIA) (Routtenberg 1968) and the involvement of the θ rhythm in hippocampal function have led to numerous suggested behavioural classifications of the EEG (e.g. Bennett 1975; Gray and Ball 1970; Berry and Thompson 1978) and to efforts to correlate variations in the θ rhythm frequency and amplitude to observable characteristics of the animal's behaviour (e.g. Whishaw and Vanderwolf 1971; McFarland et al. 1975; Fontani and Vegni 1990).

During periods of immobility there is an occasional large amplitude signal, called a *sharp wave*, that coincides with a synchronised burst of cell activity. There is disagreement in the literature about which hippocampal neurons are active during LIA. O'Keefe and Nadel (1978) observed that LIA amplitude varies with depth and undergoes an inversion just below the pyramidal layer. The anatomical correlation of sharp waves was verified and mapped extensively by Buzsaki (1986). At the same time as a sharp wave, there is a 100-200 Hz ripple pattern in the pyramidal layer (O'Keefe 1976).

The behaviour patterns that correspond to the hippocampal θ rhythm vary between species, but for a few behaviours there is nearly general agreement (for a review, see Robinson 1980). In rats, Vanderwolf (1969) found that θ is not normally present during immobility, but it can be induced by midbrain stimulation or with certain drugs such as ethyl urethane. Based on results from a series of experiments, Vanderwolf and colleagues proposed that the θ rhythm is correlated with *voluntary* movement, but not *automatic* movements.

The correlation between the θ rhythm and movement was a central part of the evidence for the cognitive map model (O'Keefe and Nadel 1978). However, they proposed that the θ rhythm coincides with displacements rather than all types of movements. An interesting example is the righting reflex, which is classified as an automatic movement, but is associated with the θ rhythm. In the cognitive map theory the θ rhythm is a clock that gates the activity of place cells.

The relationship of the θ rhythm to normal function of the hippocampus can be studied by measuring the temporal relationship between phase of the EEG and the activity patterns of hippocampal neurons. It was already pointed out, in Section 3.2, that the relationship between EEG and cellular activity is part of the classification of hippocampal cell types. Also, both theta and complex spike cells have been reported to fire in correlation with the phase of the θ rhythm (Sinclair et al. 1982; Buzsaki et al. 1983; Fox et al. 1986; Otto et al. 1991). O'Keefe found that theta cell firing is correlated with either the low-high or the high-low phase of the EEG. Two independent studies of the phase correlation of complex spike cells (Buzsaki et al. 1983; Fox et al. 1986) found that the spikes occur with a higher probability at a particular phase. However, the value for the most likely phase for complex spike activity differed by over 100° in the two studies.

The synchronisation found between hippocampal θ rhythm and complex spike cells should be evident in place cell firing. As described above, complex spike cells increase their firing rate with increased speed of locomotion (McNaughton et al. 1983b). If these two results are true, then the frequency of the rhythm should increase with the rat's speed of movement. In one of the early studies, Whishaw and Vanderwolf (1971) found a brief (100-200 msec) correlation between the running

speed of a rat on a motorised treadmill and the θ frequency, but there was no long-lasting correlation. In the same study, the initial θ rhythm frequency was shown to correlate with the height of a jump. The largest frequency occurred at the beginning of the jump, and it decreased during the jump. From these data they concluded that the frequency of the θ rhythm is correlated with vigour. A more recent study found that, during jumping, the instantaneous θ rhythm fequency correlates better with the initial speed than with impulse or acceleration (Morris et al. 1976; Morris and Hagan 1983).

In rats the hippocampal θ rhythm can be recorded only in CA1 and the dentate gyrus, and not in CA3. There is evidence, however, of θ rhythm in the activity of single cells in CA3. The θ rhythm is also found in the subiculum and the entorhinal cortex. Using a grid of electrodes, Bullock et al. (1990) measured the phase correlation along the pyramidal layer. They found long-range correlation that stopped abruptly at the subiculum.

The amplitude and phase of the θ rhythm change with position of the recording electrode perpendicular to the cell layer. In the rabbit, the phase of the θ rhythm undergoes an abrupt reversal below the pyramidal layer, whereas in the rat, the phase changes gradually.

Recording of the θ rhythm poses several difficulties. Much of the recording is differential, in which one electrode is stationary in the dentate, while the other electrode is placed in the test location. This results in the problem that the waveforms will add when in phase and will cancel when 180° out of phase. If the recording is single ended, then more noise is recorded. Several other oscillations can be misinterpreted as the θ rhythm, including thalamo-cortical spindles during quiet sitting and jaw muscle movement. The difficulties in recording the rhythm may account for some of the reported differences.

Most of the studies of hippocampal θ rhythm have been performed using acute preparations. From the response of the θ rhythm properties to pharmacological manipulation, two different forms have been identified (Kramis et al. 1975; Vanderwolf 1975). One form of the θ rhythm is present during immobility and can be

blocked by atropine, but the second form of the θ rhythm is resistant to atropine. These two forms of the θ rhythm may have different roles in hippocampal function.

3.11 Summary

This review has examined the experimental results that provide the current view of place cell properties, in the context of methodological issues. The properties are divided into the static characteristics of cell firing, and the results from manipulations to the environment. Setting aside the more difficult problem of dynamic environments, there are substantial variations in the reported properties in "unchanging" environments. A significant part of this variation may be due to the difficulties of extracellular recording in freely moving animals. Also, measurement of several of the static properties, including tests of the holistic firing hypothesis, and the distribution of place cells within an environment depend on simultaneous, accurate recording from several place cells. These properties are very important for the development of a neuron level model of the cognitive map.

The stereotrode method provides both improved isolation of single neurons and simultaneous records from several cells. In the stereotrode paper (McNaughton et al. 1983a), McNaughton and co-workers clearly point out that four electrodes in a tetrahedral arrangement can improve on two electrodes.

In the present research a four electrode recording method is developed, called the *tetrode* (Chapter 4). A new recording apparatus has been constructed in which all of the signal processing stages have been improved. This method is used to re-examine the properties of place cells in several different environments (Chapter 5). Particular attention is paid to the shape of the firing field of place cells, the homogeneity of place cells and their distribution within an environment.

In addition, as a test of the cognitive map model, the relationship between the rhythm and the speed of movement is re-examined (Chapter 6). As discussed above, the prior measurements were made in a treadmill, and without the benefit of computerised methods. Finally, the temporal relationship between the activity of place cells and the hippocampal rhythm is examined in more detail than was possible in prior published work (Chapter 7). The impact of these new data on the cognitive map model is discussed in Chapter 8.

Chapter 4: Methods

4.1 General Methods

Surgery

Lister hooded rats were implanted with one or two microdrives under deep surgical anaesthesia. Following induction with 3-4% Halothane in nitrous oxide/oxygen, rats were mounted in a stereotaxic frame and maintained on 0.5-2% Halothane in nitrous oxide/oxygen throughout the operation. Depth of anaesthesia was adjusted to keep the heart rate at 300-360 beats/minute. The skull was exposed and four or five 2 mm holes were drilled with a trephine drill to take stainless steel screws machined to a close tolerance. One or two 3 mm holes were drilled for the electrodes. Single microdrives were located over the left hippocampus (3.0-4.5 mm posterior to Bregma; 2-3.5 mm lateral). With two microdrives, both hemispheres were used. During the implant procedure the microdrives were held in micromanipulators and the electrodes inserted into the neocortex above the hippocampus through the cut dura. The deepest electrode was typically left 1-1.5 mm below the surface of the neocortex. The feet of the microdrives were attached to the stainless steel screws with dental cement. The wound margins were dusted with a topical antibiotic (Cicatrin, Wellcome), and a thin layer of dental cement covered the skin to close the wound and prevent infection. Postoperative analgesia was provided by buprenorphine (Temgesic, Reckitt and Colman 0.15 cc, i.m.). Each animal was allowed to recover for several days before recording began, and no data were collected until at least 10 days after surgery.

Microdrives

One or two small lightweight, laboratory-built microdrives were permanently implanted in each rat. The microdrive is a further development of one described by Ainsworth et al. (1969), and it is shown in Figure 4.1. Each microdrive contained two bundles of electrodes (tetrodes), one 300-500 μm above the other, in a 30 gauge cannula. One full rotation of the mechanical drive mechanism produces a vertical movement of 200 μm without rotating the cannula or the tetrodes.

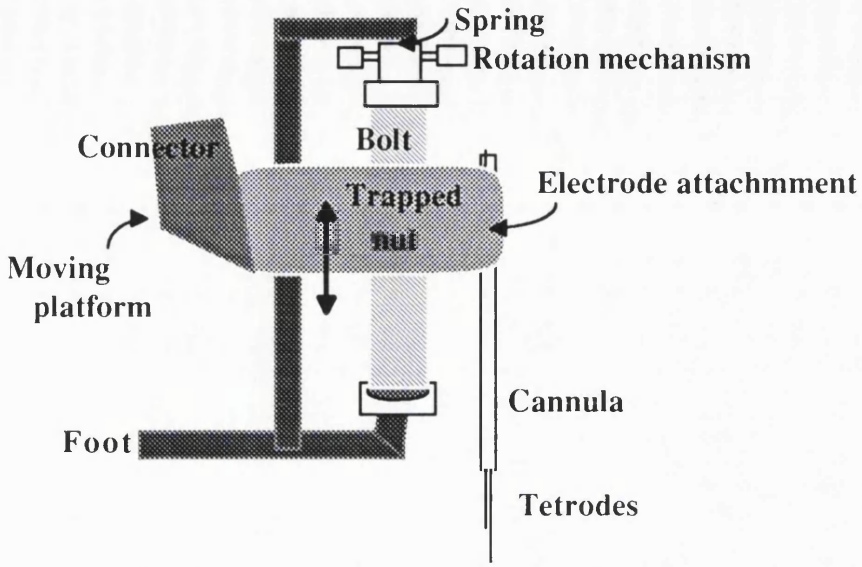

Figure 4.1 Schematic layout of the laboratory-built microdrive, which was used in all of the experiments. The bundles of electrodes that sit in the cannula are electrically attached at the top of the cannula to wires embedded in the moving platform. When the rotation mechanism is turned the platform moves up and down, along with the connector and the electrodes in the cannula.

The microdrive provides both easily controlled smooth movement and structural stability. The moving platform is constructed from a small nut embedded in dental cement. The platform is moved by rotating a bolt that is held in place by a steel spring. A stainless steel post, parallel to the bolt, holds the bolt and spring in place while providing structural support and a mechanism for attaching the microdrive to the skull. The stripped end of each electrode is wrapped around a metal post on the microdrive and is held in place by metallic epoxy. The recording ends of the two tetrodes extend from the lower end of the cannula. Typically, the longer tetrode extends 3.5 mm.

Throughout the recording from each rat the cannula remains outside the brain. This minimises tissue damage and reduces the time lag required for the electrodes to settle after they are moved. A stainless steel sleeve, which makes a sliding contact around the cannula, protects the segment of the two tetrodes that extends below the cannula and above the surface of the brain. The wires, attached to

the electrodes, end in a 9 pin connector, which is connected to the headstage (described below) during recording.

Tetrodes

The tetrode (Recce & O'Keefe 1989; Recce et al. 1991) is an extension of the stereotrode concept (McNaughton et al., 1983a). Tetrodes are twisted bundles of four strands of teflon-coated 25 μm diameter platinum-iridium (90%:10%) wire (California Fine Wire Inc.). The tips of the electrodes are slightly displaced (< 20 μm) from each other along the length of the bundle. Figure 4.2 contains a photograph of a tetrode tip as seen by a scanning electron microscope (1000x).

Figure 4.2 Scanning electromicrograph of the tip of a tetrode. Note that the tips are flat and are displaced from each other along the axis of the electrode (1000x).

Each tetrode is constructed from a 10-12 cm length of wire. The two ends of the wire are taped together. The wire loop is twisted once and the two resulting loops are threaded over an open-ended horizontal post. It is held in position, under tension, by a weight suspended by a hook that is passed through the two wire loops. The four strands are wound together under tension by rotating the suspended weight 15 turns

for every centimetre of electrode length. While the twisted strands are under tension the Teflon coating is stripped from the upper end (2 mm) of each of the four wires. The lower end of the wire bundle is cut at a slight angle with sharp scissors under a microscope to form a tip with four exposed surfaces arranged in a rectangular or diamond-shaped pattern (Figure 4.2). The electrode tips are separated by the thickness of the Teflon insulation (2-3 μm thick). The electrode bundle is then inserted into the cannula of the microdrive and electrically attached. Each stripped electrode is wrapped around a metal post and sealed with silver epoxy. A coat of varnish is used to insulate and protect the electrode attachment site.

When located in the cell layers of the hippocampus, tetrodes provide four simultaneous and independent measurements of the extracellular spikes from the same set of neurons. Depending on its spatial relationship to the tetrode bundle, each neuron contributes an action potential to some or all of the four channels. Figure 4.3 shows a schematic diagram of the technique and examples of the different recording patterns obtained from two complex spike cells. These patterns of action potentials are used to discriminate amongst the multiple spikes simultaneously recorded by the tetrode.

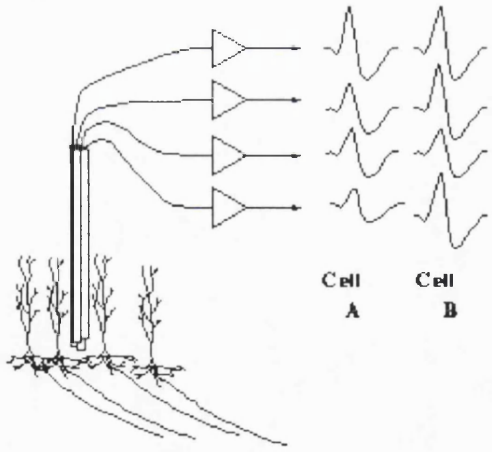

Figure 4.3 Schematic diagram of the four-channel tetrode among four pyramidal cells. The signal from each channel is led to the gate of a separate dual FET. The second input to each gate comes from a single channel of a different tetrode (not shown). On the right a set of action potentials that might be obtained from two different cells are show.

If the difference in amplitude of the action potential on the two electrodes of the stereotrode is due to a decrease in signal with distance, then from a geometrical

point of view it is reasonable to assume that increasing the number of electrodes will increase the performance. In three-dimensional space with an unsigned distance metric, four electrodes should be the optimal number.

To make this clear, consider the assumption that the extracellular medium is truly ohmic and isotropic. In this case the action potential voltage uniformly decreases with the inverse square of the distance (Rall 1960). If the electrode tip is treated as a point detector, all the neurons on a spherical shell surrounding the electrode tip will produce spikes that have the same amplitude. However, a second electrode (near the first) measures a different voltage for most of the spikes in the spherical shell centred on the first. Since the intersection of two spherical shells is a circle, only the neurons lying on this circle of intersection will have the same amplitude on both electrodes. These neurons are not separated by the stereotrode. If a third electrode is added (again near the other two), then there are only two points in space that cannot be distinguished. They are at the intersection of the circle (from the first two electrodes) and a third spherical shell. In theory, a fourth electrode uniquely identifies the location of the source.

This justification for four electrodes has assumed that the extracellular space is isotropic, which is known to be invalid. However, this assumption is not critical. The only requirement is that the action potential signal monotonically decreases at some rate in all directions from the source. If more electrodes do not increase the resolution of unit separation, it is still worth testing, since we are confident with the results only when a method surpasses requirements.

If the decrease in amplitude of action potentials, as a function of distance, is known in all directions away from the source, then the tetrode can be used to locate anatomically the position of the active neuron. Of course, if the decrease in amplitude with distance is too rapid, then there is the additional problem of limited range. Neurons further away from the tetrode can be distinguished only if they can be detected. This method could completely resolve the question of topographic firing in place cells.

Data collection

During recording, a headstage is mechanically and electrically connected to the microdrive. The headstage includes two epoxy encapsulated quad surface mount JFET-input operational amplifiers (TL074 Texas Instruments), a small DC lamp, a metal alligator clip and approximately 3 m of twisted pair hearing-aid wire. The operational amplifier has an RC high pass filter at the front end (AC coupling), and acts as a voltage follower. The amplifier circuit drives the cable, to the recording equipment, with the voltage difference between the electrode and a ground level taken from a skull screw. The operational amplifier has been selected for its very high input impedance and its low leakage current (<10 nanoamps).

The headstage cable also includes the power supply voltages for the amplifiers (± 12 V) and a separate power and ground for the DC lamp. The alligator clip provides mechanical contact between the headstage and the microdrive. The mechanical contact is intentionally separated from the electrical connector in order to avoid recording electrical artefacts, which can occur due to intermittent contact between the parts of the connector if it is mechanically stressed. The lamp is used for tracking the animal's location (discussed below).

The eight potentials (four from each of the two tetrodes) are led through the hearing-aid wires to purpose-built differential amplifiers and filters (passband 400 Hz - 5.4 kHz). Each of the four channels of one tetrode is fed into one input of a differential amplifier. None of the signals are multiplexed, each electrode has an independent wire from the headstage to the amplifiers. The signals for the other input are derived from one of the channels of the other tetrode to provide a common rejection signal to minimise noise, movement and chewing artefacts.

The programmable amplifiers have three stages. The first stage is a differential amplifier with a fixed gain (400 x). Following this, the signal is filtered with a fourth order high pass Bessel filter with a cut-off at 600 Hz and a second order low pass Bessel filter. In the final stage the gain is independently programmable for each channel (range 1 to 100,000 x). The reference for each electrode signal can be selected independently as the headstage cable is divided into miniature BNC cable for each electrode. The basic system includes four differential amplifiers, each of

which contains a filter module. The amplifiers and filters are battery powered to minimise the power line (50 Hz) pickup.

Each channel is continuously sampled at 20 or 40 KHz., with 12 bit resolution. When a spike event is detected (as a voltage above a set level on any one of the channels) the sampled points around the event are stored to yield 25 or 50 points for each of the four channels for each spike event. Each spike event was stamped with the time since the beginning of data collection and the animal's location at the time (see below). Data were usually collected in blocks of one, two or four minutes and stored on a local hard disk.

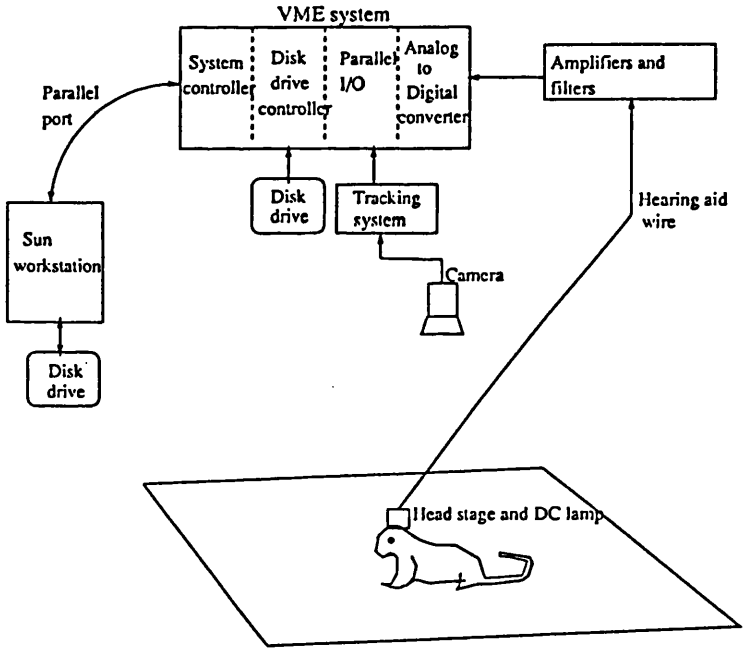

Figure 4.4 Schematic diagram of the recording apparatus. The signals are amplified in a headstage amplifier that is connected to the implanted microdrive and pass along the hearing aid cable to a bank of battery operated differential amplifiers and filters. The EEG is also filtered by Neurolog amplifiers. The amplified signals are fed into the ADC and recorded by the Force CPU onto the local disk storage. The APAL TTL-I/O board is used to read the animal's location from a camera based tracking system.

During the recording of hippocampal unit activity, the animal's location (or more precisely, the location of the DC lamp attached to the headstage) was monitored with a television tracking system (SP111, HVS Image Analysing, Kingston, UK). The location was monitored at video rate (50 Hz) and with a resolution of 256 x 256 pixels. The effective resolution of the y-axis is reduced to 128 pixels by the video interleave of alternate scan lines. These data enabled off-line analysis of the influence of the animal's spatial position and velocity on hippocampal unit activity. Figure 4.4 contains a schematic diagramof the full recording apparatus.

The EEG data were taken either from an individual channel of the tetrode or by adding the signals from all four channels of a tetrode. Only single ended recording was used. For some recordings the data were filtered using Neurolog variable filters (Neurolog System, Digitimer Inc., Welwyn Garden City, UK) but for most of the cells purpose-built EEG amplifiers and filters have been used.

In the days following recovery from surgery, the electrodes were moved down into the CA1 or CA3 pyramidal cell layers while the animal sat on a small 40 cm^2 holding platform. Once a suitable recording location was achieved, the electrodes were usually left in place for at least one day before data collection began in order to ensure maximum recording stability. The pyramidal layer was located by using the presence of 100-200 Hz ripple activity (O'Keefe 1976).

Behavioural testing

Each rat was weighed daily and given sufficient food to maintain weight at 90% of free-feeding weight. A 12 hr dark/12 hr light cycle was maintained with lights off at 3 p.m.. Most recordings took place between 2 p.m. and 8 p.m.. Units were recorded during a number of different behavioural tasks.

Four rats were trained to run back and forth along the surface of linear tracks to obtain a reward. The tracks was 1.5 m long and either 4.6 cm or 15.2 cm wide. Reward in the form of sugar-coated cereals or sweetened rice was given at each end. Rats were trained until they ran with a consistent pattern from one end to the other. During the recording of some cells, the food reward was varied between several

locations in one of the goal areas. This introduced some variability in run speed and increased the dissociation between temporal and spatial firing correlates.

Further data were collected from eleven rats as they searched for randomly distributed sugar coated cereal or drops of chocolate milk in one or more of a set of environments. The environments used included: (1) a small open 40 cm^2 platform, (2) a circular platform surrounded by black curtains and polarising extramaze cues, (3) a walled 120 cm^2 box, and (4) an elevated plus maze.

Additional data were taken from two rats that had been trained on an elevated plus maze in a cue-controlled environment. For further details of the procedure and response of place units in this situation, see O'Keefe and Conway (1978, 1980) and O'Keefe and Speakman (1987).

Data analysis

For off-line analysis, the data were transferred to Sun SPARC workstations. A new suite of data analysis programs was developed, which includes new methods for isolating the activity of single neurons, measuring the temporal interaction of simultaneously recorded neurons, and examining the spatial activity patterns. In all the experiments the activity patterns from multiple neurons were separated using a new windows based applications program called *Sample* (available on request).

The type of additional analysis varied in each of the three studies, so it is presented with the results in Chapters 5-7.

4.2 Design decisions

Design of the filters

In general, three filters are required for hippocampal extracellular recording in freely moving rats, including: (1) a high pass filter to remove slow wave activity (e.g. theta rhythm in the hippocampus), (2) a low pass filter to remove high frequency noise, and (3) a notch filter to remove pickup from the power lines (50 Hz). The design of the filters significantly affects the performance of the downstream algorithms for sorting the activity of different single neurons.

Filters are best understood by their characteristics in the frequency domain. In general a filter changes both the amplitude and the phase of each of the sinusoidal components of the input signal. It is possible to design digital filters that have no attenuation in the passband and 90% rejection outside the passband. Unfortunately this is not the case with analog filters, which have less ideal characteristics.

All the published data from extracellular recording of hippocampal neurons are based on analog filters, and most of the data have been filtered using one of a small number of commercial filtering systems. If the roll-off of the filter used in extracellular recording is not sharp enough, then one of two problems could occur. If the cut-off is too near the signal band, some of its amplitude will be attenuated, which reduces the resolution of the method. Alternatively, if the cut-off is too far from the signal band, even a large rejection ratio may not help, since the power in the low frequencies is so high. In general, filters sacrifice either the sharpness of the frequency cut-off or the amount of distortion due to the phase shift of frequency components. In addition, if the passband is too narrow, then noise can be mistaken for action potentials.

Given the importance of filters, it is surprising to find that most of the published work in this area gives little detail, most often only the passband frequency, and occasionally the roll-off at the passband. Furthermore, in most prior work commercial filters have been used. Commercial filters offer flexibility (selection of characteristics using a single switch) at the expense of better performance. Good extracellular signal isolation requires a high order filter, that cannot be switched easily, as several high precision components need to be changed. In order to address this problem the filters used in this research were designed with a plug-in filter board.

Digitised waveforms

Digital recording has the advantage that it is much easier to manipulate, but there are two disadvantages. Depending on the sampling rate, digital recording is often lower resolution than analog recording and the anti-aliasing requirements can require a high end frequency cut-off that cuts into the signal band. Secondly, with sufficient sampling rates and voltage resolution, there are difficulties in managing the incoming

data. In the four-tetrode configuration of the recording apparatus, data are collected at 200,000 samples per second, or equivalently 400,000 bytes per second. At this rate, given a disk drive with sufficient data rate capacity, less than five minutes are required to fill a 100 Mbyte disk. In fact, this data rate is near the bandwidth limit of existing computer buses. For this reason many methods try to reduce rapidly the information content or to avoid digitisation altogether. In one approach, used by Gerstein et al. (1983), the data are digitised for only the first 60 seconds, from which a set of threshold measurements is made, and then after this time only the threshold-based classification of the signals is kept, instead of the entire waveform.

The data collection software is designed to reduce the data rate by keeping only the segments of the data that contain an action potential. After the data are digitised, an independent software threshold is applied to each of the four electrode channels, and if the signal is above the threshold then one millisecond of data is saved from a simultaneous segment of each of the channels. Each of the saved data segments is time-stamped. The saved time segment includes the signal 200 μseconds before the trigger. Some signal artefacts will generate false triggers, but since all these data are saved for post-processing they can easily be removed at a later stage.

The recording system is based on the Motorola VME bus (Figure 4.4), and data are collected with a Burr-Brown programmable analog to digital converter (MPV952). The data collection process is controlled by a FORCE 68020 (CPU30) based processor board, and data are logged to a local disk drive (Micropolus 1351) with the assistance of a FORCE disk controller card (ICSI-1). The system also includes a board with 64 programmable parallel input/output lines (APAL from ELTEC). This board is a general-purpose interface used to read the animal's spatial position, to program the amplifiers, and to transfer data to a SUN Microsystems computer for analysis.

The recording system has been designed for off-line analysis, and therefore the data collection and data analysis computers are fully decoupled. This configuration has the disadvantage that large volumes of data must be managed for longer, but on the other hand it has several advantages. In the first place, the two computers are selected for peak performance in their domain rather than

compromising and finding a single machine for both functions. Secondly, the decoupling allows analysis and data collection to be carried out in parallel.

All the software for data collection is written in "C"; it is compiled on a SUN workstation and transferred using Motorola S-records to the Force CPU card. The second computer in the recording system is a SUN Microsystems workstation running the UNIX operations system that is used for data analysis. The data are transferred to the workstation at 2M words per second over a set of parallel lines from the APAL board to an MVME 952 (Motorola) added to the SUN computer. Modifications were made to the kernel of the UNIX operating system to support high priority fast data transfers. Data analysis was carried out using two software packages developed for this research, *Sample* and *Xv_eeg*.

Chapter 5: Properties of Hippocampal Place Cells

5.1 Introduction

In Chapter 3 the published properties of hippocampal complex spike cells are critically reviewed. There is considerable support for the existence of place cells, but little agreement on the details of their properties. These properties can be divided into two groups: (1) the characteristics that can be measured in static environments, and (2) the way that the representation changes when modifications are made to the environment. The properties of place cells in static environments can be further subdivided into: (1) the fraction of hippocampal complex spike cells that have place fields, (2) the spatial size and shape of place fields, (3) the consistency of the firing pattern with repeated entries of the rat into the place field, (4) the fraction of place cells that code for multiple regions in one environment, and (5) the variation of these properties from one cell to another and from one environment to another. It is perhaps most surprising to find little agreement in the literature on the properties of place cells in static environments.

This chapter begins with a description of the importance of these static properties in the process of unravelling the coding scheme used for representing space in the activity patterns of place cells. It is argued that the data available are not consistent enough to select among the models, and that the inconsistencies present in the literature are in part due to limitations in the methods used for recording extracellular potentials in freely moving animals. The methods for isolating single cells, based on the use of a tetrode, are detailed in this chapter. This is followed by results from experiments that demonstrate that the tetrode has a greater capability for isolating single cells than previous methods. The tetrode-based measurements of the static properties of place cells are reported from recordings in five different environments: (1) a linear track, (2) an open square platform, (3) a closed walled box, (4) an open circular platform, and (5) a plus-shaped open maze. Finally, it was suggested in Chapter 4 that the tetrode may provide a method for anatomically localising active place cells, and results from initial tests of this idea are presented.

Using place cells to represent spatial location

Many different schemes can be constructed to describe how the place cell activation patterns are combined to construct and use maps of space. Variation among these schemes begins with assumptions about the properties of place cells in static environments. For example, there is substantial evidence that more than one place cell is active in one spatial location, but it is not clear what is gained by the use of many cells. Does each active place cell have a different role? Are many active to achieve higher spatial acuity, or are they just redundant? Or perhaps the number of active cells is a fixed property of a spatial memory function? In this section a small number of schemes are discussed, and particular attention is paid to how they can be tested by accurate measurements of the properties of place cells in static environments.

One relatively simple scheme is to suggest that place cells provide a *value-coded* (Ballard 1987) local representation of space, which is analogous to the current model for the receptive fields of neurons in the visual cortex (Hubel and Wiesel 1977). In this scheme each place cell represents one specific location. The firing pattern of place cells would be expected to have a single peak, and the spatial firing rate distribution should be relatively constant among cells. Also, in this scheme the absolute firing rate is not used to code information, so it might be expected to be the same for all cells. In this view the spatial density of place fields and the size of each place field would directly correspond to the animal's spatial acuity. In the extreme, the most precise spatial coding would be achieved by place cells that had a spatial firing function shaped like a delta function. Furthermore, place cells would have larger place fields in regions of space that did not contain sufficient sensory information to allow precise localisation. This view would suggest that the size and shape of place fields would be consistent for different rats in a particular region of space.

Alternatively, place fields may provide a *distributed* code for locations. In one view each place cell could have a repeatable but arbitrarily shaped spatial firing rate function, which could be larger than zero at all locations in the environment. With this coding scheme each position in space corresponds to a unique firing rate for a large population of place cells (Georgopoulos et al. 1988). This scheme is less

affected by variation in the size, shape and firing rate among place cells. On the other hand this scheme depends on place cells that have a highly repeatable spatial firing rate distribution. In this view the spatial acuity would be more difficult to read from single cell firing properties, and instead would depend on the number and types of the spatial firing functions of the active set of place cells. However, if this scheme were correct it would still be possible to determine which regions of space are associated with higher or lower spatial acuity.

In both of these representation systems (value-coded and distributed) the time dimension of neuronal firing is not explicitly used. A model for explicitly using the time domain to represent information was suggested by von der Malsburg and Bienenstock (1986). In this view the binding of the attributes of an object occurs by simultaneous firing of neuron-based feature detectors. Evidence to support this type of process in the visual cortex was described by Gray and Singer (1989). Since place cells have a relatively low firing rate (Fox and Ranck 1981), and their firing is strongly linked to the phase of the θ rhythm (see Chapter 7), the hippocampus might be a good candidate for this type of representation. This type of model can be tested by analysing the temporal correlations among simultaneously active place cells.

O'Keefe (1989) proposed a model for how place cells are used to construct a map that gives a specific role to the time domain. In this model, place cells are computing precise coordinate transformations to convert poly-sensory observations of the world from an ego-centric space (centred on the animal's head) to an allocentric (world-based) map of space. In this model, the θ rhythm is explicitly used as a sine function for converting from polar coordinates to cartesian coordinates, and any timing error in the phase relationship between place cell activity and the θ rhythm corresponds to an error in the judged distance to a cue.

In addition to representing spatial locations, it has been demonstated that the place cells are part of a spatial memory system (O'Keefe and Speakman 1987). Place cells retain spatial firing in the absence of cue information. The first and clearest model for memory function in the hippocampus was proposed by Marr (1971). The value-coding scheme fits well into associative memory models that have been proposed to describe the function of the CA3 region (Marr 1971; McNaughton and Nadel 1990). Marr's model describes in detail a process, called *pattern completion*,

in which general memory patterns could be reconstructed from a small seed pattern. By reversibly inactivating the inputs to the hippocampus from the septum, Mizumori et al. (1989b) have described evidence for this pattern completion process. They found that place cells in the CA1 region still had spatial firing properties, whereas the activity rates of cells in CA3 were significantly suppressed, which suggests that the seed pattern projected in the lower fring rate from the CA3 region is completed in the CA1 region.

The storage capacity for associative memory models greatly depends on the format or representation of the data that are being stored. In a neuronal assembly which follows the Hebb rule (1949), the capacity is highest if the fraction of cells that are active at any one time (or in any particular spatial location) is small. The active fraction should be less than 5% in a randomly connected cell assembly of the size and connectivity of the CA3 region (unpublished analysis of Gardner-Medwin 1976). The storage capacity also depends on the amount of overlap between remembered patterns.

The simplest way in which an associative memory can be used to represent a set of spatial locations is by encoding each location with an active subset of place cells. When used as a memory for spatial locations, the overlap of stored patterns depends on the size of place fields (smaller is better) and on the number of times that the same neuron is part of the active subset corresponding to a location in space. If a neuron is part of two active subsets in a single environment, then it is treated as a double place field (see section on Multiple place fields, p.52) Furthermore, Gardner-Medwin (1976) has reported that significant improvement in the storage capacity of an associative memory can be achieved if the fraction of cells in each memory event is held constant, and if a gradual recall process is followed. This type of associative memory makes specific predictions about the properties of place cells in static environments, and can be tested by simultaneous recording from many place cells.

For example, if an efficient associative memory is being used, there should be a homogeneous distribution of place cell activity. Equivalently, there should be the same number of place cells representing each spatial location. It is important to note that it is not obvious how a homogeneous distribution could be constructed from

sensory inputs. In a new environment the centres of place fields might be randomly located in two dimensional space. An additional mechanism then needs to be found to develop a homogeneous distribution, perhaps during initial exploration. Secondly, if the associative memory model is correct, quantitative predictions can be made about the probability of finding multiple place fields. Finally, if the place cells in the CA3 region are participating in a progressive recall process, then there should be evidence in their activity patterns, which may involve the use of the θ rhythm to control this recall process.

While efficient spatial memory may require highly localised place fields and small active subsets of cells for each location in space, navigation models may have exactly the opposite requirements. Burgess et al. (1993) have demonstrated a navigation model that uses hippocampal place cells and the orientation selective cells found in the postsubiculum (Taube et al. 1990a,b). In this model, place cells with large and overlapping place fields provide a means for associating the animal's current location with the goal location. In this model, like the distributed representation described above, the firing rate distribution for place cells must not vary significantly with time.

Measurements of the size and shape of place fields, and the persistence of these properties will help constrain the choice of model.

5.2 Methods

In these experiments data were recorded from the dorsal hippocampus of freely moving rats using tetrodes. The general methods have been described in Chapter 4. This section gives further detail on the methods used for isolating the activity of individual neurons from others that were recorded simultaneously. Also included are methods used to measure the size and shape of place fields and the firing rate.

Isolating the activity patterns of single neurons

Each set of tetrode data from a recording session was separated into several clusters by selecting those features of the waveforms that maximally distinguished one set of spikes from the others. It was assumed that each cluster represented the action

potentials from a single neuron. In the first stage of analysis, artifact and false spike triggers were removed, using the sum of the squares of the voltage difference between each waveform and either an idealised spike or the average waveform from a clearly separated cluster. This criterion also proved effective for separating clusters from each other. Other commonly selected waveform features were the peak to peak amplitude and the voltage at a particular time after spike onset.

In addition, automatic clustering was carried out on some of the data, using the k-means algorithm (McQueen 1967). For automatic clustering, each spike was treated as a 200-dimensional vector, in which the components are the digitised voltages in the four channels after spike onset. This algorithm requires an initial guess for the number of clusters in the data. For each of these clusters, a randomly located vector is defined to be the centre of the cluster. Briefly the algorithm is an iterated two step process. During the first step spikes are assigned to the cluster that is the shortest distance away. The distance is computed between the spike vector and each of the cluster centres. In the second step the location of each of the cluster centres is changed to be the centroid of all the spike vectors that are members of the cluster. The performance of the clustering process can be measured by tracking the decrease of the mean distance of the spikes within a cluster to the centre of the cluster.

The performance of algorithms for isolating extracellular activity of single neurons (clustering algorithms) is greatly increased if higher order features of the waveshape are used in addition to the digitised voltages. In the rat hippocampus, this is useful for distinguishing theta cells and complex spike cells, but it is also sometimes useful for distinguishing between complex spike cells.

Shape of place fields

Once a single spike cluster had been isolated, its firing pattern on the maze was examined. On the linear tracks, the width of the track was ignored and the place field was plotted as a firing rate along a single dimension. The 1.5 m track was divided into 64 bins of 2.34 cm each, and the number of spikes and the number of position points per run were calculated. Dividing the former by the latter gave an average firing rate per location on the maze.

In the two dimensional environments the firing rate maps are constructed by laying a 32 x 32 grid of square bins on the environment, calculating the number of spikes fired divided by the occupancy time for each bin, smoothing (a two dimensional low pass filter of the spatial frequencies in the resulting histogram), and linearly interpolating between each grid point. Each contour represents 10% of the peak firing rate. The smoothing is equivalent to averaging over the full possible set of bins in the environment, since no particular tesselation is better than another.

On the linear track the place field of each cell consisted of a single block of elevated firing rate over a portion of the track. Detection of the field boundaries, therefore, was reduced to the problem of specifying at which point in space or time this block had been entered and exited. Since this is akin to the problem of detecting a pulse in the time domain, we used a similar criterion: the point at which the firing rate exceeded or fell below 10% of its maximum value. The number of bins between these points x 2.34 cm was used as the field length.

It is difficult to measure the firing rate of the cells and the shape of the firing field at the same time. In order to measure the shape of the firing field properly it is important to remove all false positives (spikes from other cells misclassified as the current cell). However, if all false positives are removed, then the number of false negatives will increase, leading to a spurious reduction in the measured firing rate. The same problem occurs in the measurement of the firing rate.

5.3 Results

Data were collected from 17 placements of tetrodes in the dorsal hippocampus of 11 rats. Five of these data sets were recorded in the CA3 region, and the other twelve are from the CA1 region. The activity pattern of 71 putative single neurons, called *single units*, were isolated from these data sets. Based on waveshape and activity pattern 63 were identified as complex spike cells, seven as theta cells and one as unclassified. Four data sets were collected in a small open platform, two in an open circular arena, two on a plus-shaped maze, two in a walled square environment and seven on a linear track. On average, the data sets collected in the two dimensional environments (all except the linear track) contained a larger number of active cells (5.3) than the one dimensional linear track (2.4).

Tetrodes improve the resolution of extracellular recording

In the first stage of the analysis, the hypothesis that the tetrode increases the resolution for isolating single neurons was tested. In this analysis the data are examined to determine if all of the electrodes were required for isolation, or alternatively if they just produced redundant information already present in a subset of the electrodes. Qualitative examination of the cluster centres found in clear tetrode data sets suggests that they have isolated single cells that could not have been isolated with less than four electrodes. An example of this finding is presented in Figure 5.1.

This figure contains the spatial firing pattern (left panel) and the averaged waveforms (right panel) of five cells, which were recorded simultaneously from R42 with the tetrode. In the left panel of the figure a colour-coded box has been plotted at each of the locations in which the neuron produced a spike (spike location). Note that in this type of plot the spike locations are superimposed, and therefore it does not show the increased firing rate in the centre of place fields. In the right panel colour-coded waveforms are plotted for each of the four tetrode channels of each single neuron. These waveforms are the centre of the cluster corresponding to each neuron, or equivalently the averaged shape of all of the spikes of that neuron. For example, the activity of the neuron coded with the dark blue waveforms fired when the animal was at the locations marked by the dark blue squares at the top of the plus maze. Note the similarity between the dark blue and the light blue waveforms on channels three and four. The voltage difference between these two waveforms is always less than 10 μV, which is less than the 30 μV of noise found in the raw data. Therefore the two waveforms are essentially identical on channels 3 and 4, and could only be fortuitously separated on channel 1. If these data had been recorded using a stereotrode, constructed from channels three and four, then the activity pattern would be misinterpreted as a single cell with a double place field.

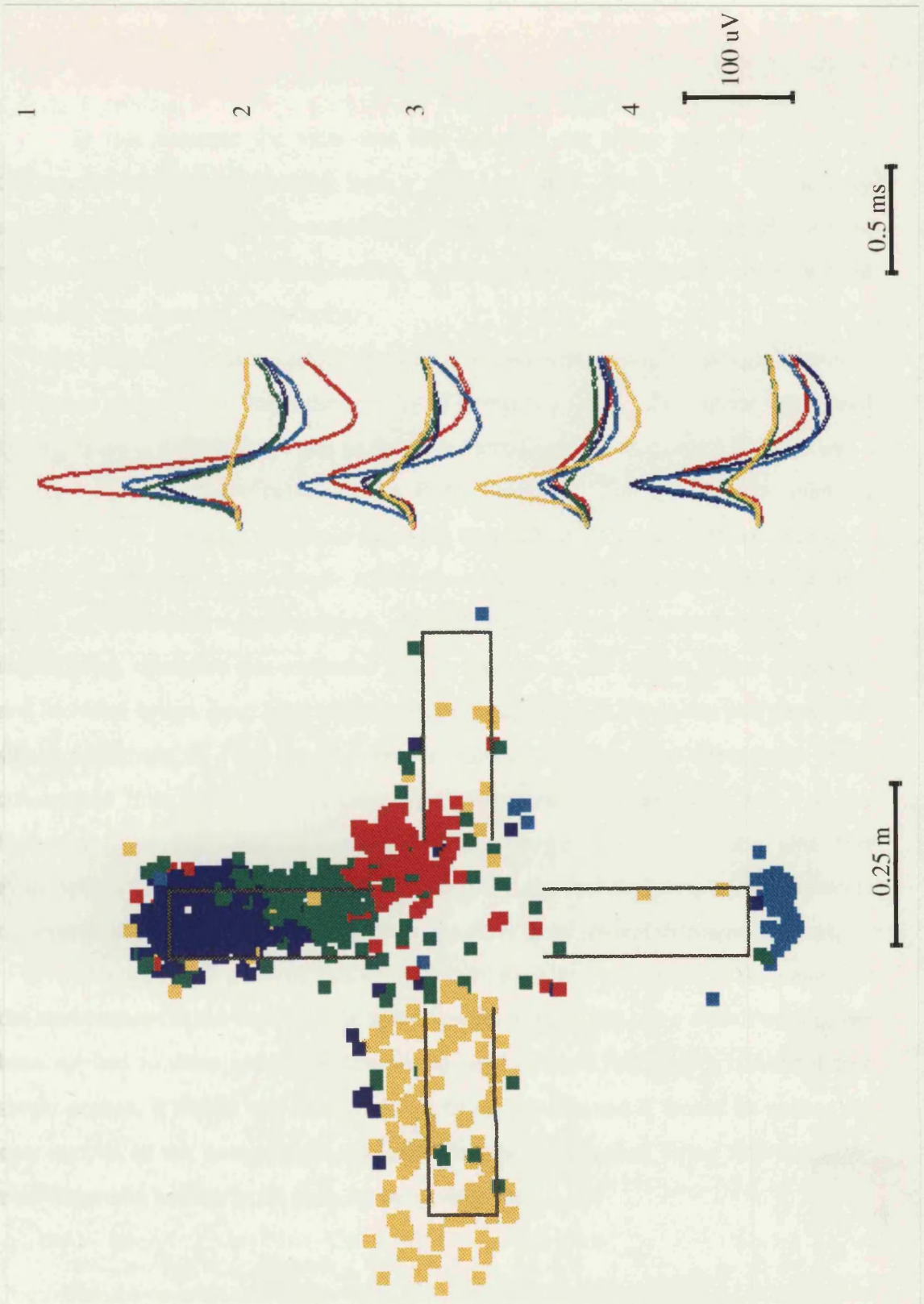

Figure 5.1 Spatial firing distribution and waveforms from tetrode-based recording of R42 on the plus maze. Each group of four colour-coded waveforms in the righthand panel of the figure is computed by averaging all of the spikes, on one channel of the tetrode, that were produced by a single hippocampal neuron. The same colour scheme is used to mark, in the lefthand panel, the animal's location at the time that each action potential was recorded. The coloured squares are printed following the sequence of spike firing in the recorded data. Note that in most cases more than two of the channels are required if the waveforms are to be separated using either the spike amplitude or shape.

In this example the view was that the data are either separated into two clusters or completely grouped into a single cluster. More likely, the activity attributed to one neuron is a complicated mixture of activity from several different neurons. This type of misclassification is more clear if the raw data are examined instead of the averaged waveforms.

Figure 5.2 is an example, which shows that a single voltage threshold applied to channel 3 includes the activity of several neurons. The upper right panel of this figure is a stereotrode plot of the signal amplitude on channels 1 (x axis) and 3 (y axis) of each of the spikes in the R164 data set. The line in this quadrant corresponds to a voltage threshold set using only the spike amplitudes on channel 3. The red highlighted points are the action potentials above the threshold, and the blue points are those below the threshold. It is clear, from this stereotrode plot, that the thresholding operation has excluded spikes that are in the cluster (false negatives) and included spikes from other clusters (false positives). In the lower two panels the signal amplitude of the same spikes is plotted in alternative stereotrode plots, constructed from other pairs of electrodes in the tetrode (channels 2 and 4 in the lower left panel, and channels four and one in the lower right panel). It is clear that those spikes that are above a voltage threshold on channel 3 correspond to elements of several different clusters, and therefore the activity of several different neurons.

The upper left panel of this figure shows the x and y position of the animal in the environment at the time that the spike was recorded. The same colour coding has been applied to these spikes. If the red spikes had been incorrectly attributed to a single neuron, it would still have a spatial firing pattern, and it would be coding for two regions in the environment. In addition, the background firing rate would be misinterpreted as high in all parts of the environment.

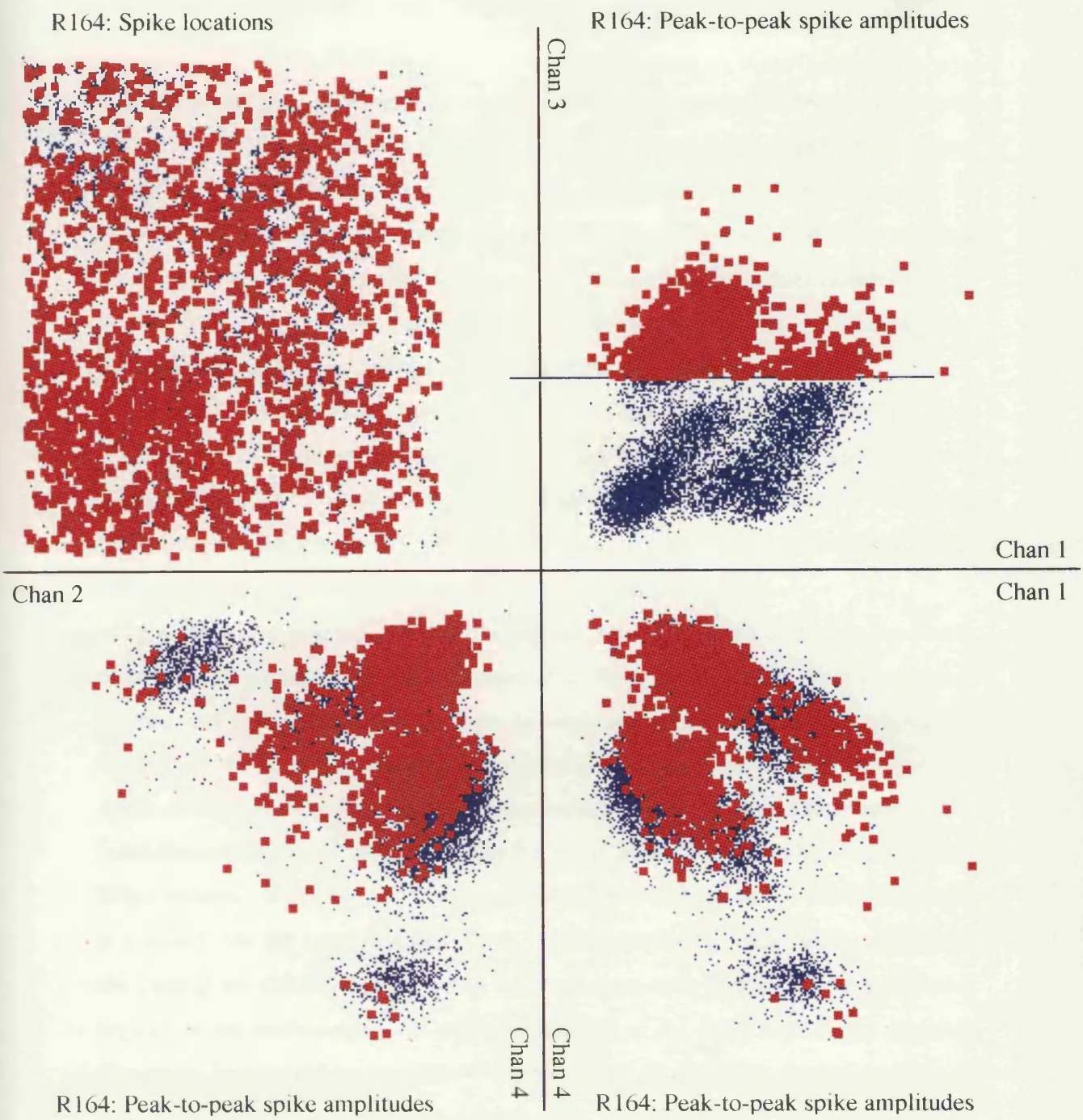

Figure 5.2 Spatial firing distribution for a "single neuron" that has been detected using one voltage threshold. In the figure, Channel 3 of a tetrode is used to illustrate the misclassification that can result when a single electrode and one threshold are used to identify the activity pattern of a hippocampal neuron. The upper righthand panel and both of the lower panels are stereotrode plots that have been constructed from two of the tetrode channels. The horizontal line in the upper righthand panel is the threshold level that has been applied only to Channel 3. The spikes that are above this level are colour-coded with red squares throughout the figure. Note that when the threshold level is viewed against the amplitude of the spikes on the second channel of the upper righthand stereotrode plot, it is clear that spikes from another cluster are incorrectly included and spikes that are part of the cluster are incorrectly excluded. The upper lefthand panel in the figure shows the spatial firing distribution that would be attributed to this neuron.

Figure 5.3 is an example of a case in which three electrodes are not sufficient. The panels are similar to those already presented in Figure 5.2, except that a different set of stereotrode plots has been selected (six are possible with four electrodes). In this example all three of the stereotrode plots that can be constructed using the first three electrodes have been used to separate the spikes into individual clusters. As in the last example, the clusters are separated by drawing lines in the stereotrode plots, but several lines are used and the lines can have any orientation.

Using the first three electrodes in this data set, five independent clusters have been isolated, and they are colour-coded in all the panels of the figure. The upper and lower righthand panels contain two stereotrode plots out of the three that were used to separate the clusters. Unlike in the prior example the clusters look well separated, but they still do not contain the activity patterns of single neurons.

The lower lefthand panel of this figure shows the result of adding the fourth electrode. The green cluster has divided into three parts and the blue cluster has divided into two parts. As in the prior example the upper lefthand panel shows the location of the animal at the time that the spike occurred. In this plot the blue and green clusters corresponded to two independent regions in the environment. The locations corresponding to the spikes in the green cluster have been highlighted using larger squares. When the two blue clusters are separated, using the fourth electrode, it is found that the two place cells have spatially separated place fields. Similarly, the three green clusters correspond to the three place cells that are active in different regions of the environment. In this case two out of the three regions are abutting. The green highlighted upper lefthand corner is two place fields. In this example, if only the first three electrodes had been used, the background rate would not be incorrect, but the number of multiple fields would be incorrect.

The place fields computed for the data set that was used in these examples, after the clusters are fully separated, are shown in Figures 5.8. In both these examples, complete separation of the clusters resulted in a bell-shaped firing distribution a background firing rate that was near zero everywhere except for a single region in the environment.

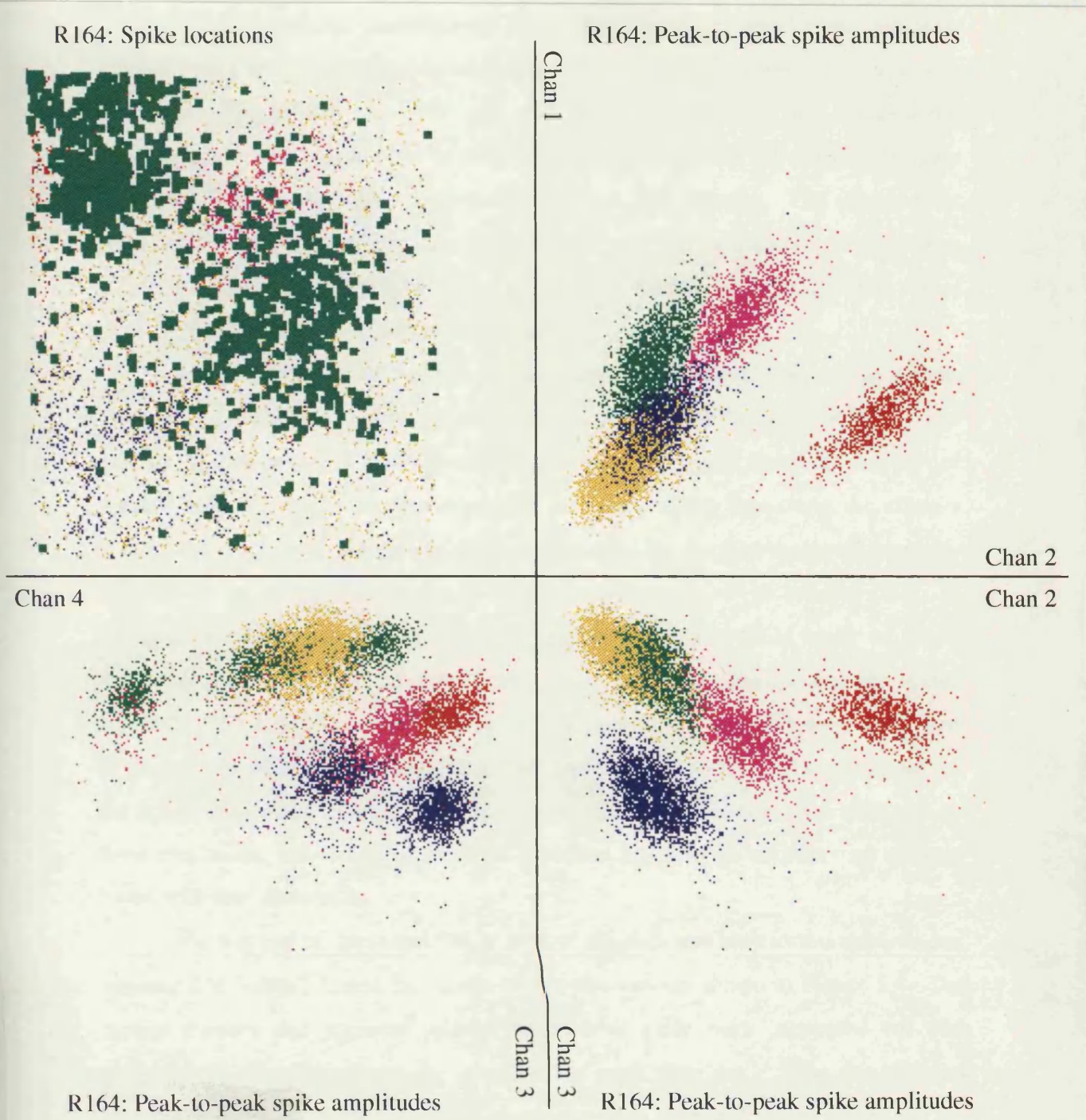

Figure 5.3 Results of cluster separation using only the first three out of four electrodes in the tetrode. The upper righthand and lower righthand panels contain two stereotrode plots that were constructed from the three channels that were used to separate the clusters. Five different clusters have been colour-coded. Note that if the fourth electrode is included, as shown in the lower lefthand panel, the green cluster divides into three separate clusters and the blue cluster divides into two parts. The upper lefthand panel is a highlighted view of the spatial firing pattern of the spikes in the green clusters. This double place field is actually three place fields of three single neurons.

To test more quantitatively the improvements in single unit isolation achieved with the tetrode, each combination of one, two, and three electrodes, was tested in each of the ten data sets that were recorded in two dimensional environments. For each number of electrodes, and in each data set, single amplitude thresholds were selected that best divided the data into clusters. The criterion for good separation of the activity of a single neuron was that, when compared to using all four electrodes, at least 90% of the spikes from the neuron were included and at most 10% of the spikes were from other neurons.

In each data set the number of electrodes was increased one step at a time. With one electrode it was always assumed that one neuron had been isolated. The number of neurons that had been isolated, called here the *apparent number* of isolated cells, increases if more electrodes are used. After separating the clusters with a single threshold, on each of the four channels, the fraction that were correctly isolated can be computed, and this is called the *actual number* of isolated cells. In the single electrode case, the actual number of isolated cells could never be larger than one, and would only be one if the cluster separation always met the above criterion. The apparent number and actual number of isolated cells were computed in the same manner using all subsets of two and three electrodes. The maximum for the actual number of isolated cells is not constrained in the same way with two or three electrodes, but clearly it must be less than the average number of clusters found with four electrodes.

The number of units isolated in each of the data sets used in this analysis are presented in Table 5.1, and the results of this analysis are shown in Figure 5.4. The actual number and apparent number of isolated cells were computed for each quantity of electrodes from the clusters in each data set. Then the different combinations of the same number of electrodes were averaged within a data set, and the mean of the averages from each data set is plotted in Figure 5.4. The plot in Figure 5.4 shows that both the apparent number and the actual number of single neurons increases as more electrodes are uesd.

These results suggest that with a single electrode, and the benefit of digitised waveforms, only 42% of apparent single neurons are actually single neurons. In some of these cases other methods could have been used to determine that the data

are not well isolated. Also, with smaller tipped electrodes better isolation might be found, but perhaps in exchange for stable recording.

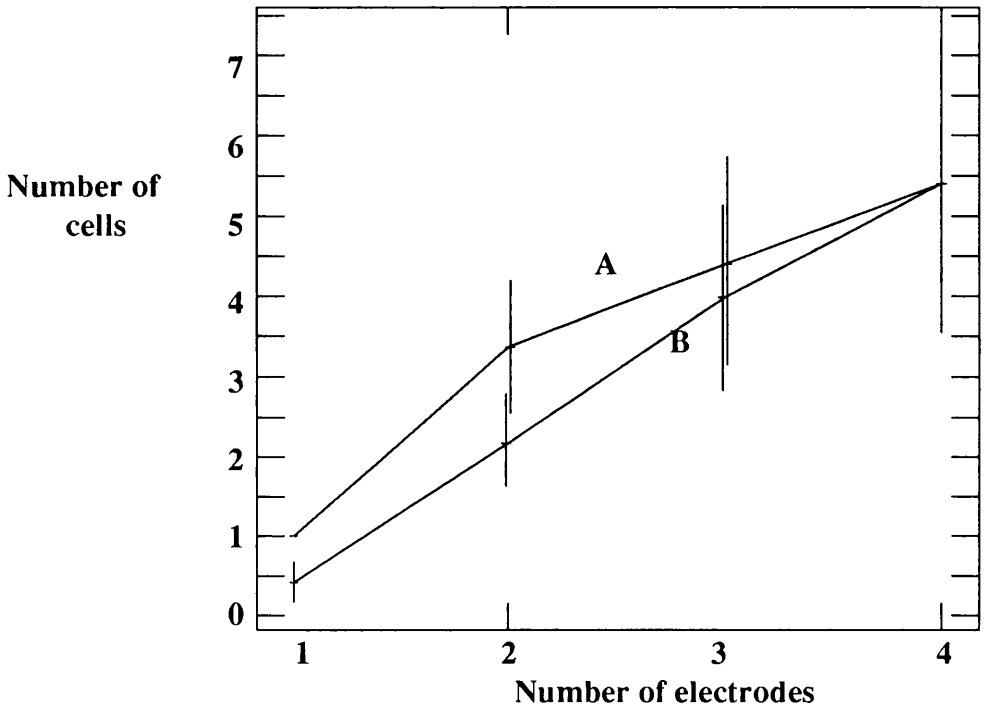

Figure 5.4 Improvement in cell isolation with increasing number of electrodes. Average values are shown for: (A) the apparent number of cells isolated as the number of electrodes used for simultaneously recording is increased, and (B) the actual number of isolated cells. The difference between the two lines are the cells that are misclassified as single cells.

The stereotrode both detects more units and achieves better isolation of single units. An average of 1.7 neurons are found on each electrode of the stereotrode. The problem is that 35% of the "single" neurons isolated are actually multiple neurons. Three electrodes are able to separate almost all of the single cells, but still fail 9% of the time. In this analysis over 72% of the clusters that were misclassified as single neurons with the stereotrode resulted in spurious multiple place fields.

This analysis only included clusters that were reasonably well isolated using four electrodes. As discussed below, in some of the cases it was considered possible that the tetrode method was still not sufficient to separate the clusters. Of course, since the analysis began with a classification with four electrodes we cannot determine if four electrodes are enough.

Place cells in a "one" dimensional space

Fourteen place cells were recorded from seven electrode placements in two rats on the linear track environment. This included two data sets from the CA3 region (4 cells in two rats), and five data sets from the CA1 region (10 cells). All of the cells had a highly directional firing pattern, and one of the cells had two firing fields.

For the analysis of cell firing rate, the linear track is divided into 64 equal size bins (2.3 cm per bin), and cell firing rate is the number of spikes in a bin divided by the total time spent in the bin. Each of the place fields consisted of an elevated block of firing over a limited extent of the maze, with virtually no firing outside this region. The size of the place fields ranged from 19 to 80 cm, but did not appear to be normally distributed. There appeared to be one group of place fields of approximately 28 cm (12 bins) and another group of larger place fields of approximately 61 cm (26 bins). Whether these represented single and double instances of a quantal field size cannot be concluded from the present small sample. The place field sizes for these cells are presented in Table 7.1 (Chapter 7, cells 2-15), along with the cell firing rate and other statistics. The average firing rates in the place fields ranged from 3.3 spikes/second to 28.5 spikes/second. The size of the place fields and the firing rates for these cells is shown in Figure 5.7.

In the linear track experiments, it is easier to make precise measurements of the spatial firing patterns of place cells. In this task the rat is largely constrained to movements in one dimension and therefore there is less variation in the spatial distribution of its behaviour. In this task the firing patterns of cells can be compared on a spike to spike basis, rather than appealing to a population based statistical meaurement of the place field.

An example of this is shown in Figures 5.5 and 5.6. Figure 5.5 contains the firing of two place cells during four runs of the animal from left to right on the linear track. The data are plotted against time, and in each of the runs it took the animal a different amount of time to run from one end to the other. The individual action potentials of each neuron are plotted above the simultaneously recorded θ rhythm, and the animal's speed during the run is plotted below.

Place cell activity during example runs along a linear track, plotted as a function of time

Figure 5.5 (On page 102) Four runs (A-D) during the recording of cells 2 and 3 from cluster 2 (CA3). The top two runs in each graph show the firing of each cell as a single vertical line. Aligned multiple vertical lines for the same cell indicate instances where the cell fired too rapidly for the individual spikes to be shown on this slow time base. The third record in each graph shows the concurrent EEG taken from an electrode at the level of the hippocampal fissure. Positive voltage is up. Calibrations are +/- 1 mV. The fourth record shows the speed of movement of the rat on the track. The x axis for all graphs is time in seconds. Each run begins after the animal leaves the left goal, and ends before it enters the right one. Runs A and D show fast uninterrupted runs, while B and C show runs where the rat slowed and paused at some point in the run. Note that the temporal relations between the firing of the two cells can vary markedly, depending on the animal's behaviour.

Place cell activity during example runs along a linear track, plotted as a function of the animals location

Figure 5.6 (On page 103) The same data shown in Figure 5.7, but with the spikes and EEG voltages plotted against the rat's position on the maze as the x axis. The firing fields of the cells are now in greater alignment. The distortion of the EEG record towards the end of runs B and C is due to the superposition of many θ rhythm cycles in the same location as the rat's speed falls to zero. The record in C is truncated because the rat turned at this point and ran in the opposite direction. Note the overlap of the spikes in the two cells in C at approximately 0.9 m, where the end of cell 2 field overlaps the beginning of the cell 3 field. Calibration +/- 1 mV for the EEG and 1.0 m for the x axis.

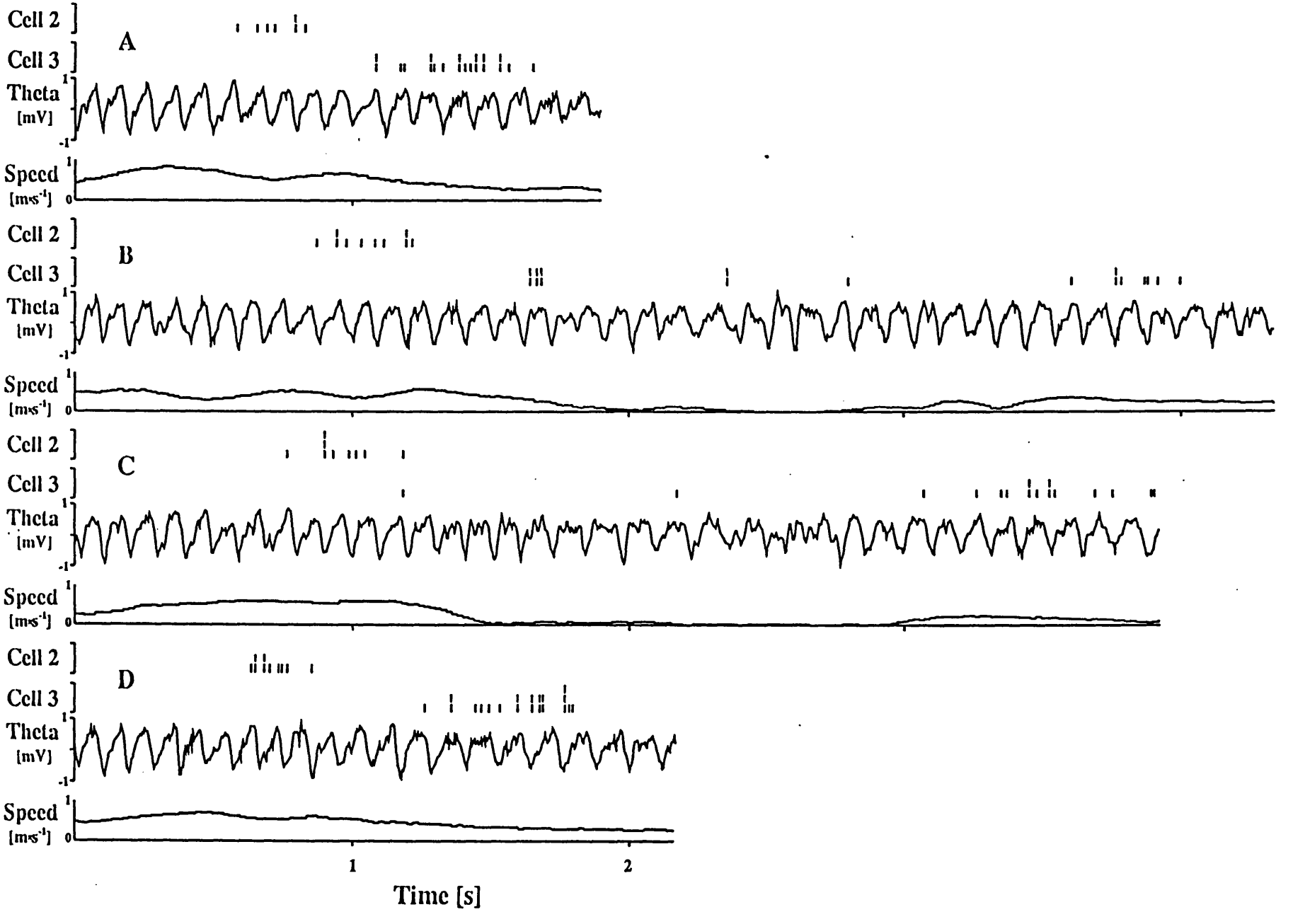
Cell 2
Cell 3
A
Theta
[mV]
1
-1
Speed
[m·s⁻¹]
1
0
Cell 2
Cell 3
B
Theta
[mV]
1
-1
Speed
[m·s⁻¹]
1
0
Cell 2
Cell 3
C
Theta
[mV]
1
-1
Speed
[m·s⁻¹]
1
0
Cell 2
Cell 3
D
Theta
[mV]
1
-1
Speed
[m·s⁻¹]
1
0
1
2
Time [s]

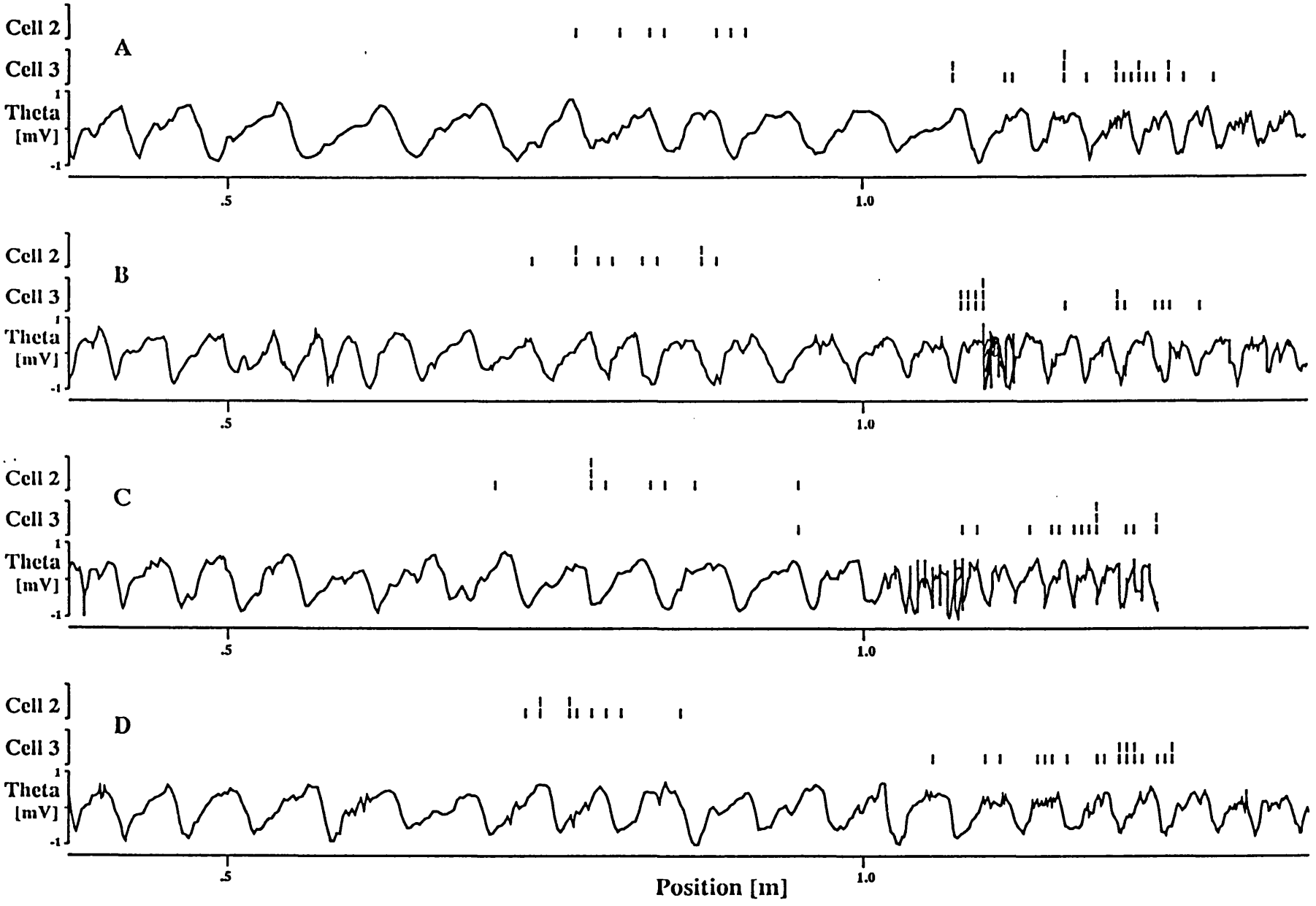
Cell 2
Cell 3
A
Theta
[mV]
1
-1
.5
1.0
Cell 2
Cell 3
B
Theta
[mV]
1
-1
.5
1.0
Cell 2
Cell 3
C
Theta
[mV]
1
-1
.5
1.0
Cell 2
Cell 3
D
Theta
[mV]
1
-1
.5
1.0
Position [m]

In Figure 5.5 the two cells do not appear to be coding for a temporal event, since they do not line up along the time axis. Also, it is unlikely that these cells are coding for the time before reaching the next goal or the time that has passed since the last reward was obtained. These same data are replotted, in Figure 5.6, as a function of the animal's location on the maze. In this figure, the firing pattern of the cells is much more aligned between runs. Note that there is no firing in these runs outside the place fields. These data demonstrate the spatial firing of place cells without appealing to the computation of an average firing rate or the occupancy time.

If only the average rate is measured, several features of the firing are lost. For example the bell-shaped average spatial firing distribution computed for these data (see Figure 5.7) can result from at lease two different mechanisms. This shaped firing function can be produced by a cell that has a constant firing rate within the place field but the start and end points of the place field are imprecise. On the other hand, as seen in the example shown in Figure 5.5, the firing rate can increase and decreease within more spatially specific place fields.

Figure 5.6 also contains the hippocampal θ rhythm plotted as a function of spatial location. Note that the length of single cycles of the θ rhythm increase as the animal runs faster. This suggests that the frequency of the theta rhythm is largely unchanged with speed (but see Chapter 6), so with faster movement the waveform is stretched. Likewise when the animal slows to a stop, as occurs two thirds of the way through the second run, the θ rhythm is shown superimposed. The fact that this waveform is not a spatial stationary wave is important in the experiments described in Chapters 6 and 7.

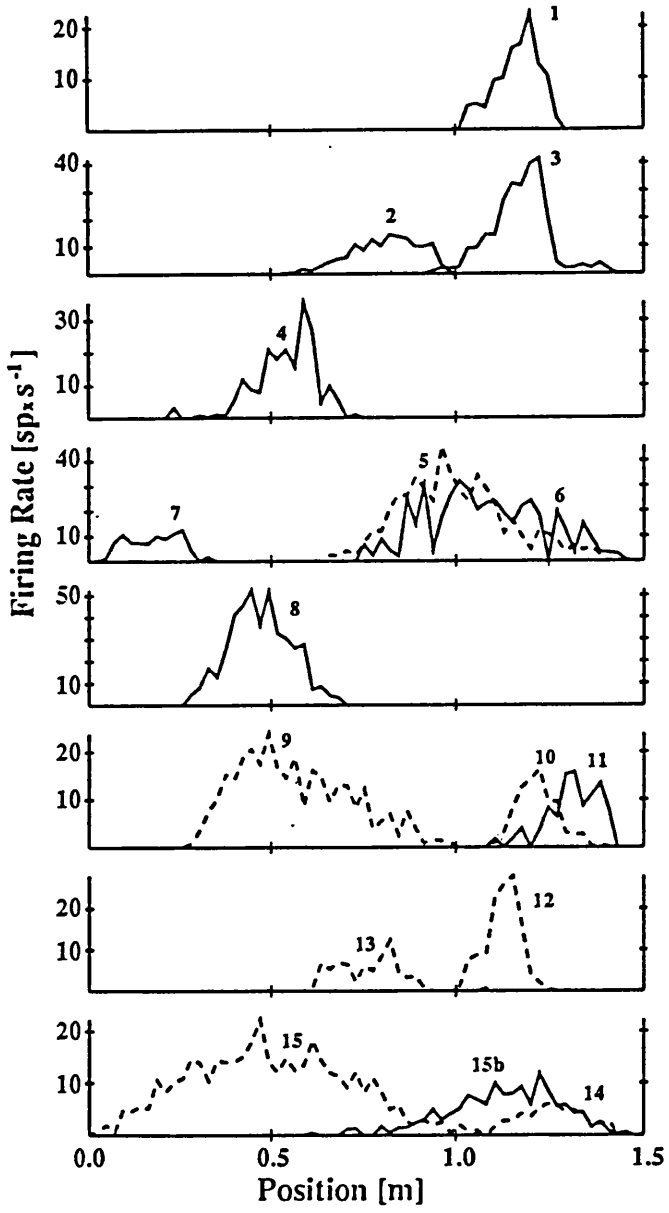

Figure 5.7 Place field location for each of the complex spike cells. The data are organised in seven clusters for each of the recording sessions. Each field is identified from the firing rate, and they are labelled as in Table 7.1. The solid lines are rate maps from cells that fire on runs from left to right, and the dashed lines are rate maps from cells that fire on runs from right to left. Note that cell number one was recorded on the plus maze, and it is included here because it was grouped together with the linear track cells in the analysis described in Chapter 7. Two place fields were found for cell number 15, and they are labelled separately as 15 and 15b in the figure.

Place cells activity patterns in two dimensional space

Ten of the data sets were recorded in environments with a full two dimensional structure. In eight of these data sets data were recorded as the rat randomly searched for food rewards (drops of chocolate milk, rice cereal, or sweetened cooked rice) and in the other two the animal performed the perceptual component of the cue controlled memory task (plus maze) developed by O'Keefe and Speakman (1987). This range of environments was selected as part of a search for a pattern in the hippocampal representation of space. It was deemed possible that the expected benefits of the tetrode (i.e. better isolation of single cells and more simultaneously recorded cells) might reveal some consistency in the coding pattern. Nineteen of the cells discussed here were recorded from the CA3 region and thirty four were recorded in the CA1 region. The characteristics of each of the cells are included in Table 5.1.

Rat:Cell	Environment	Electrode Location	Cell Type	Field Size (bins)	Peak Firing Rate (spikes/sec)	Clustering Performance (x1000)
R83:1	small box	CA1	place	147	7	11
R83:2	small box	CA1	theta	616	33.3	6
R83:3	small box	CA1	place	251	1.8	9
R83:4	small box	CA1	place	323	2	12
R83:5	small box	CA1	place	205	2.8	9
R83:6	small box	CA1	place	78	13.2	8
R90:1	small box	CA3	place	131	1.1	58
R90:2	small box	CA3	place	144	4.9	5
R90:3	small box	CA3	place	143	1.1	16
R90:4	small box	CA3	place	74	1	10
R90:5	small box	CA3	place	163	0.6	13
R90:6	small box	CA3	place	238	0.5	28
R90:7	small box	CA3	place	46	1.3	27
R90:8	small box	CA3	place	89	0.9	18
R87:1	small box	CA1	place	204	15.5	8
R87:2	small box	CA1	place	210	4.6	15
R87:3	small box	CA1	place	204	12	33
R87:4	small box	CA1	place	213	6.1	20
R89:1	small box	CA1	place	135	12.5	7
R89:2	small box	CA1	place	249	7.5	9
R89:3	small box	CA1	place	117	7.8	24
R89:4	small box	CA1	place	204	13.4	8
				This Table	is continued on	the next page.

R108:1	open circular	CA1	place	52	10.4	22
R108:2	open circular	CA1	place	47	15.8	13
R135:1	open circular	CA3	place	86	8.4	27
R135:2	open circular	CA3	place	87	6.7	23
R135:3	open circular	CA3	place	67	5.8	56
R135:4	open circular	CA3	place	104	10.8	34
R135:5	open circular	CA3	place	126	7.6	39
R135:6	open circular	CA3	place	81	18.5	16
R42:1	plus maze	CA1	place	15	34.4	21
R42 :2	plus maze	CA1	place	36	7.7	10
R42 :3	plus maze	CA1	place	47	4.9	24
R42 :4	plus maze	CA1	place	31	21.2	16
R42 :5	plus maze	CA1	place	72	9.4	40
R62:1	plus maze	CA1	place	118	12.5	10
R62:2	plus maze	CA1	place	54	12.9	31
R62:3	plus maze	CA1	place	69	16.9	53
R62:4	plus maze	CA1	place	56	9.3	12
R164:1	walled box	CA1	place	74	28.7	22
R164:2	walled box	CA1	place	90	16.9	14
R164:3	walled box	CA1	place	184	6.3	28
R164:4	walled box	CA1	place	67	23.1	18
R164:5	walled box	CA1	place	168	3.6	28
R164:6	walled box	CA1	theta	652	8.3	17
R164:7	walled box	CA1	place	106	10.5	19
R164:8	walled box	CA1	theta	517	6.2.	35
R149:1	walled box	CA3	place	104	28.5	8
R149:2	walled box	CA3	place	114	16.7	26
R149:3	walled box	CA3	theta	670	62.5	6
R149:4	walled box	CA3	place	137	36.4	4
R149:5	walled box	CA3	place	112	38.5	5
R149:6	walled box	CA3	place	208	3.3	31

Table 5.1 The characteristics of each of the cells that were recorded in two dimensional enviornments. The environments are each divided into a grid of 32 x 32 bins, and the ratio of the number of spikes and the occpancy time is computed for each bin. These data are then filtered with a low-pass 2-D spatial filter, and the peak firing rate is measured. All bins that have at least 10% of the peak firng rate are included in the place field The *clustering performance* (described p.111-2), included in column 7, is a measure of the separation between the clustered activity of each cell and the centre of the nearest cluster.

The firing properties of place cells showed more variation in two dimensional environments, than on the linear track. The peak firing rate of the place cells ranged from less than 0.5 to 38.5 spikes/second (mean 11.1, σ=9.6) and the peak rate of the theta cells ranged from 6.2 to 62.5 spikes/second. The true firing rate is difficult to measure from averaged data, since the data have been filtered, and the rates depend on the spatial distribution of the animal's behaviour. Also, as

described above the firing rates are significantly affected by the cluster separation process. There is better cluster separation if false positives are lost at the expense of a larger number of false negatives. There was more variation in firing rates between data sets than within each data set. The true firing rate cannot be measured from these data, but the variance in the overall spike activity rate of the uncut data suggests that, independent of the spatial filtering, there is a large range of firing rates.

The shapes of the place fields are shown in Figures 5.8, 5.9, 5.10, 5.11, 5.12, and 5.13. In all of these figures, except for 5.8, each of the place field plots has been scaled to use the full colour spectrum, and the firing rate range between contour bands is 10% of the peak rate. In Figure 5.8 all of the place field plots, from the R164 data set, are produced with a common firing rate scale. This data set, which had well separated clusters (presented in the example plots in Figure 5.2 and 5.3) there appears to be a simple spatial code. There are four narrow place fields (mean size 84 bins) and two broader place fields (mean size 176 bins), and the firing rate is essentionly zero outside of the place fields.

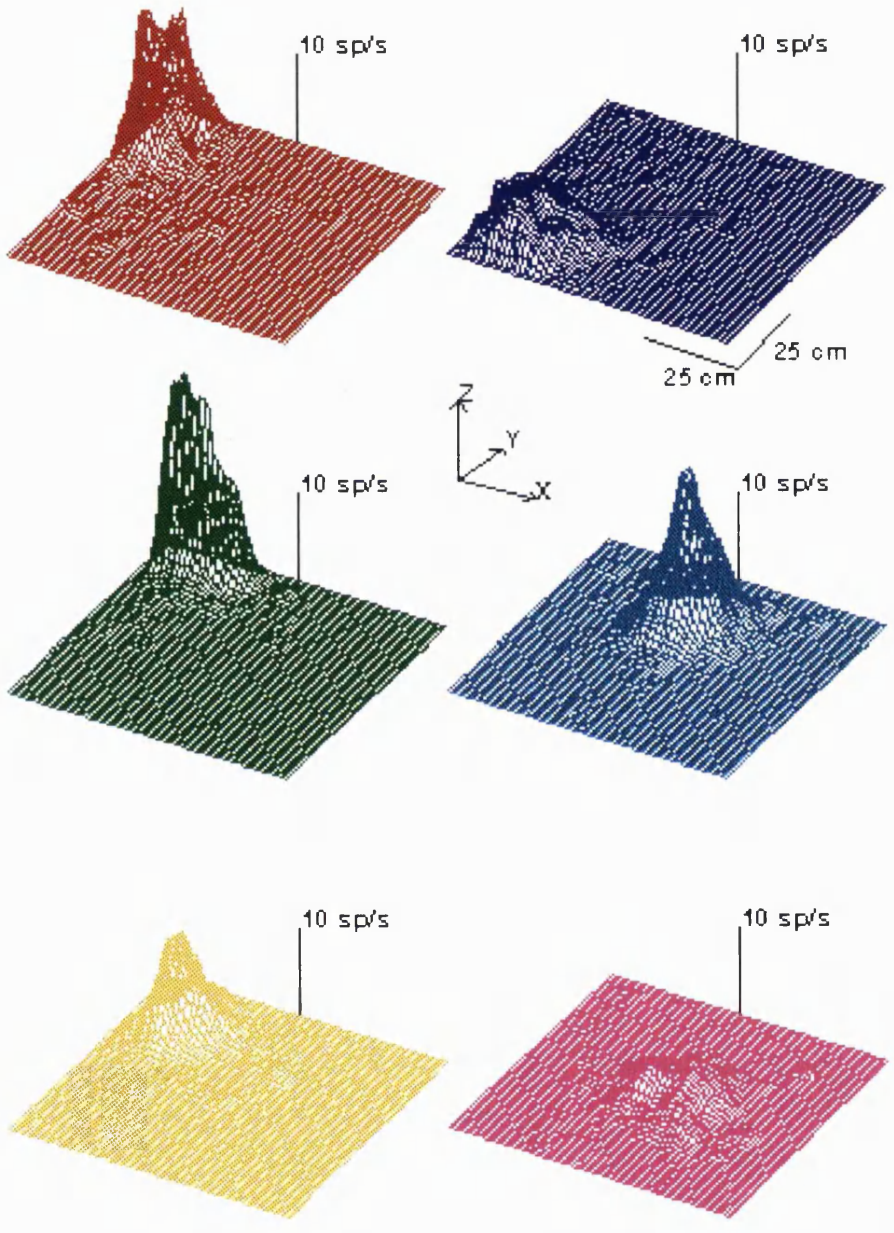

Figure 5.8 The firing rate of the six place cells in the R164 data set plotted as a function of location within the walled box recording area. These data are suggestive of a simple coding for spatial location in the activity of place cells. The correspondance between the place fields and the cells is: R164:1 (red); R164:3 dark blue; R164:4 green; R164:2 light blue; R164:7 yellow; R164:5 violet.

Other data sets did not have such simple place fields. For example in the small box there were several edge-shaped place fields (R87:1, R90:3, and R83:4,6). Also several of the place cells had significant levels of activity outside of the place fields. Some of the activity outside of the place fields is probably caused by insufficient separation of the spikes from different neurons. For example in the R90 data set, cell R90:6 has background firing in the same spatial region that is the place field of cell R90:8. This suggests that the data may not be sufficiently well separated into clusters, and that an objective measure is required to determine which of the data sets are well isolated, and therefore represent the true hippocampal coding pattern.

The k-means clustering algorithm, among others, uses a distance metric to group each spike into the nearest cluster. In this case, the metric is the Euclidean distance between the individual digitised voltages of the spike and the average waveform (or equivalently the cluster centre). The mean distance between the spikes that are in a cluster and the cluster centre should decrease as the algorithm separates the data. Independent of the method that is used to separate the data, the mean distance to the cluster centre, which reflects the spread of a cluster, is one way to evaluate the performance. If the mean distance from a cluster of spikes is measured instead to the center of a different cluster then the resulting value indicates the amount of overlap between the two clusters.

A matrix of all of the mean distances between the spikes in a cluster to the center of each of the clusters, computed from the spikes in the R164 data set, is shown in Table 5.2. In this table, for example, the number in the first row and first column, is the distance between all of the spikes in cluster one and the center of cluster one. The other numbers in the same row are the mean distances from the spikes that are in each of the other clusters.

Mean Distance	Spikes in Cluster 1	Spikes in Cluster 2	Spikes in Cluster 3	Spikes in Cluster 4	Spikes in Cluster 5	Spikes in Cluster 6	Spikes in Cluster 7	Spikes in Cluster 8
Centre of Cluster 1	16	38	42	66	45	50	49	53
Centre of Cluster 2	47	21	46	80	35	54	57	56
Centre of Cluster 3	97	87	40	120	74	68	73	90
Centre of Cluster 4	73	72	57	20	64	66	37	84
Centre of Cluster 5	121	79	86	154	50	85	101	102
Centre of Cluster 6	74	64	43	87	45	25	53	52
Centre of Cluster 7	63	60	41	43	49	47	22	72
Centre of Cluster 8	92	78	66	133	65	61	96	26

Table 5.2 Mean distance between the digitised spikes in each of the clusters and the centre of each of the clusters.

As expected, the smallest numbers in this matrix (Table 5.2) are along the diagonal, which indicates that most of the spikes are in the correct cluster. Note that the matrix is not symmetric. This is due to the fact that spikes within a cluster are not uniformly distributed around the cluster center. The smallest element in this matrix is 35 which suggests that, out of all of the combinations, the spikes in cluster 5 are closest to the centre of cluster 2. The average waveforms (cluster centres) of all of the single cells in this data set are shown in Figure 5.14. It this figure it is clear that the waveforms for cell R164:5 (cluster 5) and cell R164:3 (cluster 2) are most similar.

If the diagonal element in a row is much smaller than all of the other elements in the same row, then most likely the spikes in the cluster are far from other cluster centres. One measure of the overlap between clusters is the difference between the diagonal element in each row and the next smallest element. Of course this only measures the overlap with the nearest cluster. Other measures could be proposed. For example, the difference between the smallest matrix element in a row and the average of the other distances indicates how far the rest of the clusters are on average from the spikes in the current cluster.

These matrices were computed for each of the data sets and the difference between the diagonal element in each row and the next smallest element are included

in column 7 of Table 5.1. Note that the two waveforms, in Figure 5.1, that were difficult to separate using only two channels have the smallest values for clustering performance in that data set (R42:2;R42:4). Also, the three cells with the lowest scores for clustering performance (R83:2; R90:2; R149:4) have comparitively poor spatial specificity in the resulting place fields, while the three cells with highest scores (R90:1; R135:3;R62:3) have essentially no background firing outside of the place fields. Note that the R164 data set, which is suggestive of a simple coding scheme, has relatively high clustering performance scores for each of the cells.

The clustering performance score can be used as a criteron to select the subset of the data that are most well isolated, and that therefore provide the clearest indication of how space is represented in the activity of place cellls. The nine clusters with a clustering performance score greater than 30 contain spikes from cells: R90:1; R87:3; R135:3,4,5; R42:5; R62:2,3; and R149:6. Out of these cells only R149:6 has a multiple place field (see Figure5.13). In addition all of these cells have low out of place field firing rates.

All four of the theta cells contained in these data have firing patterns which are uniform over most of the environment (R83:2 in Figure 5.9; R164:6, R164:8, R149:3 in Figure 5.13). The theta cells also have a surprisingly broad range of firing rates. The theta cell were identified in part from the narrow width of the recorded waveforms. As an example the waveforms from the two theta cells in the R164 data set are presented in Figure 5.14.

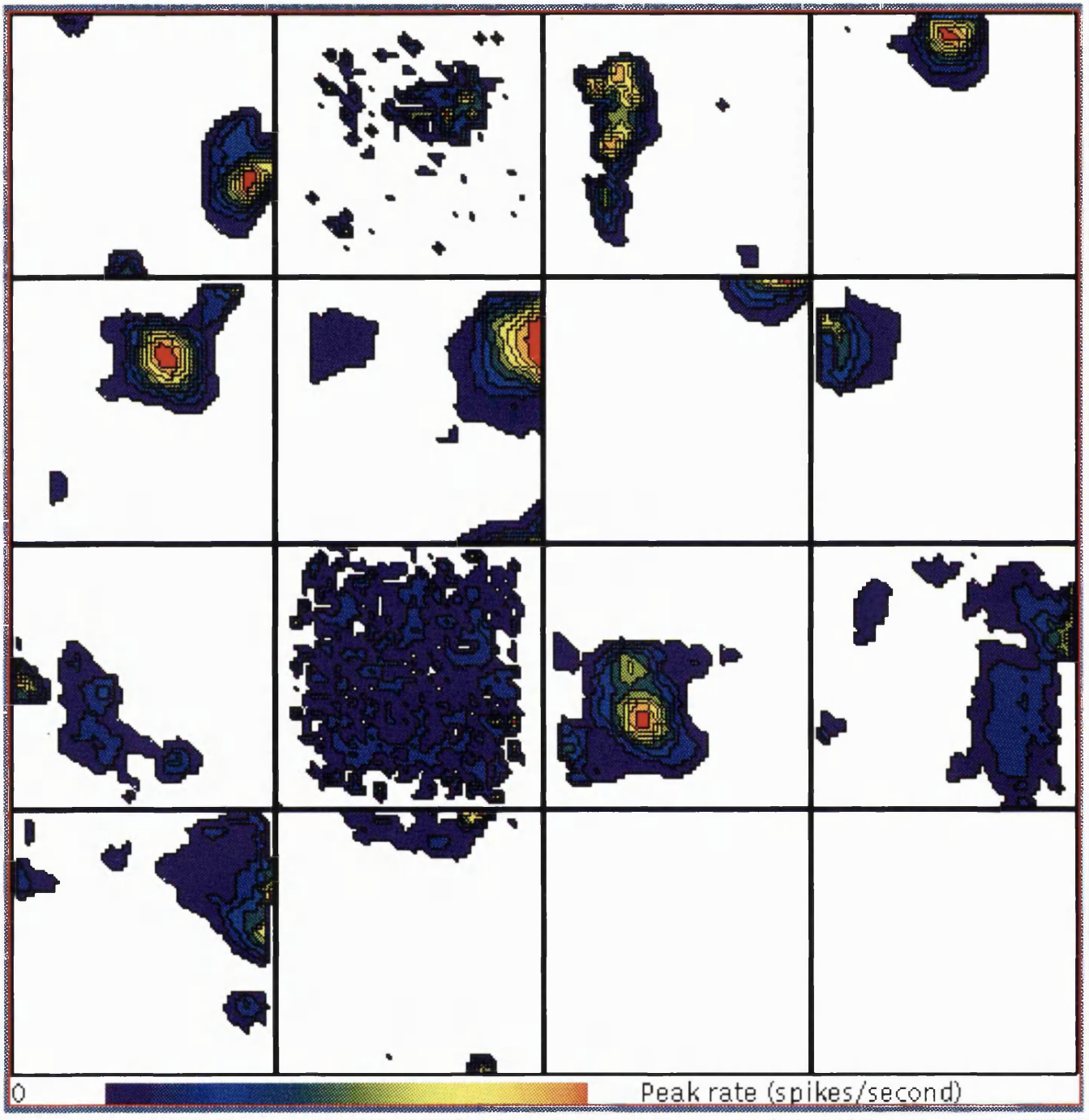

Figure 5.9 Firing rate maps for the R90 and R83 data sets. The top two rows contain the cells recorded from R90, and they are numbered in sequence from left to right and top to bottom. The second two rows contain the cells recorded from R83. The colour scale indicates shows the range of firing rate, and it is independently applied to each plot. The contour bands indicate a change of 10% of the peak firing rate. See Table 5.1 for the friing rate peak values, and the text for a description of how the plots are constructed. The high end of the colour range is obscured in some of the panels by the black contour lines.

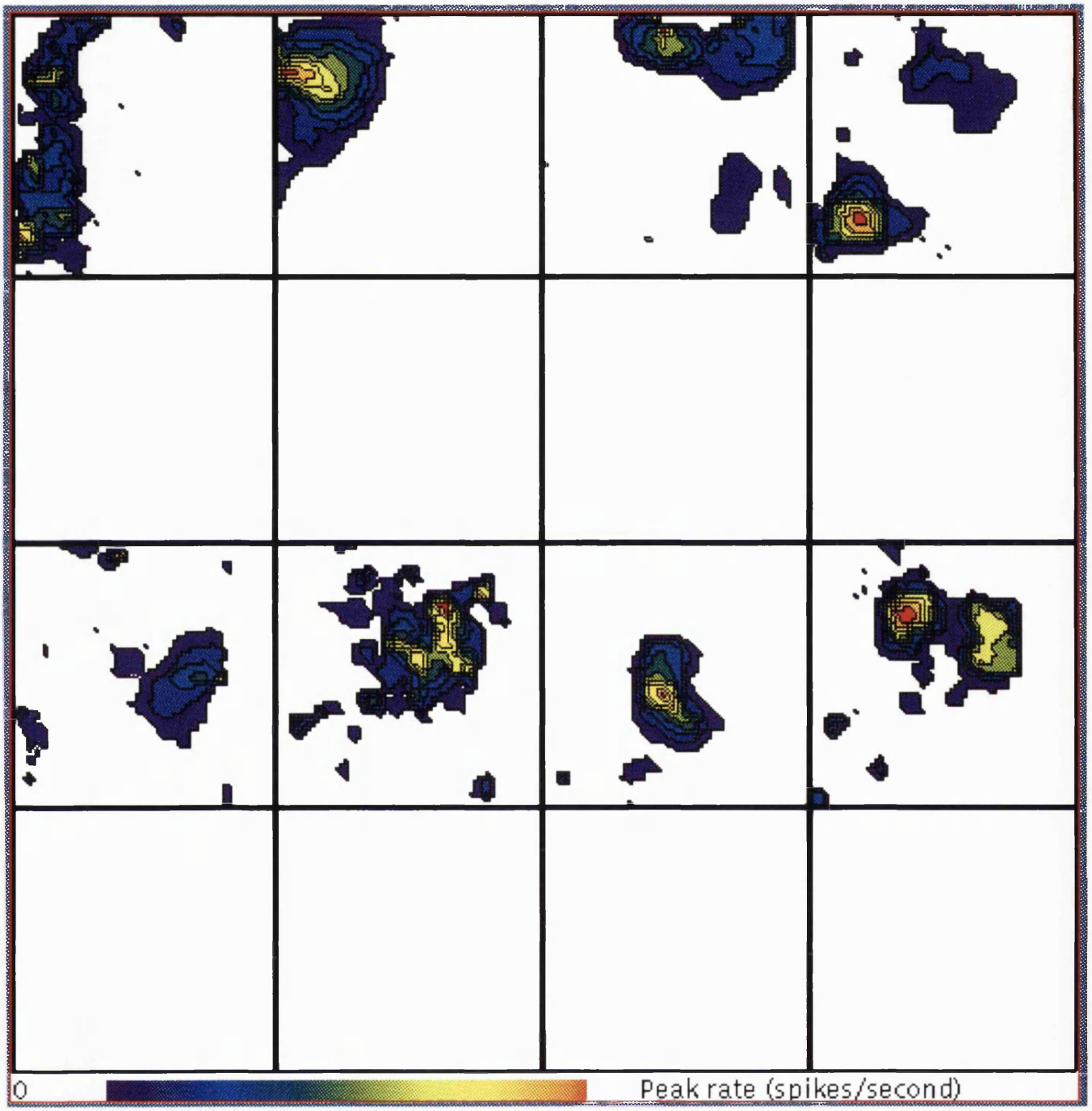

Figure 5.10 Firing rate maps for the R87 and R89 data sets. The top row contains the cells from R87, and they are numbered in sequence from left to right. The third row contains data recorded from R89. The colour scale indicates shows the range of firing rate, and it is independently applied to each plot. The contour bands indicate a change of 10% of the peak firing rate. See Table 5.1 for the firing rate peak values, and the text for a description of how the plots are constructed.

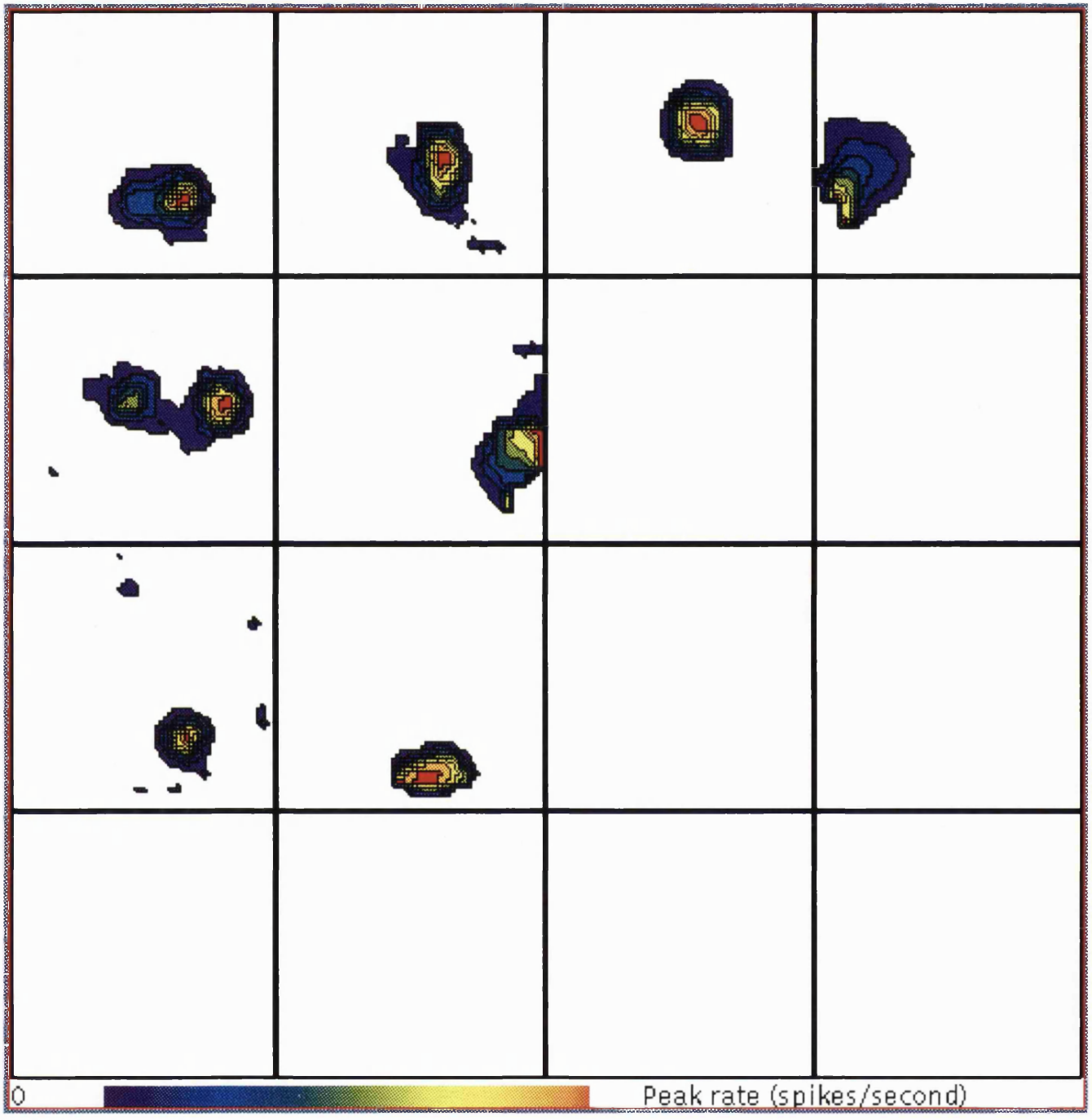

Figure 5.11 Firing rate maps for the R135 and R108 data. The top two rows contian the cells recorded from R90, and they are numbered in sequence from left to right and top to bottom. The third row contains the data recorded from R108. The colour scale indicates shows the range of firing rate, and it is independently applied to each plot. The contour bands indicate a change of 10% of the peak firing rate. See Table 5.1 for the firing rate peak values, and the text for a description of how the plots are constructed.

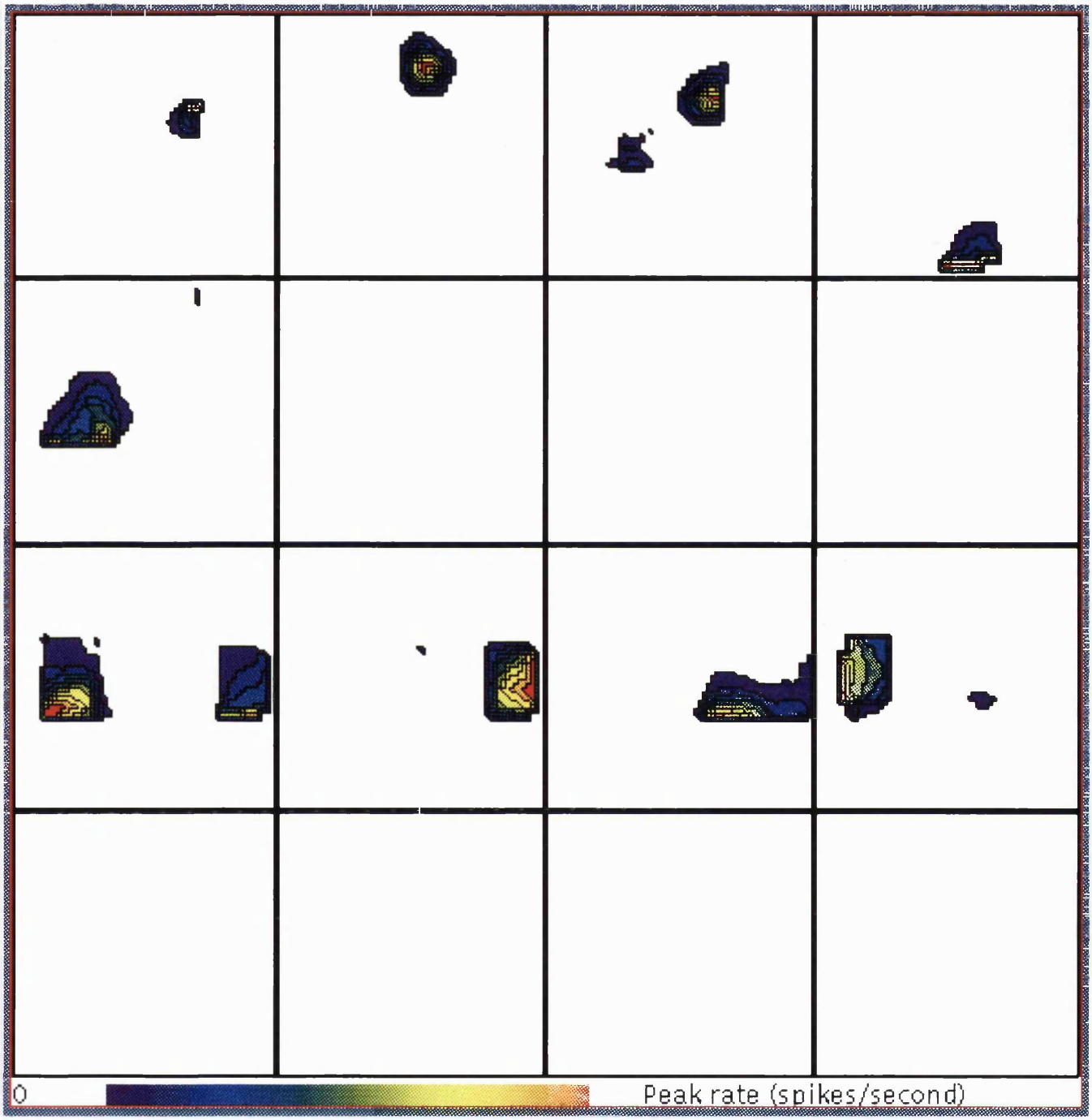

Figure 5.12 Firing rate maps for the R42 and R62 data sets. The top two rows contain the cells recorded from R42, and they are numbered in sequence from left to right and top to bottom. The third row contains the data recorded from R62. The colour scale indicates shows the range of firing rate, and it is independently applied to each plot. The contour bands indicate a change of 10% of the peak firing rate. See Table 5.1 for the firing rate peak values, and the text for a description of how the plots are constructed.

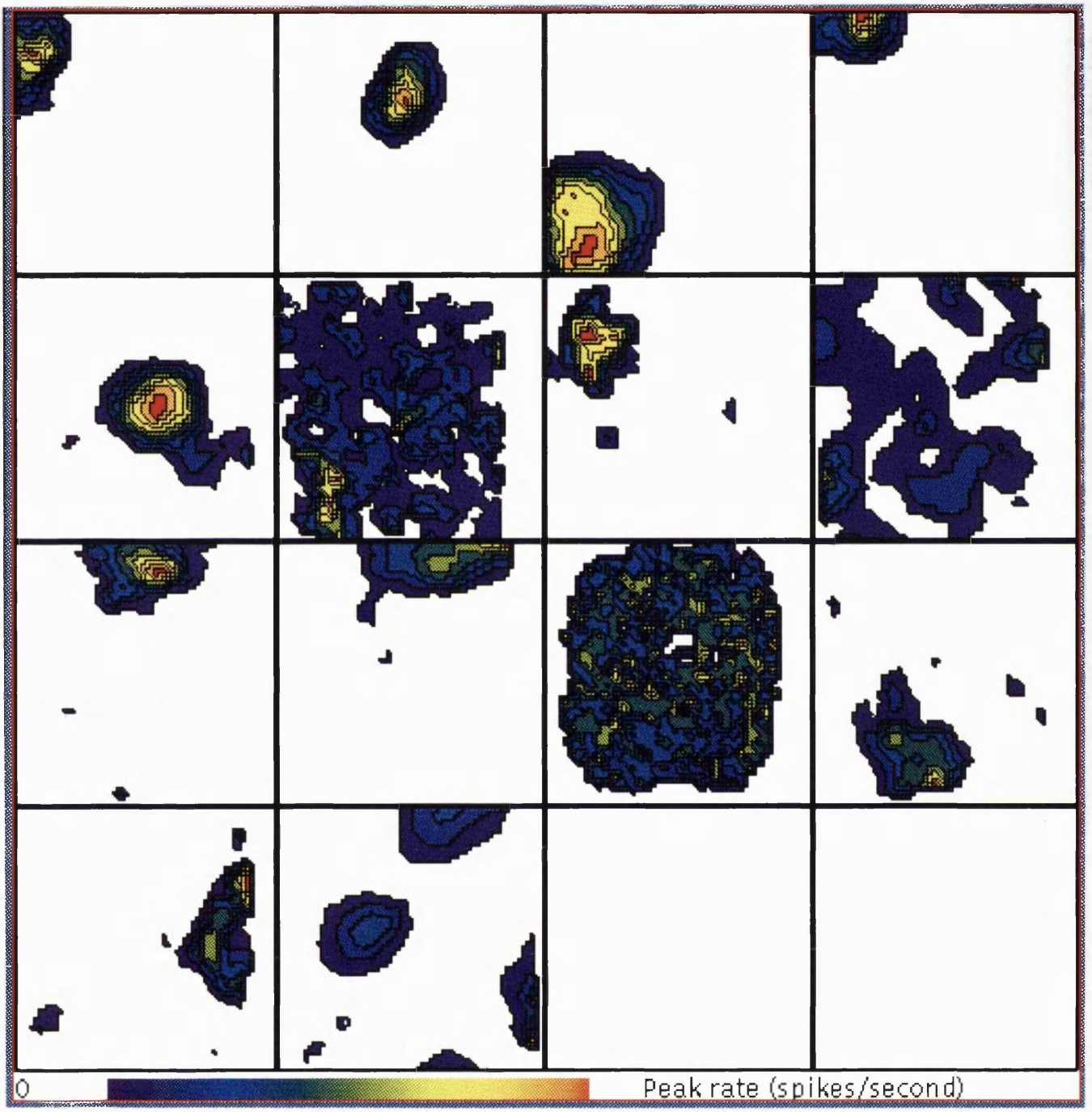

Figure 5.13 Firing rate maps for the R164 and R149 data sets. The top two rows contain plots of the place fields of cells recorded from R164, and the are numbered in sequence from left to right and top to bottom. The second two rows contain the data recorded from R149. The colour scale indicates shows the range of firing rate, and it is independently applied to each plot. The contour bands indicate a change of 10% of the peak firing rate. See Table 5.1 for the firing rate peak values, and the text for a description of how the plots are constructed.

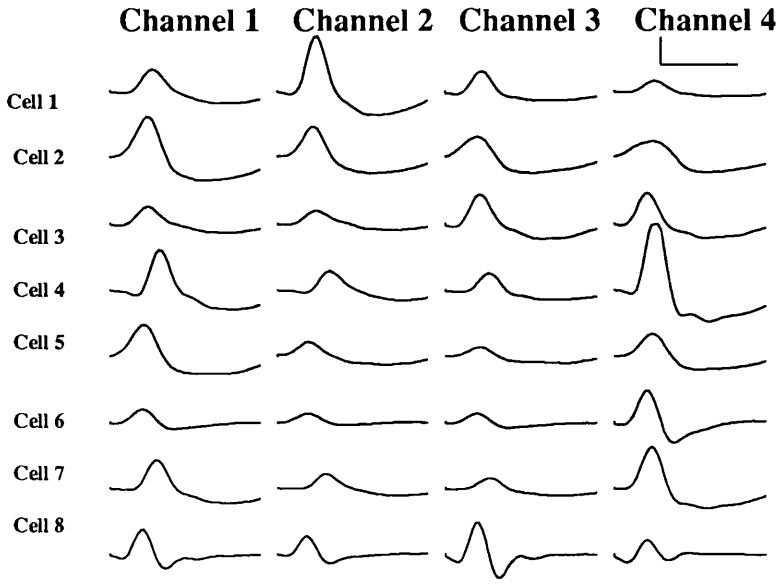

Figure 5.14 Average spikes for the 8 cells in the R164 data set. The averages computed for each independent channel of the tetrode areplotted in each row. The vertical scale bar is 100 μV and the horizontal bar is 500 μsec.

5.4 Discussion

These data have demonstrated that clearer single unit records can be obtained using tetrode-based recording than was possible with previous methods. Furthermore the present data suggest that many of the prior reported properties of single hippocampal place cells were confounding the activity of more than one cell. The stereotrode method was found to increase the number of cells found in a single electrode placement, but 35% of the single units included more than one cell.

However, this analysis made several assumptions which are disadvantageous to fewer electrodes, and should be considered. To simplify the analysis only voltage thresholds were allowed, and in practice the waveshape can also be use in single electrode or stereotrode recording. Secondly it was assumed that the potentials recorded from two electrodes in a four electrode bundle would be the same as those recorded from two single electrodes. However a larger bundle of electrodes both makes more damage to neuronal processes and places the electrodes further away from the electrical sources.

The more important demonstration of the improved performance of the tetrode technique is the differences in the observed properties of place cells in static environments. The cells recorded on the linear track, and the better isolated cells in the two dimensional environments were virtually inactive during displacement movements outside of the place field. Also, the number of multiple fields and the size of place fields found in these data were smaller than described in previous reports.

There was more variation found in the data from two dimensional environments. Some of this variation may have been due to the need for further improvements in recording methods. A measure of clustering preformance was proposed and applied to the data, and the clusters that had the highest performance score with this measure were further analysed. One of the data sets that was well isolated had place fields suggestive of a simple spatial code in which all of the place fields were single peaked functions, with a well localised spatial extent.

Chapter 6: The Frequency of Hippocampal θ Rhythm is Correlated with Speed of Movement

now syntax settled round the orderless,
joining action and reflection in the arch,
then adding desire and will: four walls:
four walls, a house.'How simple' people said.

Lawrence Durrell

6.1 Introduction

At present only a small number of hippocampal single neurons (<100) can be simultaneously recorded, which provides a limited picture of the overall function of the region. Measurements of the hippocampal EEG provide complementary information. The EEG is composed of the cumulative intracellular potentials of a large number of cells, and is therefore a useful measure of the overall activity of a part of the hippocampus. As previously reviewed (see Chapter 3), during movements the EEG in region CA1 and in the dentate gyrus has a large amplitude sinusoidal pattern called the θ rhythm that has been correlated with various behaviours.

The changes in the frequency of the θ rhythm are particularly important in an analysis of the spatial function of the hippocampus. A sufficient increase in the frequency of the θ rhythm with faster movement could generate a spatial standing wave pattern, in which the peaks and troughs have persistent spatial locations. However, it is already clear from experiments described in Chapter 5 (see Figure 5.5) that the θ rhythm is not a spatial standing wave.

O'Keefe and Nadel (1978) proposed that the θ rhythm acts as a clock for place cell activity. This hypothesis has been supported by evidence that on average the firing of single hippocampal cells occurs at a preferred phase of the θ rhythm (Sinclair et al. 1982; Buzsaki et al. 1983; Fox et al. 1986; Otto et al. 1991). New evidence is presented in Chapter 7 that indicates that the phase of firing of place cells systematically shifts as the animal runs through a place field. The phase alignment of place cell activity imposes restrictions upon when the cell can be active, which exist independently of restrictions upon where it can be active.

The question is: what happens when the animal runs more quickly or more slowly through a place field? If, for example, the θ rhythm has a fixed frequency of 10 Hz, and the rat is moving at 0.5 metres/second, then one cycle of the θ rhythm will occur while the animal moves 5 cm. A place cell that is time-locked to the θ rhythm can fire at only one spatial position within the 5 cm movement that occurs during each cycle, so that on a second run through the region a variation in the relative timing of the θ rhythm could lead to the firing of the place cell at any point within the 5 cm specified by each θ cycle. Similarly, the jitter in the spatial location

for the place cell activity is increased to 10 cm if the animal runs at 1.0 metres/second. If this suggestion is true, then the jitter of place cell firing imposed by the timing to the θ rhythm places a bound on the minimum size of place fields and on the animal's spatial acuity. Furthermore it predicts that the rat's spatial acuity decreases linearly with the rate at which it moves through an environment.

As summarised in Chapter 3, the correlation between speed and θ frequency has been tested in a running wheel, on a treadmill and on a jumping stand, without completely consistent results. In the first of these studies, Whishaw and Vanderwolf (1973) tested for variations in θ rhythm during wheel running, bar pressing, avoidance tests and swimming. In the running wheel experiments the animals ran for eight hours in motorised wheels turning at three different speeds. This experiment showed no lasting correlation between the average speed and the θ rhythm frequency. However a consistently higher instantaneous frequency was found during the first one or two cycles of the θ rhythm in a motorised running wheel that was turning at 60 ft/min (0.3 metres/second). Previously, Bland and Vanderwolf (1972) had described higher running speed and correspondingly higher θ rhythm frequency in the first second of wheel running following posterior hypothalamic stimulation. These data, combined with their finding (Whishaw and Vanderwolf 1973) that higher θ rhythm frequency is correlated with farther distance during jumping, led to a hypothesis that the θ rhythm frequency signals the degree of *vigour* at the initiation of movement.

In contrast, McFarland et al. (1975) found that a linear correlation between the running speed and the θ rhythm frequency persisted during five minute episodes of running on a motorised treadmill. However, they did not directly measure the frequency. Instead they electronically counted the number of times that the θ rhythm exceeded a voltage threshold during a fixed interval. With this method they only obtained an average for each running speed, and without frequency measurements it impossible to quantitatively compare their data to other published findings. In addition they selected four slow running speeds, all less than 25 cm/sec (approx. 1.2 m/sec is peak running speed for rats).

Vanderwolf's hypothesis that the θ rhythm frequency coded for the amount of vigour was also tested using jumping experiments in which the animal carried lead weights on its back (Morris et al. 1976; Morris and Hagan 1983). The conclusion of these studies was that the θ rhythm frequency correlates better with the jump height, velocity and peak force, than with impulse or acceleration.

In most of the literature, changes in the θ rhythm frequency are correlated with the behavioural state of the animal. For example, Gray and his colleagues (Gray and Ball 1970; Gray 1971) divided the observed θ rhythm frequency into three bands: (1) frequencies less than 7.5 Hz were associated with consummatory behaviours, (2) frequencies greater than 8.5 Hz occurred during approach to reward or avoidance of punishment, and (3) the band of frequencies 7.5 to 8.5 Hz had a role in processing new information. In part these categories arose from observations that during exploration the θ rhythm had a lower frequency range than during running. O'Keefe and Nadel (1978) re-interpreted these data as an increase in frequency with increased velocity.

In the experiments described in this chapter, the relationship between running speed and the frequency of the θ rhythm is re-examined. Using the new computer-based methods described in Chapter 4, the correlation between θ rhythm frequency and movement variables can be measured with high resolution (each θ cycle) and in an automated manner. These new methods also make it possible to use a more natural task. Instead of using a motorised running wheel or treadmill, the animal runs back and forth along a linear track to obtain a food reward at each end.

6.2 Methods

The EEG is recorded from one or more movable teflon-coated 25 μm platinum-iridium micro-electrodes (filtered 1 to 100 Hz bandpass, 50 Hz notch) in a monopolar configuration, using a large steel screw in the parietal bone as a ground reference. The EEG is digitised continuously at 244 samples per second (4.1 msec per sample) with a resolution of 12 bits. For some of the data, the EEG was recorded using an additional stationary electrode (75 μm tungsten), which was in either the dorsal CA1 region or in the dentate gyrus.

EEG was recorded from four rats while they ran back and forth along the surface of linear tracks to obtain a reward. The track was 1.5 m long and either 4.6 cm or 15.2 cm wide. Reward in the form of sugar-coated cereals or sweetened rice was given at each end. Rats were trained until they ran with a consistent pattern from one end to the other. During some of the recording, the food reward was varied between several locations in one of the goal areas. This introduced some variability in running speeds. Additional data were taken from a fifth rat, which was trained on an elevated plus maze in a cue-controlled environment. For further details of the procedure in this situation, see O'Keefe and Conway (1978, 1980) and O'Keefe and Speakman (1987).

As previously described in Chapter 3, the rat's position was recorded using an overhead TV tracking system that collected the (x,y) location of a DC. lamp on the animal's head at video rate (50 Hz). The location of the light was lost in less than 10% of the readings, and these were corrected by interpolation. These coordinates were subjected to a moving average filter (width 100 msec, cosine windowing function), and the instantaneous speed of locomotion was computed using the Euclidean distance between sequential position readings. The average speed for each cycle of the θ rhythm was computed from the 25 values (102.5 msec) of instantaneous speed data following each negative peak of the θ rhythm.

In order to determine the instantaneous frequency of the θ rhythm, the θ rhythm was modelled as a set of independent sinusoidal waves, where the transition from one wave to the next occurs near the positive to negative zero crossing. Each cycle of the θ rhythm was extracted in a sequence from the beginning of the data set. The EEG segment corresponding to each cycle of the θ rhythm was found by shifting each out of a set of templates along the data, and comparing the goodness of fit. The goodness of fit was determined by computing the Euclidean distance (sum of the squares of the differences) between the data and the template. This distance to the best fit template for each cycle of the θ rhythm (T_D) also indicates how well the data have been fit. The templates consisted of half period inverted sine waves, that ranged in frequency from 11.1 to 20.3Hz, and in steps of 0.4 Hz (see Figure 6.2).

In this analysis, for each extracted EEG cycle, the best-fit has two independent parameters: (1) the frequency of the selected template, and (2) the

amount of time shift that was required. The amount of time shift varied over a range of 102.5 msec, and in steps of 4.1 msec. In order to select the best fit, all of the possible templates and shifts were tested.

During the recording sessions there were periods, particularly at the endpoints of the linear track, during which the animal was not moving and the recorded EEG contained the characteristic LIA pattern. These segments were not included in the analysis. They were discarded by defining a minimum value for the template distance (T_D). This criterion resulted in the loss of some (<1%) noisy periods of normal θ rhythm. Cycles of the θ rhythm which occurred during slow movements (speed < 0.1 meters per second, or at the ends of the linear track were also removed.

In the runway task the rat's behaviour can be divided into *episodes* of running separated by periods of relative immobility. Usually these movement episodes correspond to complete runs from one end of the track to the other. However, if the rat stopped in the middle of the track then the run is divided into individual movement episodes. Figure 6.1 shows the animal's speed of movement during 15 seconds of recording. During this period, three movement episodes have been identified by the automatic analysis program. The correlations between the θ rhythm and movement variables can be examined independently for each episode (see Figure 6.5). The beginning of each run was identified either as the point at which the speed exceeds 0.1 meters/second or a point a certain distance down the track.

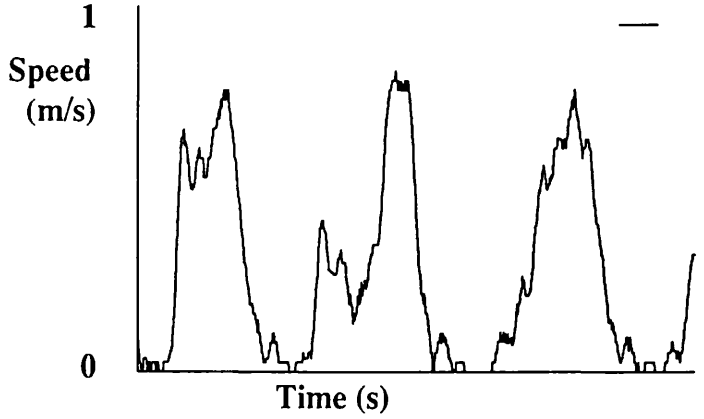

Figure 6.1 Speed of movement during 15 seconds of recording of R149 on the linear track. The calibration bar at the top of the firgure is one second.

The Pearson correlation coefficient and the probability that the correlation could occur in random data were computed for each movement episode within a recording session, also called a data set, and separately for all of the runs within each recording session. In the overall analysis of a data set, equal weighting was given to each cycle of the θ rhythm rather than to each movement episode, which meant that longer episodes had effectively larger weighting.

After the final recording session, the electrodes were left in place for at least one day before the animal was sacrificed. Animals were deeply anaesthetized with Pentobarbital sodium (Lethobarb 0.7ml/kg, Dupham) and perfused with saline followed by 10% Formol saline. The brains were left in Formol saline for several weeks and then sectioned every 50 μm in the sagittal plane and stained with Cresyl Violet. The location of each recording electrode was measured, using the gliosis pattern made by the electrode penetration.

6.3 Results

A significant correlation between the frequency of the θ rhythm and the animal's speed of locomotion was found in the overall data from each rat, and for most of the individual movement episodes. A particularly clear example of the correlation for one movement episode is presented in Figure 6.2. The top part of this figure (A) contains the θ rhythm recorded in the molecular layer of the dentate gyrus as the animal (R149) ran for about four seconds along the linear track. The best fit half sine wave function, computed for each cycle of the θ rhythm, is plotted under the recorded data (B). The instantaneous frequency for each cycle of the θ rhythm, plotted in part C of the figure, is the reciprocal of the time difference between the negative peak in two sequential cycles. The correlation of the frequency with the rat's speed of locomotion (D) is clear.

At the beginning of the run there is a transition from LIA to the θ rhythm, and at the end of the run there is a transition back to LIA. The presence of LIA can be seen both in the high frequency components of the EEG and in the value of T_D (the distance of the best fit between the EEG and the half sine wave template) that is shown for each cycle in part E of Figure 6.2. These data are not consistent with

published evidence in several different species, including the rat, that the θ rhythm continues after the movement has ended (Klemm 1970; McFarland et al. 1975). The time interval between LIA and the θ rhythm can be measured objectively with a globally applied threshold on the value of T_D.

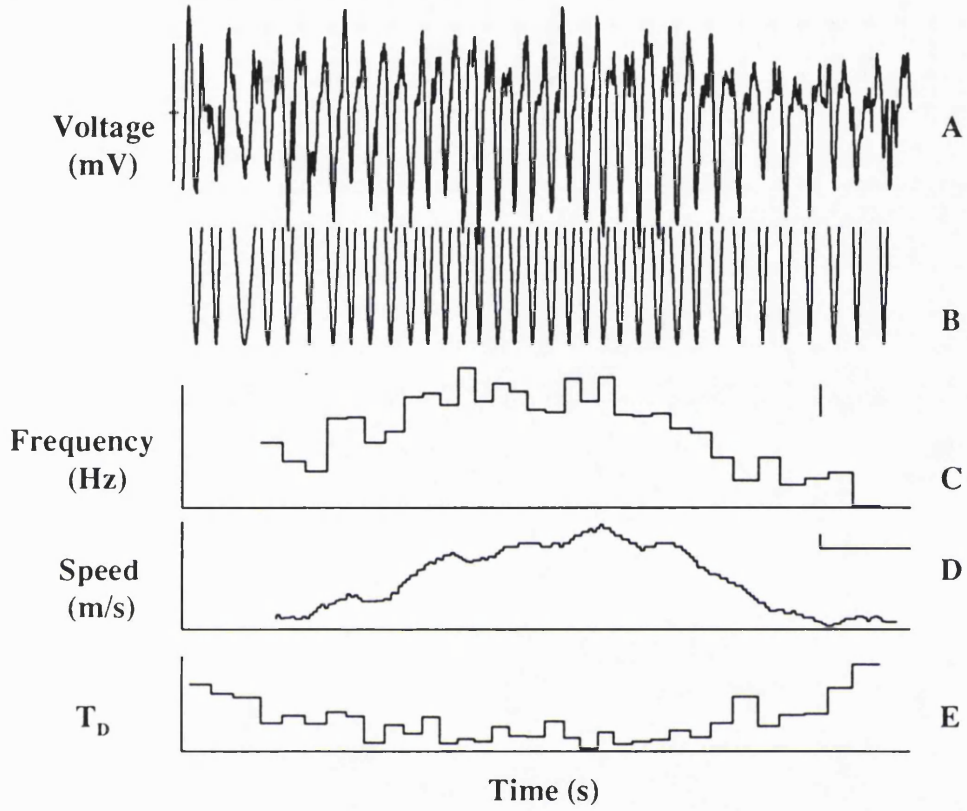

Figure 6.2 Segment of recorded θ rhythm shown with the results from the frequency measurements. (A) The θ rhythm during an approximately four second movement episode (range on axis is -0.5 to 0.5 mV). (B) The templates which fit best to the lower half of each cycle of the θ rhythm. (C) The instantaneous θ rhythm frequency (measured from the start of one θ cycle to the next), which is computed from results of the template fit plotted above (vertical calibration bar is 1 Hz; range 7.5 to 11.6 Hz). (D) The animal's speed of movement measured from the head lamp (vertical calibration bar 0.1 m/s, horizontal bar 0.5 s). (E) The value of T_D, the distance between the best fit template and the θ rhythm for each cycle, as measured from the fit in part B.

The relationship between the θ rhythm frequency and speed for this episode (Figure 6.2) are plotted in Figure 6.3. The analysis includes only the cycles of the θ rhythm that occur during the movement episode. In this figure each dot corresponds to a single cycle of θ rhythm, and the movement speed has been averaged over the single cycle. The Pearson correlation coefficient is 0.8, and the best fit line indicates

a change in frequency from 7.8 to 11.6 Hz with speeds ranging from stationary to one metre/second.

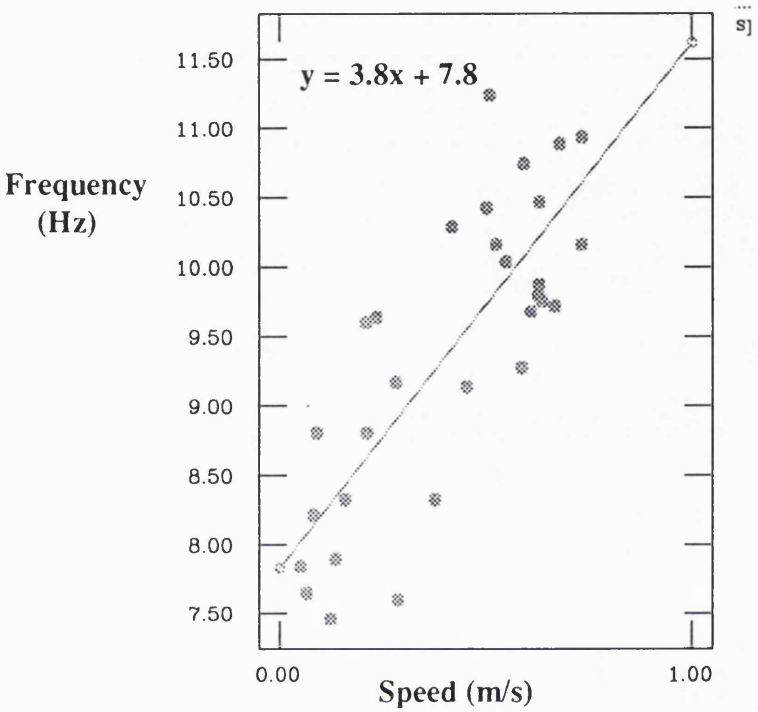

Figure 6.3 Correlation between running speed and the θ rhythm frequency for a single movement episode in R149. Each data point represents the average speed during a single cycle of the θ rhythm.

The accumulated data, and the regression line, from 9658 cycles of the θ rhythm recorded while R149 ran in 266 individual movement episodes on the linear track are plotted in Figure 6.4. The data are divided into ten bins (0.1 metres/second for each bin) and the plot shows the mean and range of the standard error computed for each bin. The number of cycles of θ rhythm for each speed are shown in the histogram in part B of Figure 6.4. The Pearson correlation coefficient for these data is 0.50. The correlation was computed separately for runs from left to right (0.48), and in the runs from right to left (0.51), but there was not a significant dependance on the direction of the run.

The best fit line for these data indicated a frequency change from 8.5 Hz in the extrapolated stationary state to 10.6 Hz at one metre/second. However, the correlation coefficient improves and the slope of the best fit line increases if speeds

greater than 0.7 metre/second are excluded from the analysis. This is expected, since the θ rhythm frequency appears to reach a plateau near this speed. In the individual episodes of movmement the plateau did not occur at a consistent speed, nor was it present in all of the data (e.g. Figure 6.3). Variability in the presence of this plateau has reduced the correlation of the larger data sets. This plateau may be explained by the fact that the sequence of frequencies in the movement episodes occur before the sequence of speeds (discussed below).

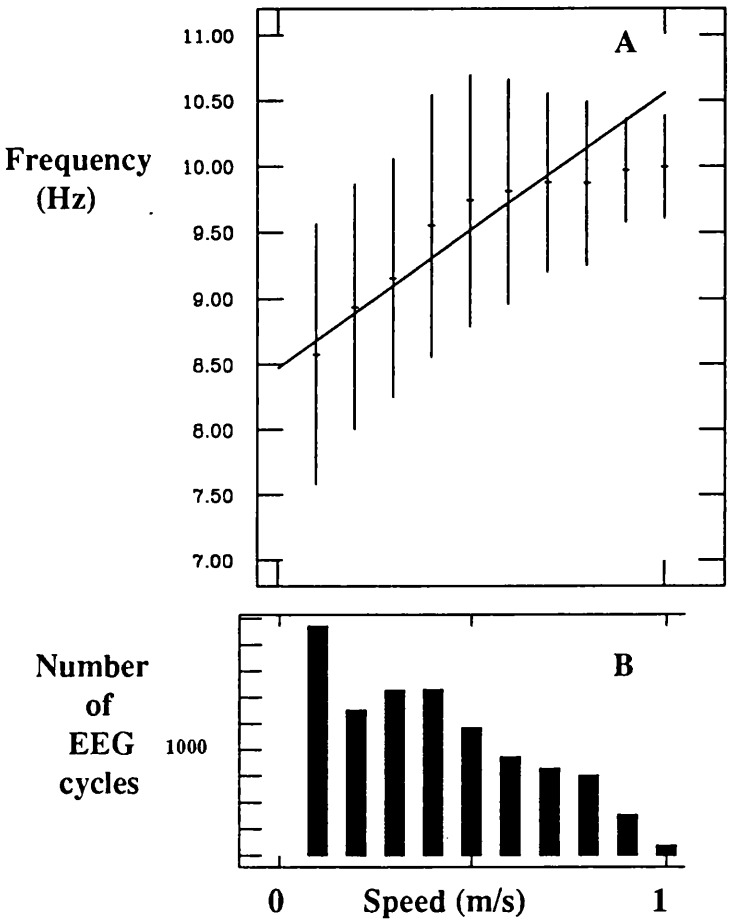

Figure 6.4 (A) Plot of the correlation between speed of movement (x-axis) and the frequency of the θ rhythm (y-axis). The data are divided into bins and the mean and standard error measure for each bin is plotted. The line is a least squares fit to the data. (B) The number of θ rhythm cycles present in each of the speed bins. Cycles of the θ rhythm that occurred at speeds of less than 0.1 meters/second were excluded (see above).

The best fit line and correlation coefficient were computed in the same manner for each of the data sets from an additional four rats, and the results are shown in Figure 6.3 and in Table 6.1. The Pearson correlation coefficient, computed

for each of the full data sets, ranged from 0.43 to 0.57, and these are summarised, along with the slopes and intercepts of the best fit line, in Table 6.1.

Rat	Data set (code)	θ Rhythm cycles	Movement episodes	Slope	Y-Intercept	Correlation	Electrode lodcation (Comments)
R149	o182-191	9,658	266	2.1	8.4	0.5	dentate gyrus
	o172	846	23	3.1	8.2	0.57	dentate gyrus
R173	o233	422	22	1.6	8.1	0.43	dentate gyrus
R192	o50	966	36	2.6	7.8	0.44	CA1 (wide arm)
R195	o24-5	1,338	60	1.6	8.2	0.4	CA1 (wide arm)
R42	o321	401	14	2.3	8.1	0.41	dentate gyrus (+ maze start arm)

Table 6.1 Correlation between the θ rhythm frequency and speed of movement in each of the data sets.

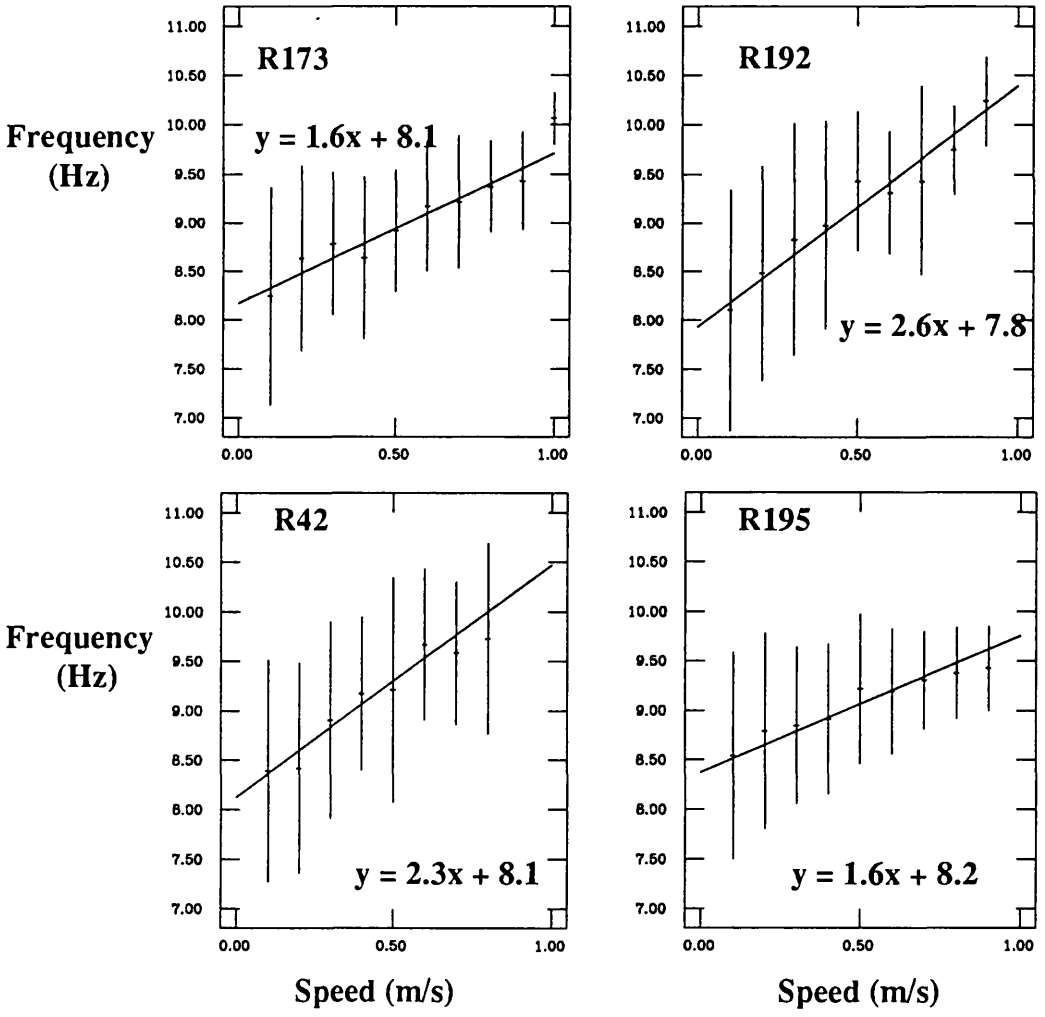

Figure 6.5 Linear fit to the correlation between running speed and the θ rhythm frequency in each of the data sets.

The slope and intercept are largely consistent across the data sets. The slopes and intercepts appear to divide into two groups. There are two sets with a shallower slope (1.6), and four sets from three rats with steeper slopes (2.1-3.1). It is interesting to note that this grouping does not correspond to the recording site. In these data there is little variation in the correlation found in the dentate gyrus and in the CA1 region. Also, there was more variation in the slope and correlation of the data from the one rat with two data sets, than there was between other rats and recording sites.

Some variation in the slope and intercept is due to the fact that the data do not have an equal spread of speeds, and a plateau at higher speeds will tend to decrease the slope of the best fit line. Variation in the correlation may also depend on specific characteristics of the animal's movement pattern that are not detectable using a single lamp on its head. For this reason it is also not possible to establish from these experiments if the correlation is with head or with body movements.

One of the key differences among the results of the prior studies (Bland and Vanderwolf 1972; Whishaw and Vanderwolf 1973; McFarland et al. 1975) was the time duration of the correlation between speed and the θ rhythm frequency. In the present data the duration of the running episode did not have a large effect on the Pearson correlation coefficient. An example of the effect of the length of the running episode is shown in Figure 6.5, which contains 266 movement episodes recorded from R149. The majority of the movement episodes lasted from three to four seconds, but some lasted over ten seconds. The worst correlations were found in very short movement episodes, which may either have been large head turning movements or short displacement movements. The short movement episodes do not have a large impact on the overall correlation, as they do not contain many cycles of the θ rhythm. There is possibly some decrease in the correlation in longer movement episodes.

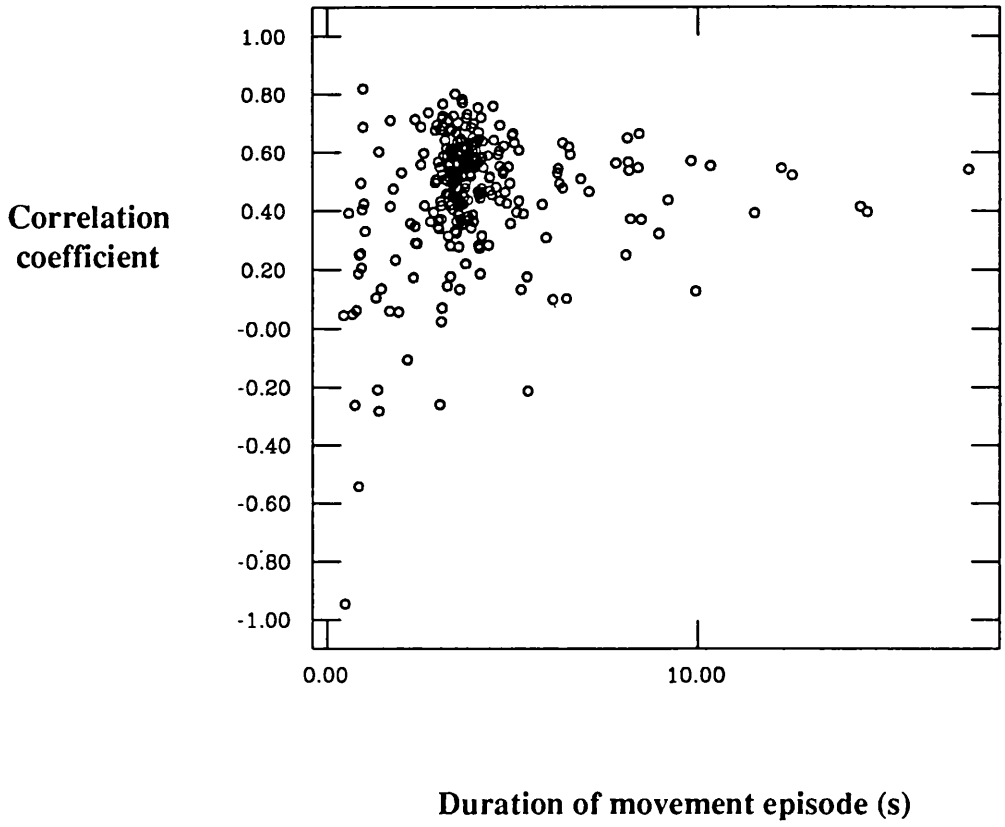

Figure 6.5 A scatter plot of the correlation coefficient for each of 266 movement episodes plotted against the length of the episode.

In Figure 6.2 the amplitude of the θ rhythm is largest near the center of the movement episode coinciding with the highest frequencies. Overall the amplitude of the θ rhythm was also found to be correlated with the rat's speed of locomotion. Figure 6.6 contains a plot of the θ rhythm amplitude against the animal's running speed. The correlation coefficient for the R149:o172 data set is 0.36, which is significantly less than the 0.57 the correlation with the speed. There appears to be only a slight increase in amplitude with increased speed. The θ rhythm amplitude reaches a plateau at 0.4 metre/second.

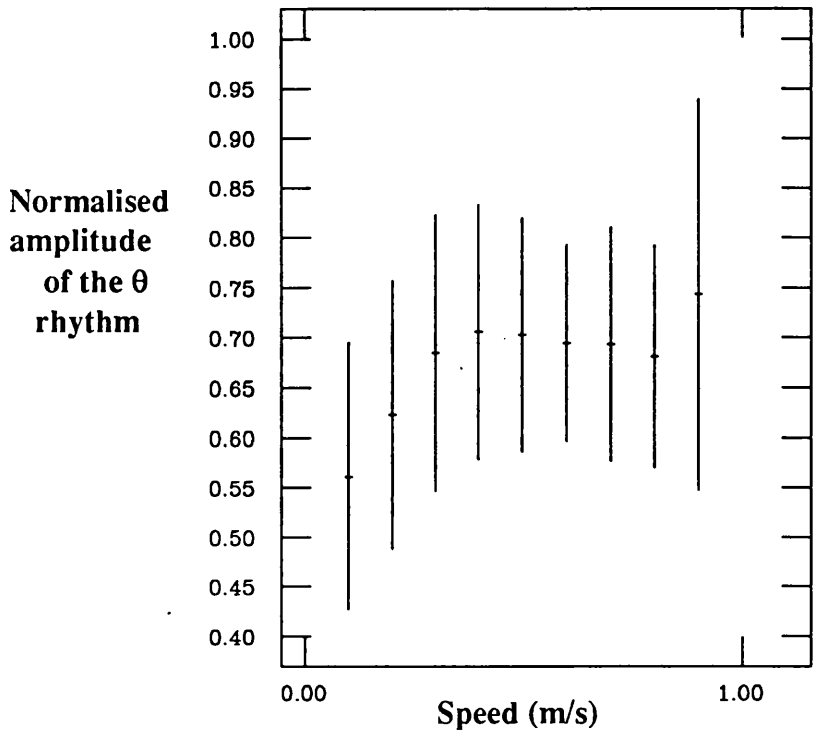

Figure 6.6 Correlation between the amplitude of each cycle of the θ rhythm and the running speed in the data from trial o172 in R149.

The instantaneous frequency of the θ rhythm, which is correlated with speed of movement, was computed from the time interval between sequential negative peaks (minima) in the recorded EEG. As described above, there are two independent parameters used in the determination of instantaneous frequency: (1) the length (or characteristic frequency) of the half sine wave template, and (2) the amount of time shift between successive fits to the EEG. When the rat runs faster, the corresponding higher frequency that is measured can be produced either by decreasing the width of the negative peak of the θ rhythm cycle, or by decreasing the time between two peaks without changing their shape.

In order to distinguish between these two possibilities the correlation between the frequency of the best fit template to the running speed was tested, and found to be not correlated. Therefore the θ rhythm periods are generated at a higher rate with increasing speed but the shape of the negative going part of the waveform is not affected. This point is discussed further in the next section.

Theta rhythm frequency predicts speed of movement

A correlation coefficient of 0.40 to 0.57 is not sufficient to explain all of the variation present in the data. On closer inspection an additional source of variation is evident. In Figure 6.7 the speed and computed frequency from Figure 6.2 are replotted and overlaid. The sequence of θ rhythm frequencies follows the same pattern as the sequence of speeds but the sequence of frequencies appears to finish earlier. This is either due to a systematic shift in time between the two sequences or to the fact that the sequence of frequencies occurs slightly faster than the sequence of speeds. To test these hypotheses one of the data sets was systematically shifted or compressed.

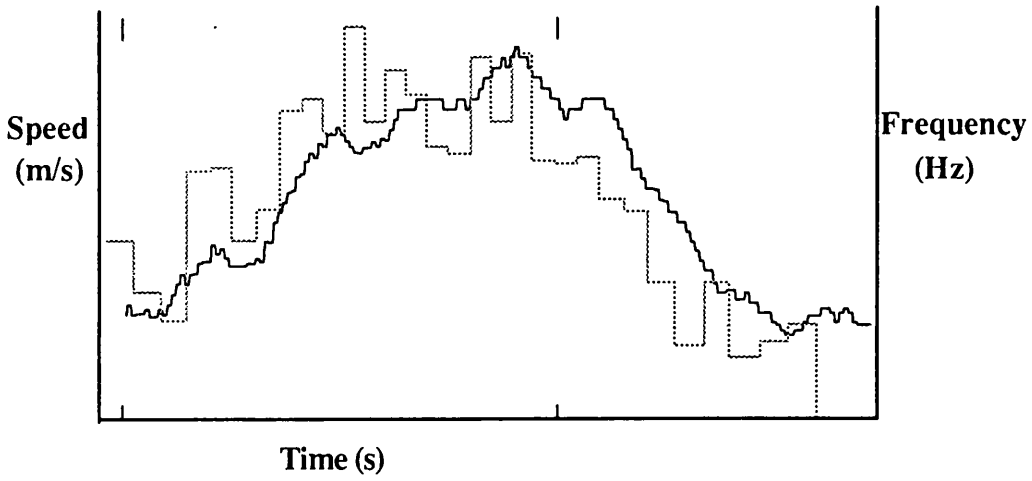

Figure 6.7 Movement episode from Figure 6.2 replotted with frequency (light shade) and speed overlaid. The time between the tick marks on the horizontal axis is two seconds.

The largest improvements in the correlation were found by keeping the sequence of θ rhythm frequencies and speeds time aligned at the beginning of the movement episode, but compressing the time axis of the speed data. This is equivalent to shifting the speed within a movement episode by an amount proportional to the time that has passed since the beginning of the movement. Figure 6.8 shows the result of a 15% compression of the speed data in the episode previously shown in Figure 6.3. For this episode the correlation coefficient has increased from 0.8 to 0.88, the slope of the regression line has increased from 3.8 to 4.2 and the y-intercept has decreased from 7.8 to 7.7 Hz.

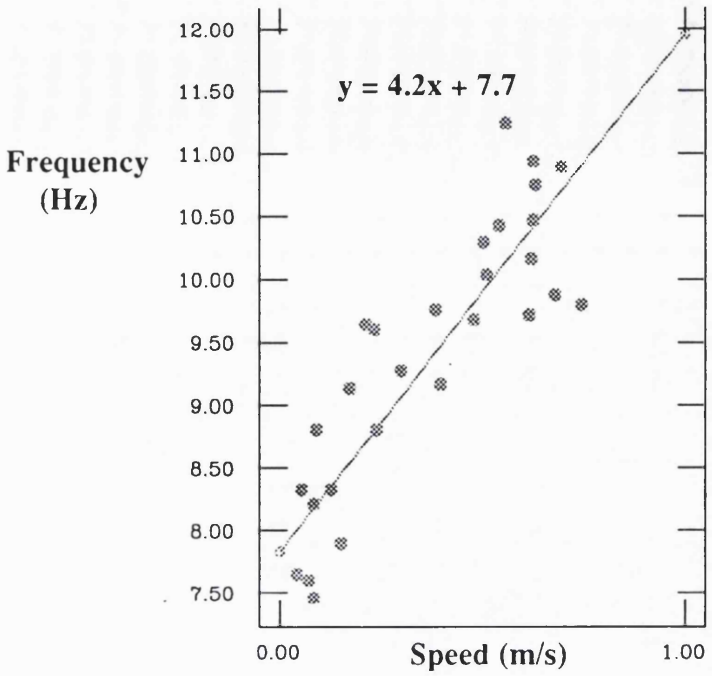

Figure 6.8 Correlation between the running speed and the θ rhythm for a movement episode in which the speed data has been compressed in along the time axis by 15%. The same data are plotted without compression in Figure 6.3.

The improvement in the correlation with this shift is even more evident in the set of 266 movement episodes previously shown in Figure 6.5. The correlation coefficients of these episodes, with speed data compressed by 15%, are replotted in Figure 6.9 as a function of the length of the episode. For these 266 movement episodes (9657 cycles of the θ rhythm) the overall Pearson correlation coefficient increased from 0.50 to 0.57, the slope of the regression line increased from 2.1 to 2.3, and the y-intercept increased from 8.4 to 8.5. More striking, however, are the changes in individual movement episodes. Clearly since the data are being compressed along the time axis, in this analysis there is greater dependence on correct determination of the beginning of an episode. Notice that the correlation coefficient significantly increases in the majority of the episodes (three to four second duration in Figure 6.9 vs. Figure 6.5) but decreases in some of the longer episodes. This decrease may be caused by two episodes that are grouped together into a single episode. This kind of error can occur if the animal stops for a sufficiently short period of time that the decrease in velocity is lost through filtering.

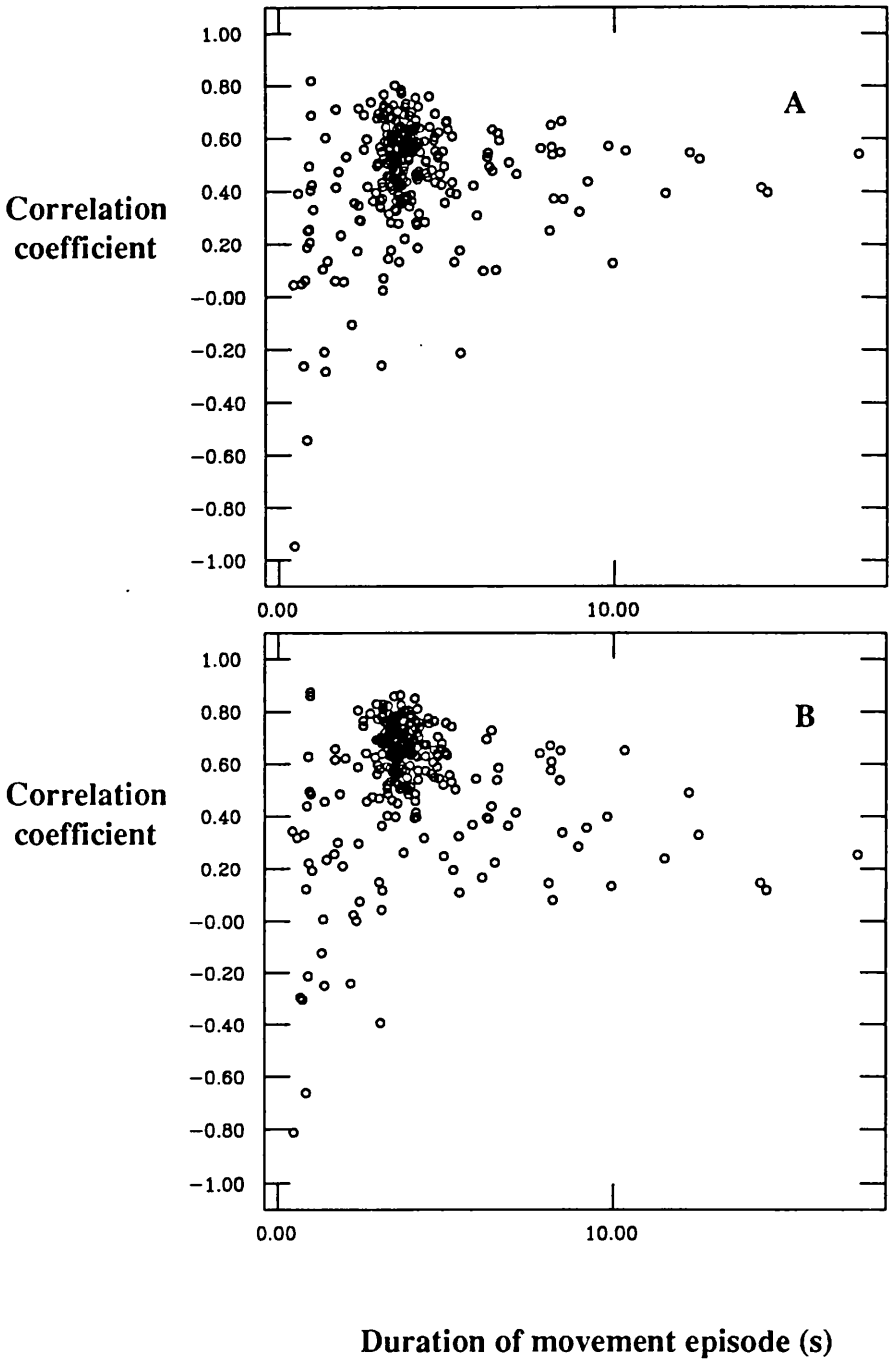

Figure 6.9 Scatter plots of the correlation coefficient for each of 266 movement episodes plotted against the length of the episode. (A) The data from Figure 6.5 are replotted for comparison with (B) the data in which the speed sequences have been compressed by 15% along the time axis, within each movement episode.

The improvement in the correlation between the θ rhythm frequency and the speed, that occured with this compression of the speed sequence time scale, was not present in all of the data sets. The average increase in the correlation coefficient in the two data sets from R149, and the data set from R173 was 0.077, but the correlation decreased in the the other data sets. In one case, the R42 data set, there was no significant correlation between the θ rhythm and the time compressed speed measurements.

6.3 Discussion

These results demonstrate a high degree of correlation between the speed of unrestricted movement in a rat and the frequency and of the monopolar recorded θ rhythm in region CA1 and in the dentate gyrus of the dorsal hippocampus. The best correlation is to the frequency, when found using a sine wave fit to each period of the θ rhythm.

Prior correlation studies of the θ rhythm frequency sought only to find an average correlation to continuous running at a fixed speed, and found inconsistent results. The present data show that the instantaneous frequency is linearly correlated with the speed and follows the same sequence of variations during normal movement episodes. Furthermore these data show that the sequence of frequencies begin at the same time as the sequence of speeds but ends earlier.

Consistency with prior studies

Evidence for the speed correlation of the θ rhythm is present in the literature, if one looks closely enough. Using a voltage triggered counter, McFarland et al. (1975) measured the rate that an EEG voltage threshold was crossed as a rat ran at four different slow speeds, with a duration of five minutes, on a treadmill. They found a linear correspondance between the trigger rate and the animals running speed. However, they did not measure the frequency directly and not give quantitative data on the amount of the frequency change, so it is not possible to compare the present data further with their results.

A related study was reported by Bland and Vanderwolf (1972), in which the θ rhythm and behaviour of rats were monitored following posterior hypothalamic stimulation. They measured the running speed in a wheel and the frequency of the θ rhythm as the intensity of the stimulus was increased. They found that for the first second after the stimulation pulse, there was a correlation between the stimulus voltage and both the running speed and the θ rhythm frequency. Their data are plotted as the θ rhythm frequency against the speed of running, after being averaged and converted to metric units, in Figure 6.10. These data, viewed in this way, are remarkably consistent with the new results described in this chapter. However, there are still several differences. Their results were based on a measurement of the average θ rhythm frequency and average running speed. Also the correlation that they found did not last beyond the first second.

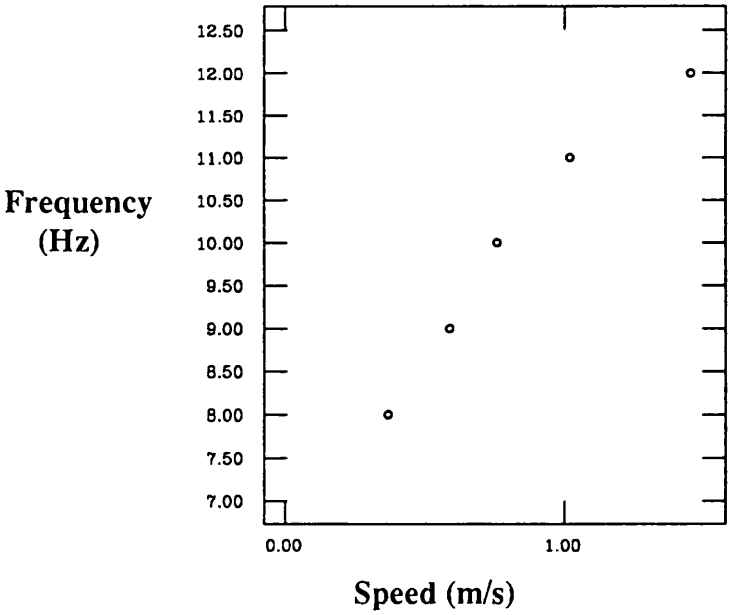

Figure 6.10 Correlation of the θ rhythm with wheel running speed, reproduced from a posterior hypothalamic stimulation experiment (Bland and Vanderwolf 1972).

Indirect suggestion of a correlation between the θ rhythm and the speed of movement can be found in the firing patterns of hippocampal neurons. McNaughton et al. (1983b) found that the firing rate of both complex spike cells and theta cells increased with speed of movement. In their data the increase in firing rate saturated

at about 0.3 metre/second, which is considerably lower than found in the present study. In part, the increase in firing rate is due to an increase in the spikes per period of the θ cycle, but a component due to increased frequency of cycles cannot be ruled out from the present findings. In contrast, Wiener et al. (1989) reported that each complex spike cell is tuned to a specific speed of movement, with decreasing firing rate at both higher and lower speeds.

Predicting the speed and location

In 1989 Muller and Kubie published results showing an improvement in the spatial specificity of place cell firing when the animal's location in space is shifted forward in time relative to the cell firing time, suggesting that the place cells were predicting the animal's location by approximately 100 to 200 milliseconds. Wiener et al. (1989), however, did not find this phenomenon in their data. One interpretation of this effect is that the head-lamp, used for tracking, was too far behind the animal's head. At a running speed of 0.1 metre/second, a prediction of 100 milliseconds corresponds to a one cm displacement of the head lamp. An alternative possibility is that there is a predictive component in the overall spatial function of the hippocampus. From the present data it is reasonable to suggest that the θ rhythm and some aspect of the place cell firing reflect a motor program that is passing through the hippocampus to generate a trajectory in space. This possiblility is discussed further in Chapter 8.

One of the implications of the present correlation analysis is that at the end of a five second movement episode the θ rhythm frequency, in some of the data sets, is predicting the movement speed by 750 msec. Other studies have found neuronal correlates that predict behaviour, but the apparent magnitude of this prediction is large in comparison.

The nature of the theta rhythm

It was previously suggested (Whishaw and Vanderwolf 1973) that the amplitude and frequency of the θ rhythm change independently in the normal rat; the θ rhythm amplitude was thought to reflect the number of cells firing and the θ frequency was considered a measure of vigour. In contrast, the present data show a correlation between frequency and amplitude in the normal rat. This finding, however, does not rule out the possibility that the amplitude and frequency can be uncoupled by pharmacological or other manipulations.

One interpretation of these data is that the θ rhythm can be described as a forced, damped harmonic oscillator. On this interpretation, the delay parameter reflects the forcing function that presumably originates in the medial septum, while the period of the sine wave is due to the dynamical properties of the oscillator itself. These may be identified with some aspect of the dynamics of the pyramidal and granule cells. The amplitude of the θ wave is due in part to the state of the oscillator at the time of the forcing function.

Implications for the cognitive map model

The result that the frequency increases with speed of locomotion alone only weakly supports the existence of stable sized place fields with changes in speed, and the cognitive map theory. At the beginning of this chapter it was suggested that a proportional change in the θ rhythm frequency with running speed would support the purported clocking function of the θ rhythm. The problem with this simple suggestion is that the best fit line to the data has a large y-intercept and a relatively small slope. This means that the change in θ rhythm frequency provides some correction but not enough to provide stable place fields.

An interesting possibility, previously suggested by O'Keefe (1985), is that two frequencies are combined to construct a stable wave packet. The superposition of two similar frequencies is a beat, and the wavelength of the envelope of the beat function is determined by the difference between the two composite frequencies.

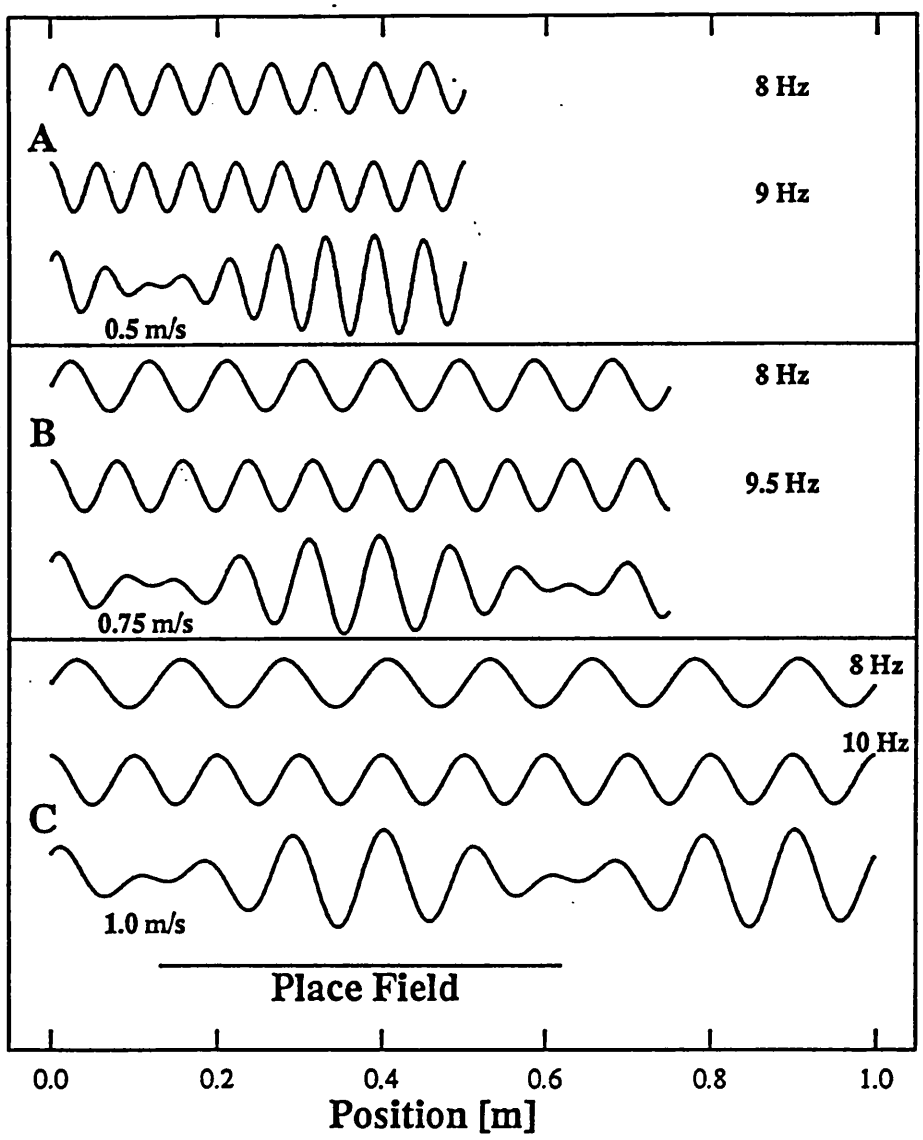

Figure 6.11 Model for constant place field size using beats. The three parts of the figure (A,B and C) each show the combination of two frequencies as a hypothetical rat runs for one second at a constant speed. One of the two frequencies is the value measured for the θ rhythm that corresponds, from the present data, to the speed in each part of the figure, and the second frequency is a fixed 8 Hz sine wave. Since the data are plotted with the animal's position on the x axis, the distance traveled in one second is different in each of the three cases. Note that the 8 Hz sine wave appears to change wavelength as the constant running speed is changed, but this is a result of plotting the data as a function of position. The result of combining the observed θ rhythm frequency with a fixed frequency of 8 Hz is a spatially stable wavepacket, which may represent a place field.

This idea may provide a mechanism for the construction of spatially stable place fields, as shown in Figure 6.11. In the figure a hypothetical rat is run along a linear track at a constant speed. Three different speeds are chosen to illustrate a potential mechanism for constructing place fields that begin and end at the same spatial location, independent of movement variables. In part A of Figure 6.11 the hypothetical rat is run for one second at 0.5 metre/second along the linear track. The first curve is a 8 Hz sine wave, which is assumed to be an intrinsic oscillation frequency inside the cell. The second curve in part A of the figure is a 9 Hz sine wave, which is approximately the frequency of the θ rhythm that corresponds to 0.5 metre/second in the present data. The third curve is a beat function, which is the sum of the 8 Hz and 9 Hz sine waves. Since the animal only travels 0.5 metre the curves stop at this point.

In part B of the figure the same 8 Hz fixed frequency is added to a 9.5 Hz sine wave, which again corresponds to the θ rhythm frequency for that speed in the present data. Note that the 8 Hz sine wave in part B appears to have a longer wavelength. This is the result of plotting the sine wave as a function of space instead of as a function of time. The envelope of the beat function in part B of the figure begins and ends at the same spatial locations as the envelope in part A. The frequencies were combined in part C of the figure for a constant speed of 1 metre/second, with the same result.

If the constant 8 Hz oscillator is inside the wavepacket or place field for each cell can be independently moved by slight phase changes in the internal oscillator. If for example the phase of the internal oscillator is shifted by 180° then the place field or wave packet would move by half of its spatial extent.

It is also important to note that the size of the envelope of the wave packet very closely corresponds to the size of the small place fields that were found in the linear track data. This model may explain the observed phenomenon that place fields are spatially well localised, independent of changes in the movement variables. The use of a wave packet to model the data is discussed further in Chapters 7 and 8.

Chapter 7: Phase Relationship Between the Theta Rhythm and Hippocampal Single Cells

7.1 Introduction

The last two chapters described results from experiments in which hippocampal place cell activity and the sinusoidal EEG θ rhythm were separately correlated to movement parameters. In both cases the higher resolution of the new computer-based methods resulted in data that alter and constrain hypotheses for the function of the hippocampus. At the same time, new questions were raised. For example, in Chapter 6 it was demonstrated that the frequency of the θ rhythm increases with higher speeds of movement in the rat, but the frequency change was not sufficient to produce place fields that were stable with variations in speed. However, the arguments about the maintenance or loss of stability assumed a fixed phase relationship between the place cell firing and the θ rhythm. In the experiments described in this chapter, this assumption is tested.

Several studies have found that hippocampal cell firing is phase-locked to the θ rhythm (Sinclair et al. 1982; Buzsaki et al. 1983; Fox et al. 1986; Otto et al. 1991). However, in all these cases the phase relationship was determined by measuring averages over long periods of recording. In the present experiments, instead of using the average phase correlates, the phase of place cell activity is examined independently for each cycle of the θ rhythm.

This relationship is important in determining both the true spatial coding performed by place cells and the timing conditions for synaptic change. Recently it has been shown that long term potentiation (LTP) preferentially occurs on the positive peak of the dentate θ rhythm (Pavlides et al. 1988), and there is some suggestion that the timing of the activity of pre- and postsynaptic cells determines the amount (Larson and Lynch, 1989) and possibly the direction of synaptic change (Stanton and Sejnowski 1989).

7.2 Methods

Following the procedures outlined in Chapter 4, Lister hooded rats were implanted with one or two microdrives, containing tetrodes. With two microdrives both hemispheres were used. Complex spike cells were recorded from either the CA1 or the CA3 region while the animal ran back and forth on a 1.5 m linear track for a food

reward at both ends. During the recording, the location of a DC lamp on the animal's head was tracked with an overhead camera and recorded together with the extracellular data (for more detail see Chapter 4). In each case the recorded data included the activity of several simultaneously recorded single neurons, which were separated following the methods described in Chapter 5. The time point at which each spike occurred was measured to within 20 μsec. The EEG was recorded at the same time, and stored in records with the complex spike data. Measurements of the EEG were made every 4.1 msec. The EEG data were collected either from the same microdrive as the complex spike cells or from the contralateral hippocampus.

The phase of hippocampal θ rhythm was computed for each spike. For this analysis the individual cycles of the EEG were extracted in the same way as previously described in Chapter 6. The positive to negative zero crossing that was measured as the beginning of the best fit template was treated as the beginning of a cycle (0°), and the ending of the prior cycle (360°). As described in Chapter 6, the frequency changed with movement speed, so the time period corresponding to one cycle of the θ rhythm varied.

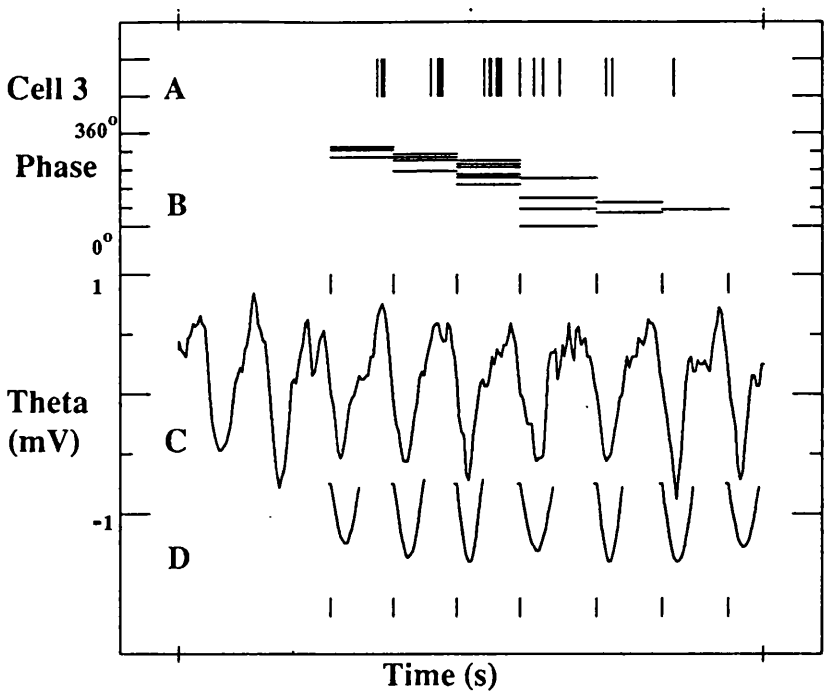

Figure 7.1 Extraction of the firing phase shift for each spike during a single run through the field of a CA3 place cell on the linear track. (A) shows each firing of cell 3 as a single vertical line during the one second of data. (B) represents the phase of each spike relative to the θ cycle within which it falls as a horizontal line. (C) shows the hippocampal θ activity recorded at the same time as the single place cell. In (D) the result of the template matching algorithm is shown. Note that the amplitude and the time between onsets of each template match varies to fit the variations in the θ rhythm. The small vertical ticks above the EEG and below the template fits mark the beginning of each θ cycle. The cell clearly fires six bursts of spikes during this run through the place field. Comparison of each burst with the concomitant θ wave shows that each successive burst fires at an earlier part of the θ rhythm. This is shown clearly by the descending staircase of the phase correlates in B. EEG voltage in C is +1 to -1 mV. Total time between marks on the x axis is 1 sec.

An example of the process used to find the phase of each spike is shown in Figure 7.1, which contains one second of data from a typical complex spike cell as the animal ran through the place field. Part A shows one vertical bar for each spike plotted against the time at which it was recorded, and Part C shows the EEG. At the bottom (D) are the best fit templates for each EEG cycle. A tick mark is plotted above the EEG and below the template to indicate the computed beginning of each cycle. In order to highlight the measured phase for each of the spikes, they are replotted in B as horizontal bars against the phase angle as the vertical axis.

The EEG phase of firing was determined relative to the location of the animal on the track and, separately, to the time from the beginning of the place field. The location on the maze was assessed by dividing the 1.5 m track into 256 bins of 0.58

cm each (the camera system pixel size). The time of each spike into the field was taken as the time after the animal crossed the point identified as the field onset (10% of maximum firing rate).

The correlation of the unit-EEG phase with each of the variables was determined by linear regression, or equivalently by finding the values of "m" and "b" which minimise

$$\Sigma_N(\phi - (mx + b))^2$$

for the N data pairs (x,ϕ). The standard approach cannot be used because the phase (ϕ) is periodic (360° = 0°), and large values would mistakenly be treated as far away from small values. Figure 7.2A contains an example data set, with the firing phase of each spike from a typical complex spike cell plotted against the position of the animal at the time of the spike. Since the phase is periodic, the data are actually distributed on the surface of the unit cylinder, which is constructed by joining the two dashed lines in the figure.

Conventional least squares minimisation with respect to m and b cannot be performed on these data, so the best fit line was found using exhaustive search. The distance of the data from 72,000 different lines was tested, and the best fit line was selected. Due to the rotational symmetry of the unit cylinder, the value for b must be between 0° and 360°, and in this analysis values for b were selected in steps of one degree. The slope of the line (m) took on values ranging from ten rotations in the clockwise direction over the length of the cylinder to ten rotations in the counterclockwise direction, in steps of ±0.01 turns. The distance between the data and the model was computed for each of the lines, and the best fit line was selected. The data were replotted (as in Fig.7.2B) with 360° added or subtracted from data points to unwrap them from the unit cylinder. It was then possible to compute the Pearson correlation coefficient for each data set.

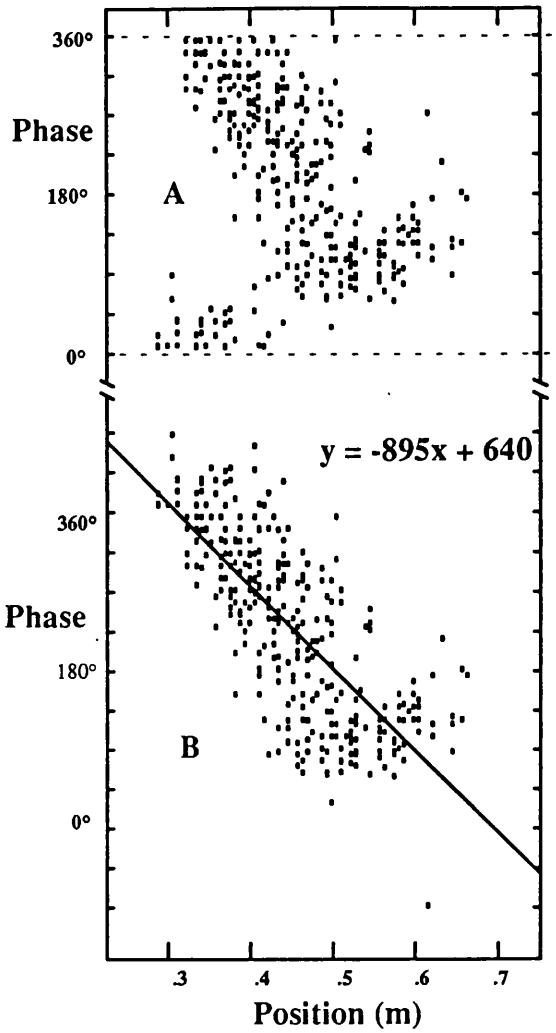

Figure 7.2 Histogram demonstration of the effect of the data mapping procedure to find the best fit line to periodic phase data for cell 8. (A) shows each spike location plotted against the phase of the θ wave. The spikes at the beginning of the field between 0.3 and 0.4 m on the track have clearly wrapped around the 0°/360° line and fall in the lower phase range. (B) portrays the data pattern that results from the application of the unwrapping program. Imagine that the graph of A has been cut along the dotted line and rolled into a unit cylinder. The cylinder is rotated until a single straight line can be drawn through the data points. Many of the points in the left lower part of the graph have been wrapped to the left upper quadrant, and it is clear that a straight line provides a good fit to these data.

7.3 Results

Basic observations

Data were collected from three rats at eight electrode placements that were observed to have at least one cell firing on the maze during the recording session. From these eight multi-unit clusters, 19 cells were isolated in the analysis phase: 15 were

classified as complex spike cells, three as theta cells and one as unclassified, on the basis of wave-shape and pattern of firing on the linear track. In this chapter data are presented only for the 15 complex spike cells. The location of each of these single cells within the hippocampus is given in Table 7.1, together with other statistics. There were eleven CA1 and four CA3 complex spike cells. Of the 15 complex spike cells, 14 had a single localised region of firing on the track as the animal ran in one direction but failed to fire above the 10% threshold rate along the rest of the track or in the opposite direction. One complex spike cell fired in both directions on the track but in symmetrical locations rather than in the same place. There were therefore 16 sets of runs from 15 complex spike cells available for the phase analysis.

Cell	Location	Firing Rate (spikes/s)	Field Size (bins)	Correlation (position)	Correlation (time in field)	Start Phase	End Phase	Phase Change	Slope (degrees/m)	Intercept (degrees)
1	1-CA1	10.4	11	0.59	0.21	390.3	102.7	287.6	-1,116	1,527.5
2	2-CA3	8.1	17	0.68	0.37	383.1	32.1	351	-880.8	888.8
3	2-CA3	24.1	10	0.56	0.4	344.8	157.8	187	-796.8	1,158.8
4	3-CA1	14.8	13	0.73	0.5	437.4	82.8	354.6	-1,164	887
5	4-CA1	21	23	0.67	0.52	193.5	-5.9	199.4	-369.6	-99
6	4-CA1	17.5	21	0.52	0.11	250.5	101.2	149.3	-302.4	474.5
7	4-CA1	8.8	10	0.65	0.6	308.6	6	302.6	-1,291.2	384.1
8	5-CA1	28.5	15	0.76	0.25	378.4	63.4	315	-895.2	640.8
9	6-CA1	11.8	26	0.74	0.67	442.5	120	322.5	528	-34.9
10	6-CA1	8.3	10	0.8	0.35	381.6	95.1	286.5	1,221.6	-1,266.1
11	6-CA1	7	14	0.46	0.54	405.3	305.8	99.5	-302.4	735.8
12	7-CA3	15.4	8	0.57	0.22	266.3	71.8	194.5	1,036.8	-986
13	7-CA3	6	12	0.78	0.61	334.2	6.2	328	1,166.4	-717.8
14	8-CA1	3.3	16	0.76	0.55	205.9	-64	269.9	720	-814.7
15	8-CA1	11.2	34	0.7	0.54	224.5	-24.1	248.6	312	-49.7
15b	8-CA1	4.7	29	0.54	0.37	215	-9.5	224.5	-328.8	450.7

Table 7.1 The location column contains the cluster number and hippocampal region. The firing rate is averaged over the place field and is in spikes x s^{-1}. The field size is in bins where 1 bin = 2.34 cm. The correlation (position) is the Pearson correlation coefficient of the phase vs. the location on the track, while the correlation (time) is the phase vs. the time after the start of the field. The start phase and end phase are taken from the best fit line at the two ends of the place field. The phase change is the difference between the start and end phases, and the slope and intercept are the parameters of the best fit line to the data. The slope is in degrees per metre and the intercept is in degrees.

Phase correlate of the place cells

A clear example of the phase shift phenomenon is shown in Figure 7.1. This CA3 cell fired a series of six bursts as the rat ran through the place field. Within the sequence, from the first to the last of these bursts, the midpoint of the cell firing occured at a successively earlier stage of the concomitant θ cycle. On average, the number of spikes within each burst increased towards the middle of the field and then decreased as the animal exited from the field, but this was not invariable from trial to trial. In some cells the phase shift was reduced towards the exit of the field.

In order to quantify the phase shift phenomenon, the θ waves were modelled with sinusoids and each spike in the field firing burst was assigned a phase correlate relative to the modelled wave. In order to assess the relationship of this phase to spatial aspects of behaviour, the phase of each spike was correlated with the animal's location on the maze. Figure 7.6 shows this correlation for place cell number 10, which was recorded from the CA1 region (EEG from 300 μm deeper in the CA1 field). It is clear that there is a good correlation with the location of the animal.

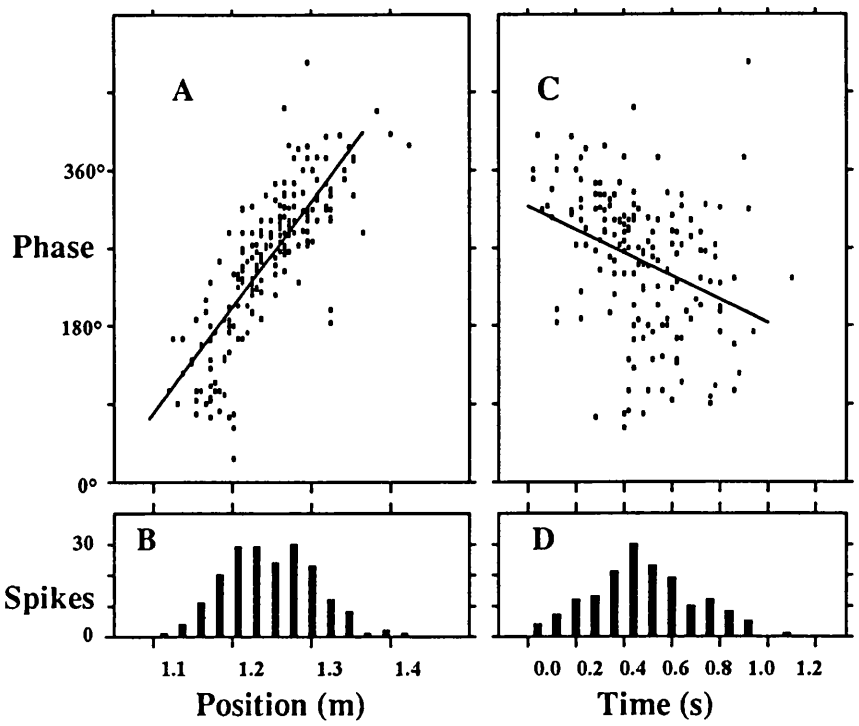

Figure 7.6 (A), plot of phase of cell 10 (CA1) (y axis) against position on the linear track (x axis). Hippocampal EEG was recorded from an electrode 300 μm deeper in the CA1 field than the unit recording electrode. Positive voltage up. 0°/360° phase was selected as described in the text. (B), number of spikes at each location on the track during the 41 runs used to construct the plot in A. (C), phase data from the same runs plotted against time after field entry. (D), number of spikes at each time after entry into field. Note that the correlation of phase with position ($p = 0.80$) is much better than the correlation with time into field ($p = 0.35$). Position calibration in B is for A and B, time calibration in D is for C and D.

One simple explanation of the phase shift phenomenon is that the positional correlate is secondary to a temporal correlate, that is, that each cell burst shifts by a fixed part of a θ cycle once the place field is entered, irrespective of the animal's speed (see Discussion). In order to test this possibility, the correlation of the phase with time after entry into the field was computed and compared with the phase vs. position correlation. Figure 7.6C shows the result of this analysis for cell 10. It is clear that the scatter of the spike phase vs. time is greater than for phase vs. position.

The application of these analyses to the set of 16 direction/runs substantiated the above findings. Table 7.1 column 5 shows the correlations of all the cells to location on the track, and column 6 to the time into the place field. In 15 of 16 cases the temporal correlation is lower than the corresponding spatial correlation, and this is reflected in the large difference between the averages (0.66 ± 0.026 s.e.m. vs. 0.42 ± 0.041).

However, in this analysis there is a bias against a possible temporal correlate of the phase shift. The temporal correlate depends on accurate determination of the time that the animal enters the place field. The start of the place field has been defined as the spatial location with 10% of the peak firing rate, which depends on accurate measurement of the firing rate. Since the firing rate is difficult to measure (as discussed in Chapter 3) the start of the field is also difficult to measure accurately. The accuracy of this measurement can be improved by using the centre of the place field (measured from the spatial centre of mass of all of the spikes). For the data presented in Figure 7.6, this improves the correlation coefficient for the temporal correlation (part C) from 0.35 to 0.39.

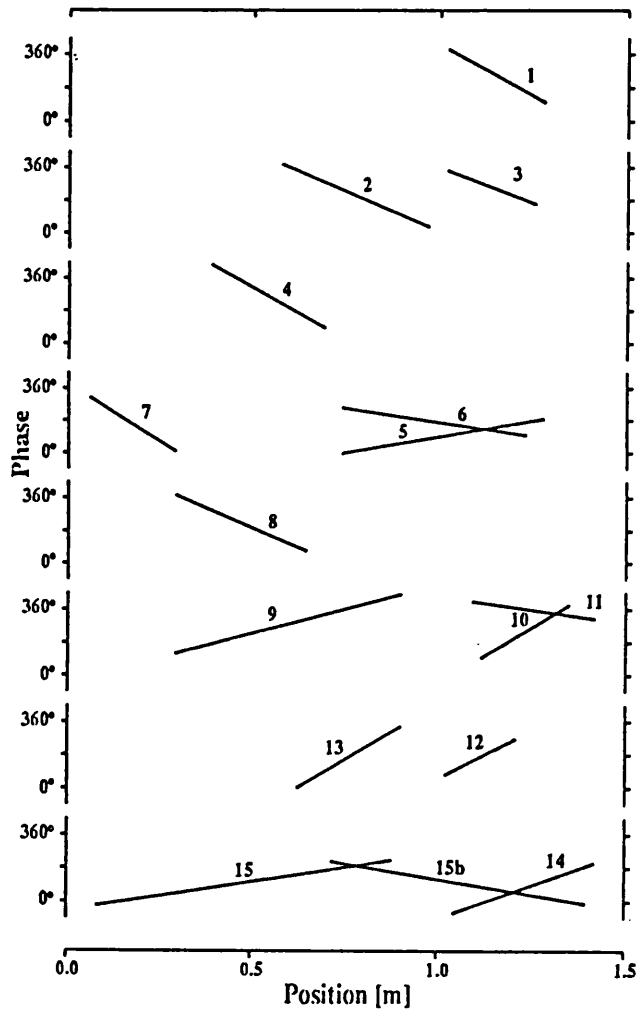

Figure 7.7 Phase profiles for the 15 place cells. Each of the eight sections represents one cluster. Phase shift is always in the descending direction, so that shifts which ascend from left to right are from cells that fired as the rat ran from right to left.

All place cells had phase shifts (range 100° to 355°) that were related to the animal's location on the maze. Figure 7.7 gives a graphic illustration of all the fits and Table 7.1 column 5 gives the numerical details. For a given cell, the phase shift began at approximately the same point of the θ cycle on each run, but this point varied from cell to cell. For all the data sets, the phase shift was in the same direction. The best fit lines in Figure 7.7 that have a negative slope correspond to cells that fire when the rat runs from left to right, whereas the lines with a positive slope are from cells that fire during movement in the other direction. As noted above, the relative phase amongst the EEG recording electrodes was not systematically recorded so no significance should be attributed to the absolute phase measures. There did not appear to be a relationship between the field sizes or the firing rate and the slope of the phase shift. The background firing rate of place cells outside the place fields was too low to determine the firing phase.

7.4 Discussion

The results of this experiment show that firing of hippocampal place cells is not locked to a constant phase of the θ rhythm. Instead the first burst of firing in the place field of a cell consistently occurs at a particular phase of the reference θ rhythm, and each successive burst systematically shifts to an earlier phase. This sequence of phase shifts often completes a full cycle as the animal runs through the place field, reaching a phase correlate at the end of the place field which is similar to that measured at the beginning of the place field. In the linear track environment, the overall phase shift within a place field does not exceed one cycle of precession independent of the speed at which the animal ran.

In this section, the present results are discussed in conjunction with findings in earlier studies. The present results suggest that the phase of a burst of place cell activity is a more accurate measure of the animal's spatial location than the firing rate of the cell. The implications of this result are discussed below, along with a description of mechanisms that could produce the phase shift phenomenon.

In previous studies (Buzsaki et al. 1983; Fox et al. 1986; Otto et al. 1991), the overall preferred θ rhythm phase of complex spike cell firing was reported from

averaged data. Fox et al. (1986) studied the firing correlates of hippocampal cells while the rat was running on a treadmill, and hence unlikely to be in the place field. They found that the main correlate of the CA3/4 complex spike cells on the treadmill was after the peak of the dentate θ rhythm positivity (at 19°), while the peak for the CA1 phase correlate was before the θ rhythm positivity (at 310°). In contrast, Buzsaki et al. (1983) found peaks at an earlier phase (270°) for CA3/4 and a later phase (0°) for CA1. Otto et al. (1991) found that the phase correlate of the first spike in each burst varied from 275° to 312° depending on the task. The present results cannot be compared directly to these previous findings, since the firing phase of the data from different electrode placements are not referred to the θ rhythm recorded in the same location. It is clear from the present data, however, that at least in the place field, the identification of a single phase correlate does not adequately describe the firing pattern of the cells. Instead, one must establish the phase as it changes across the field. The phenomenon can be characterised, instead, in terms of starting phase and total phase shift. The present data suggest that within any one cluster the phase onsets appear to be roughly the same, but nothing can be said about the phase relations between different parts of the hippocampus. The results have important implications for understanding the way in which place is represented by the complex spike firing.

Representation of spatial location

The results suggest that the place cells have a much higher spatial resolution on narrow armed mazes than had previously been thought (on the basis of experiments using firing rate as the sole measure of spatial information). Not only does the phase information provide a second measure of location which may be independent of firing rate, but in one sense it is superior. If we assume that most place fields are symmetrical and approximately Gaussian, then there is an ambiguity for any given level of firing rate as to whether the animal is on one side of the centre of the field or the other. No such ambiguity exists with the phase correlate, since it is a monotonic function of location, each phase identifying a unique location. Whether this also applies to open field situations in which the place cell firing is non-directional must

remain open at this point (see Muller et al. 1987). It is possible that the phase angle is the primary index of location and that the firing rate is secondary, or even carrying additional information. Since the background firing tends to occur at a constant phase, the start and end of the place field could be defined using the phase of the spikes. Furthermore, it suggests that the readout of hippocampal activity could be performed by phase-sensitive detectors. These downstream cells would be able to distinguish between activity in the field and either spontaneous out of field activity or spikes that occur during LIA.

Mechanism underlying the phase shift

The phase shift for each of the 15 cells fits well to a straight line, which can be explained only if the bursting rate of each cell has a higher frequency than the corresponding EEG θ rhythm. Figure 7.8 shows this effect for cell 3 where the autocorrelation of the cell is compared with the θ rhythm period taken from the EEG recorded as the animal ran through the field (i.e. excluding the data recorded outside the field). It is clear that the peak value of the θ rhythm period is slightly shifted to the right of the cell autocorrelation function, suggesting that the latter has a higher frequency than the former.

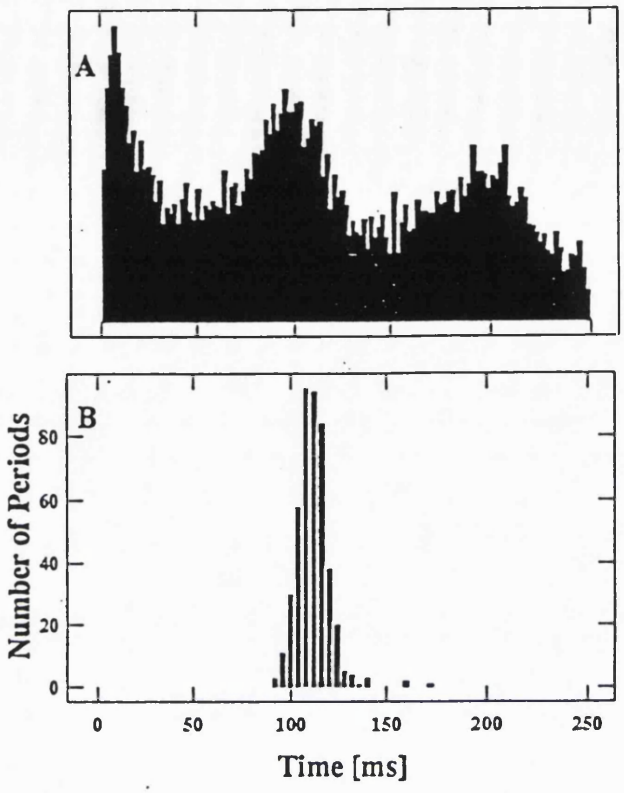

Figure 7.8 Comparison of the spike period and the EEG wave period. (A), autocorrelation of the spike data from cell 3. The y axis scale is in arbitrary units. Bin width is 2 msec. (B), interval histogram of the EEG periods derived from the sine wave fit program. Only θ waves during unit firing were used. Bin width is 4 msec. y axis shows the number of instances of each θ rhythm period within the place field. Note that the peak of the θ rhythm period in B is shifted to the right of the autocorrelation peak in A.

The simplest model of the bursting of place cells is that they are voltage-controlled oscillators (Hoppensteadt 1986) which are turned on for the spatial duration of the place field. The fact that the cells are bursting at a slightly higher frequency than the concurrent θ rhythm (Figure 7.8) is sufficient to lead to the observation of a phase shift between the two signals, even if they are not related to one another.

However, this does not account for the systematic occurrence of the first burst of spikes at a particular phase of the θ rhythm on each entry of the animal into the place field. Given this requirement, the EEG and place cell activity must be phase-locked for at least one instant during each entry of the animal into the place field. In addition, observation that the phase shift is limited to 360° or less suggests

that the θ rhythm and the place cell activity must be correlated for the duration of the run.

The correlation results illustrated in Figure 7.6 and presented in Table 7.1 provide clearer evidence that the correlation between the θ rhythm and place cell activity lasts for the duration of the movement. In general, the correlation between phase and time after field entry is considerably worse than the correlation between phase and position. As discussed, from the present data we cannot rule out the possibility that the difference between the spatial and temporal correlations is due to the fact that the method used to measure the temporal correlation introduces more variation. If the phase shift is more correlated to the animal's spatial location then on slower runs through the place field the phase shift must be less in each cycle of the θ rhythm so that the total phase shift, as a function of position, remains the same.

The deficiencies of the single oscillator model can be overcome if there are at least two different rhythmic generators operating within the system, and if they are oscillating at slightly different frequencies. Furthermore if the assumption is made that both of these oscillations are impinging on each cell, the generation of the firing pattern within the place field might be due to the interference patterns set up by the two oscillations (see O'Keefe 1985). There are several ways this could happen. First, consider the possibility that both oscillations are continuously impinging on the cell but that throughout most of an environment they are roughly of equal amplitude and of opposite phase, cancelling each other out or at best resulting in the occasional spike at the peak of one of the phases. Within the field, however, the frequency of one of the oscillators increases slightly relative to the other. Under these conditions the output of the cell, evinced in its firing pattern, will be represented by the interference pattern resulting from the summation of the two waves. Figure 7.9 illustrates this effect for waves of frequencies 9 and 11 Hz. The wave packet produced is governed by the general wave equation for the summation of two spatio-temporal sinusoids of differing frequencies:

$$y = 2a \cos[0.5(k_1 + k_2)x - 0.5(\omega_1 + \omega_2)t] \\ * \sin[0.5(k_1 - k_2)x - 0.5(\omega_1 - \omega_2)t]$$

where k is the spatial propagation number of each wave and ω is the angular frequency of the temporal component.

As can be seen, there are four components to this equation, two spatial and two temporal. The average difference of the two frequencies [e.g. the $0.5(\omega_1 - \omega_2)$ term] determines the period of the wave packet envelope (in the example, 1 Hz) while the average of the two frequencies [e.g. the $0.5(\omega_1 + \omega_2)$ term] gives rise to the oscillations within the wave packet (in the example, 10 Hz). The present suggestion is that the envelope of the wave packet determines the place field, while the amplitude of the beat oscillations determines the firing rate within the wave packet. Note, for example, that the amplitude of the oscillations within the wave packet rises and falls giving rise to the bell-shaped profile of the place field. Furthermore, if one assumes that one of the input waves is reflected in the frequency of the gross EEG θ rhythm, the model also predicts the precession of the phase shift. Note how the peak of the wave packet progressively moves to earlier phases of the B wave.

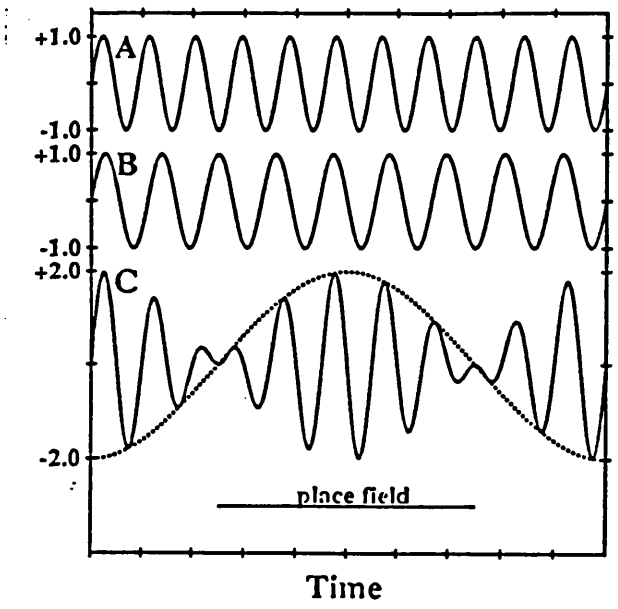

Figure 7.9 Interference pattern model of place field formation. Two sinusoids of the same amplitude but different frequencies (A, B) will sum to produce the pattern shown in (C). The top cosine (A) has a frequency of 11 Hz, the assumed rate at which the data are projected to the cell. The middle sine (B) has a frequency of 9 Hz, read from the EEG interval data. The bottom wave (C) oscillates with an average frequency of 10 Hz, and a beat frequency of 1 Hz. The firing in the place field is determined by the compound wave, with the amplitude of the + peaks determining the average phase relative to the EEG wave. The + phase of the slow beat wave (dotted line) determines the temporal extent of the field.

Alternative simple explanations of the phase shift are difficult to identify. For example, it might be thought that the depolarisation of the cell increased as the animal approached the centre of the field and then decreased as it moved out again, and that this interacted with a depolarising phase of the θ rhythm. This would explain the increased firing rate into the field and to some extent the precession forward, since the cell might tend to fire at an earlier point in time, when it was more depolarised. It fails, however, to account for the continued precession as the animal runs out of the field, coupled with a decrease in firing rate, unless an additional mechanism is invoked. This additional mechanism must be one that allows for an increased excitation to account for the continued precession and a decreased excitation to account for the decreased number of spikes per cycle.

Chapter 8: Discussion and Summary

Tiger got to hunt,
Bird got to fly,
Man got to sit and wonder "Why, why, why ..."

Tiger got to rest,
Bird got to land,
Man got to tell himself he understand.

Kurt Vonnegut Jr.

8.1 How is space represented in the activity of hippocampal cells?

This research has sought to test and extend the cognitive map model of hippocampal function, through measurements of the spatial correlates of extracellular neuronal activity in freely moving rats. New computer-based methods have been developed in order to achieve better isolation of the activity of individual neurons. Instead of using averages, measurements were made of the correlates of individual action potentials and single cycles of the θ rhythm. In this chapter new results found during this research are summarised and the implications of these results are discussed.

8.2 Tetrode based recording

Have single neurons been isolated yet?

In Chapter 1 it was argued that a method for measuring an unknown quantity needs to exceed the resolution requirements in order to ensure that the measurements are correct, or to show that a less powerful system would be sufficient. The present data demonstrate that if one wants to isolate single cells in the hippocampus convincingly, then any fewer than four electrodes is not enough. Furthermore, four electrodes are not guaranteed to solve the problem either. Currently, recording with four electrodes only sometimes meets, and does not exceed, the resolution requirements. In addition, based on the argument from geometry, more electrodes should not improve the performance of extracellular recording.

The next step will be the development of better electrodes and more precisely constructed tetrode bundles of electrodes. There was clear variation in the quality of recording between data sets, which is probably due to variations in the characteristics of the electrode tips. The quality of the recording depends on the impedance of each of the electrodes, the shape at the tip and the geometrical arrangement of the four electrodes in the bundle. It is also likely that other materials or sizes of tetrode, none of which were tested, could be better.

Improvements in single unit isolation will also be made with further development of clustering algorithms (see below), and metrics for testing how well separated the clusters are within a data set. As demonstrated in Chapter 5, these metrics can be used to direct the attention to the most fully isolated data, and therefore possibly the true correlates of the cells.

Place fields are smaller and more localised

The place fields measured with the tetrode are smaller and more localised than might have been found if the same data had been collected with less than four electrodes. It is likely that in many cases, the place cells that have been described in the literature were not single neurons. The same phenomenon is present in the firing rates. In much of the present data, place cells either have a small firing rate or are completely silent during movements outside of the place field. Some of the background firing attributed to place cells in the literature is probably a result of poor isolation of the activity of single cells.

An additional complication is the synchronous bursting that occurs during the LIA periods of hippocampal EEG (Ranck 1973), which can be misinterpreted as background firing. The template fitting method that is applied to single cycles of the EEG in Chapters 6 and 7 can be further developed and used to separate these action potentials from the rest of the data.

In some of the data sets, and in a large part of the linear track data, the firing rate distributions within place fields were single bell-shaped functions. There is some suggestion in the data that there may be a simple and uniform coding of places. In these data the locations of place field centres on the linear track appeared to be more aligned between animals than would have been expected if the place fields were randomly spatially located. Also the size of place fields in the linear track data did not appear to be randomly distributed. It was not possible to determine from the current data, but the sizes of place fields may form two groups, in which the average size of the larger place fields is nearly twice that of the smaller place fields. This also seems to be the case in the best of the data sets recorded in a two dimensional environment (see, for example, Figure 5.8). In this data set the place fields appear to be simple two dimensional bell

shaped functions, which are also clustered into two size groups. In addition the length of the smaller linear track cells is the same as the square root of the area of the smaller two dimensional place fields in the R164 data set.

If the neurons are part of an associative memory system, then the size of place fields and the number of cells with multiple place fields are important properties of the spatial code. However there are not sufficient data to analyse directly how the place cells could be part of an associative memory of spatial locations. In addition to the number of double fields, the fraction of hippocampal place cells active in a single location still needs to be measured. Thus far, the fraction of cells that are active has only been measured by comparing place coding with neuronal activity during sleep (Wilson and McNaughton 1993). A better measurement could be made with tetrodes that have a suitably constructed and precisely known tip geometry. In this case, it may be possible to determine the relative anatomical location of active neurons.

Performance of clustering algorithms

As described in Chapter 5, some of the clustering of the multi-unit data into the activity of single cells was performed using the k-means clustering algorithm. The performance of this algorithm was better than several others that were evaluated, but it was not sufficiently powerful to be used on all the data. During the present research several different methods for clustering neuronal activity were developed and evaluated. The first method developed was a variant of the CART algorithm (Breiman et al. 1984), which was used to construct clusters from the waveshape variation between individual spikes (Recce and O'Keefe 1989). Also a form of the back-propagation algorithm (Werbos 1974) was trained on a clustered subset of the data and then used to classify and filter the remainder of the data set (Callippi and Recce 1992). Finally, a variant of the Kohonen self-organising map algorithm (Kohonen and Makisara 1989) was used to find clusters in some of the data sets (Bilge and Recce unpublished). The goal was to make the process as objective and automatic as possible, but the problem has proved to be difficult. The most successful of these methods were incorporated into the analysis software, but the requirement remained for decisions made by the experimenter.

Several algorithms have been proposed for automatic clustering of multi-unit data (Abeles and Goldstein 1977; Dinning and Sanderson 1981; Gerstein et al. 1983; Schmidt 1984; Yang and Shamma 1988). However, in general these approaches are more suitable for cortical recording, where there is greater variation in wave shape. One complication in automatic clustering is the assumption that all of the noise is additive, and in the present data there is often a component of the noise which grows in proportion to the size of the spike. The changes in amplitude during a complex spike burst also make the clustering process more difficult.

More improvements are needed

In Chapter 5 it was argued that measurements of the properties of place cells in static environments are important to guide the development of theories of hippocampal function. This research has come some way towards making these measurements, but more data are required. At least three improvements are needed to obtain these data: (1) improvements in the quality of the electrodes, as discussed above, (2) a method for recording from many tetrodes at the same time, and (3) better measures of the spatial specificity of place cell firing. Recently, Wilson and McNaughton (1993) have demonstrated a system for recording simultaneously from twelve tetrodes, which is an important step towards obtaining these data. The third of the suggested improvements may be less critical if, with more data, the firing rate distribution of place cells ends up looking like a simple bell-shaped function.

8.3 Correlation between movement speed and the θ rhythm

A significant correlation was found between running speed and the frequency of the θ rhythm. The scale of frequency change was consistent among the animals that were tested. More variation was seen in the correlation of individual movement episodes. This may be due to the current simple approach used for tracking, which can lead to misinterpretation of some movements; or it may be that the correlation is to a component of the movement, rather than to full body movements. With these data it

was not possible to test whether the correlation was to head or to full body movements. Also it was suggested that different gaits or movement patterns might produce different correlations. Tests of this phenomenon will require the development of more sophisticated systems for tracking the animal's location and behaviour.

In the task that was used in these experiments the animal was usually making stereotyped movements, back and forth along a linear track. It was therefore not easy to find out whether this kind of correlation is present in other types of movement.

Most of the data contained a roughly 2 Hz change in frequency between the stationary state and movement at 1 metre/second. This frequency change will not produce a spatially stationary θ rhythm pattern (see, for example, Figure 5.6). It was suggested that stationary wave packets could be constructed if a hidden frequency of 8 Hz exists.

Movement episodes, saccades and motor programs

One surprising result in the present data is that, in some of the data sets, the sequence of frequency changes occurs on a compressed time scale to that of the actual movement. The movement episode appears to begin at the same time as the frequency changes, but ends later. In some cases this means that the frequency of the θ rhythm is predicting the speed of movment by over 750 msec. This type of prediction could only exist in planned or repeated movements, and it is easy to imagine how this phenomenon could be tested.

One interesting possibility is that body movements, like eye movements, are divided into two groups, one similar to smooth pursuit and the other like saccadic eye movements. Ideally, movements in animals or machines are controlled by continuously comparing the target location with an actual location, which is determined using some form of sensor. The problem with biological sensors is that they are very slow. When movements are made that are too fast to be measured and controlled through use of the sensors, then they must be made without the advantage of feedback. Perhaps displacement movements can also be divided into two similar types. This might explain

why the finding that place cell firing predicts spatial location (Muller and Kubie 1989) has not been replicated (Wiener et al. 1989). Perhaps during slow movements, in which sensory feedback is used, there is no prediction of location, whereas during fast movements not only the speed is predicted, but also the animal's future location.

A correspondence might also exist between these two hypothesised types of movement and methods for localisation in space. The localisation method most often used for the control of mobile robots is inertial. The total amount of movement in two cartesian directions and the total amount of rotation are monitored and accumulated. The current position is known only from the distance moved from the last location. Alternatively, in cue-based localisation the position is determined, as in modern maritime and aviation navigation systems, from measurements of the angle and distance to landmarks or beacons.

The two types of movement might correspond to the two forms of localisation. The suggestion here is that during cue-based localisation movements the activity of place cells might slightly follow the observation of cues. However, during fast movements the full trajectory is programmed through the map that is present in hippocampal place cells, providing a prediction of the target position within the environment.

8.4 The phase shift of place cell firing

The phase relationship between place cell firing and the hippocampal θ rhythm that was found from measurements of the phase of individual action potentials, was different from the phase-locked relationship that was previously suggested. The firing phase was shown to systematically shift as the animal ran through the place field, and the phase was shown to be most highly correlated with the animal's location in space. This finding has implications both for how spatial position is represented by place cell activity, and for the conditions for synaptic change within the hippocampus.

Synaptic changes

It is widely believed that learning involves synaptic modifications and that one important variable for this is the temporal relationship between different afferents onto a postsynaptic cell and between the pre- and post-synaptic activations (Collingridge and Bliss 1987). Recently, interest has developed in the relationship between the optimal parameters for synaptic enhancement and the firing patterns observed in freely moving animals (Larson and Lynch 1989; Otto et al. 1991). The pattern of firing associated with the phase shift places interesting conditions on the temporal relations between synaptically coupled cells and thus on the possibility that synaptic connection between place cells will be strengthened (or reduced) in a given environment.

One possibility is that the timing of the pre-synaptic input relative to the θ rhythm cycle is important. Pavlides et al. (1988) reported good long term potentiation if the electrically induced afferent barrages impinged on the cells during the positive phase of the dentate EEG, and no change or a decrease in synaptic efficacy if the inputs occurred at the negative phase. It is possible that afferent inputs to the cell at some phases in the θ cycle could be most effective in producing synaptic enhancement. This might mean that only spikes occurring at one part of the place field (e.g. at the edge of the field) would be effective in strengthening the synapses onto the downstream cells.

An alternative is that the absolute phase of theta at which the burst occurs is less relevant than the relative timing of the spikes in the two cells. In this case the relative spatial location of place cells could influence their synaptic coupling. Muller et al. (1991) have assumed that the synaptic coupling strength falls off as a monotonic function of the time between place cell activations, and therefore that cells with neighbouring fields will be more strongly coupled than those with distant ones. However, the phase shift phenomenon suggests that the relationship between synaptic coupling and place field location is more complex.

If it is assumed that the effective time window for synaptic modification is less than one θ rhythm cycle, and further, that all of the cells in a region of the hippocampus (e.g. the CA3 field) fire with a phase shifts that begins at the same phase of the θ

rhythm, as appears to be the case in the data shown in Figure 7.7. With this assumption it follows that the synaptic coupling function between connected cells of similar field sizes will not be a monotonic function of distance. Cells with completely overlapping fields will experience the strongest coupling, because the spike trains will coincide throughout each run through the fields (ignoring the delays introduced by the conduction and EPSP rise times). As the place field centres are shifted relative to each other, the time separating the bursts in one train will shift relative to those in the second spike train. At the point where one field centre is shifted to lie on the periphery of the second field (50% overlap of the fields) the temporal spike patterns will occur 180° out of phase with each other, and a maximum temporal disparity will be reached. As the fields separate even further, however, the spike bursts in one train will approach the bursts of the next θ cycle in the second train, and the temporal disparity will begin to decrease. The next maximum would occur at the point at which the fields were completely separated and abutting, but this maximum would not reach the same strength as the complete overlap condition, since only the spike bursts at the beginning and end of the trains would occur contemporaneously. The synaptic strengthening function, on this model, would have two peaks: a large one when complete overlap occurs, and a smaller one when fields are edge-abutting. If long term depression (LTD) exists, and can be shown to occur when two spike trains have a 180° phase relation, it would enhance the above effect.

This type of synaptic change could provide a mechanism for the construction of maps that have a uniform representation of spatial locations. Consider, for example, that in a new environment place cells have a fixed radius, but the centres of the place fields are randomly distributed. In this case many more place cells will be active in some random locations, as compared to others. However, as the animal explores the environment, only overlapping or abutting place fields will meet the conditions for synaptic change. Furthermore if interneurons suppress the activity of completely overlapping place cells then the number of place cells active in each spatial location will gradually become more uniform. However if the time window for synaptic change is

longer than one θ rhythm cycle, as some data suggest (Gustafsson and Wigström 1990) than this model will not hold.

8.5 Hidden frequency models

In the discussion sections of Chapters 6 and 7, second frequencies (other than the observed θ rhythm) and the notion that each pyramidal cell acts as an oscillator were suggested as a method to model how the place cell firing could have a stable spatial pattern. This model raises many questions for future consideration. The first concerns the origin of the two frequencies. One possibility is that they are both external to the hippocampus, and that the hippocampal cells are essentially passive devices whose sole function is to sum their inputs. The alternative view is that the hippocampal cells act as oscillators, perhaps as voltage controlled oscillators (Hoppensteadt 1986), whose dynamics translate input voltages to output frequencies. This leads to questions such as whether each cell has a fixed natural frequency, or alternatively whether the frequency varies with the environment. The phase shift vs. position curves for some cells are best approximated by straight lines, suggesting that the second input frequency in the field has a fixed difference from the EEG θ rhythm. In others (e.g. Figure 7.1) the curves may have a more sigmoidal shape, which would be more in keeping with a second frequency that rises, peaks and then falls. In some curves there is evidence of a lessening of the phase precession as the animal exits the field, which is clear evidence of a frequency reduction. There are several suggestions as to how the membrane and channel properties of single cells might enable them to oscillate either as individuals (Llinas 1988) or when imbedded in networks (Traub et al. 1989).

More work is required to fit these results within a single model. The speed correlation required a hidden frequency that was lower than the θ frequency, but the wave packets proposed in the discussion of the phase shift required a missing frequency that was higher than the θ rhythm frequency. It is not yet clear how this model can be extended to incorporate all of the new results. In particular, there is a problem in the model if all of the hidden frequencies are outside of the cell. In this case, each cell

might add the same two frequencies and it would be difficult to construct independent place fields for each of the two cells. However, if one of the hidden frequencies is internal to the cell then a place field that is constructed from a beat function can be shifted by changing the phase of the interal constant frequency oscillator.

Also the fact that, in some of the data sets, the sequence of changes in the θ rhythm frequency was found to predict the speed does not fit with the notion of spatially stable place fields. The model in which the θ rhythm frequency is combined with a hidden lower frequency to produce stable wave packets requires that the frequency changes at the same time that the speed changes. However, as suggested above, this may be explained by a difference in the way that the animal is moving through space. If it is using the cue-based navigation system then stable place fields occur, whereas if it is using an inertial navigation system the entire place field is predicted.

Suggestive new findings have resulted from this research, but many questions are left unanswered. There are hints of a simple spatial coding for environments, which further developments of the present methods may help resolve. The approach of looking at individual action potentials and cycles of the hippocampal θ rhythm has provided some new insight. However, changes in these variables will be easier to interpret if better simultaneous measurements are made of the animal's behaviour. The θ frequency correlation with the animal's speed can be further investigated with a more controlled task in which the animal can be asked to switch between the hypothesised navigation systems. Also, further theoretical work is necessary to piece together these new data into a better model of how the hippocampus represents spatial locations.

References

Abeles,M. and Goldstein,M.H. Multispike train analysis. *Proc.IEEE* 65:762-773, 1977.

Ainsworth,A., Gaffan,G.D., O'Keefe,J. and Sampson,R. A technique for recording units in the medulla of the awake, freely moving rat. *J.Physiol.* 202:80-82P, 1969.

Alonso,A. and Kohler,C. Evidence for separate projections of hippocampal pyramidal and non-pyramidal neurons to different parts of the septum in the rat brain. *Neurosci.Lett.* 31:209-214, 1982.

Alonso,A. and Kohler,C. A study of the reciprocal connections between the septum and the entorhinal area using anterograde and retrograde axonal transport methods in the rat brain. *J.Comp.Neurol.* 225:327-343, 1984.

Amaral,D.G. A Golgi study of cell types in the hilar region of the hippocampus of the rat. *J.Comp.Neurol.* 182:851-914, 1978.

Amaral,D.G. and Dent,J.A. Development of the mossy fibres of the dentate gyrus: I. A light and electron microscopic study of the mossy fibres and their expansions. *J.Comp.Neurol.* 195:51-86, 1981.

Amaral,D.G. and Witter,M.P. The three-dimensional organization of the hippocampal formation: a review of anatomical data. *Neuroscience* 31:571-591, 1989.

Amaral,D.G., Ishizuka,N. and Claiborne,B. Neurons, numbers and the hippocampal network. In: *Progress in Brain Research* 83, edited by J.Storm-Mathisen, J.Zimmer and O.P.Ottersen. Elsevier, Amsterdam, 1990.

Andersen,P., Eccles,J.C. and Loyning,Y. Location of postsynaptic inhibitory synapses on hippocampal pyramids. *J.Neurophysiol.* 27:592-607, 1964.

Andersen,P., Bliss,T.V.P. and Skrede,K.K. Lamellar organization of hippocampal excitatory pathways. *Exp.Brain Res.* 13:222-238, 1971.

Ballard,D.H. Interpolation coding: a representation for numbers in neural models. *Biol.Cybern.* 57:389-402, 1987.

Barnes,C.A., McNaughton,B.L. and O'Keefe,J. Loss of place specificity in hippocampal complex spike cells of senescent rat. *Neurobiol.Aging* 4:113-119, 1983.

Barnes,C.A., McNaughton,B.L., Mizumori,S.J.Y.. Leonard,B.W. and Lin,L.H. Comparison of spatial and temporal characteristics of neuronal activity in sequential stages of hippocampal processing. In: Understanding the Brain through the Hippocampus: the hippocampal region as a model for studying brain structure and function, *Progress in Brain Research* 83, edited by J.Storm-Mathisen, J.Zimmer and O.P.Ottersen. Elsevier, Amsterdam,1990.

Becker,J.T., Walker,J.A. and Olton,D.S. Neuroanatomical bases of spatial memory. *Brain Res.* 200:307-320, 1980.

Bennett,T.L. The electrical activity of the hippocampus and the process of attention. In: *The Hippocampus, Vol.2: Neurophysiology and Behavior*, edited by R.L.Isaacson and K.H.Pribram. Plenum Press, New York, 71-99, 1975.

Berger,T.W., Rinaldi,P.C., Weisz,D.J. and Thompson,R.F. Single-unit analysis of different hippocampal cell types during classical conditioning of rabbit nictitating membrane response. *J.Neurophysiol.* 50:1197-1219, 1983.

Berry,S.D. and Thompson,R.F. Prediction of learning rate from hippocampal EEG. *Science* 200:1298-1300, 1978.

Best,P.J. and Ranck,J.B. Reliability of the relationship between hippocampal unit activity and sensory-behavioral events in the rat. *Exp.Neurol.* 75:652-664, 1982.

Blackstad,T.W. Commissural connections of the hippocampal region in the rat, with special reference to their mode of termination. *J.Comp.Neurol.* 105:417-537, 1956.

Bland,B.H. and Vanderwolf,C.H. Diencephalic and hippocampal mechanisms of motor activity in the rat: effects of posterior hypothalamic stimulation on behavior and hippocampal slow wave activity. *Brain Res.* 43:67-88, 1972.

Bland,B.H., Andersen,P., Ganes,T. and Sveen,O. Automated analysis of rhythmicity of physiologically identified hippocampal formation neurons. *Exp.Brain Res.* 38:205-219, 1980.

Bland,B.H. The physiology and pharmacology of hippocampal formation theta rhythms. *Prog.Neurobiol.* 26:1-54, 1986.

Bland,B.H. and Colom,L.V. Preliminary observations on the physiology and pharmacology of hippocampal theta-off cells. *Brain Res.* 505:333-336, 1989.

Bliss,T.V.P. and Lømo,T. Long-lasting potentiation of synaptic transmission in the dentate area of the anaesthetized rabbit following stimulation of the perforant path, *J.Physiol.* 232:331-356, 1973.

Boss,B.D., Turlejski,K., Stanfield,B.B. and Cowan,W.M. On the numbers of neurons in fields CA1 and CA3 of the hippocampus of Sprague-Dawley and Wistar rats. *Brain Res.* 406:280-287, 1985.

Bostock,E., Muller,R.U. and Kubie,J.L. Experience-dependent modifications of hippocampal place cell firing. *Hippocampus* 1:193-206, 1991.

Brashear,H.R., Zaborszky,L. and Heimer,L. Distribution of GABAergic and cholinergic neurons in the rat diagonal band. *Neuroscience* 17:439-451, 1986.

Breese,C.R., Hampson,R.E. and Deadwyler,S.A. Hippocampal place cells: stereotypy and plasticity. *J.Neurosci.* 9:1097-1111, 1989.

Breiman,L., Friedman,J.H., Olshen,R.A. and Stone,C.J. *Classification and regression trees*. Wadsworth International Group, Belmont, California, 1984.

Brodmann,K. *Vergleichende Lokalizations lehre der Grosshirnrinde in inhren Prinzipien dargestelldt auf Grunde des Zellenbaues*, Leipzig: J.A.Barth, 1909.

Brummer,S.B. and Turner,M.J. Electrochemical considerations for safe electrical stimulation of the nervous system with platinum electrodes. *IEEE Trans.* BME-59-63, 1977.

Bullock,T.H., Buzsaki,G. & McClune,M.C. Coherence of compound field potentials reveals discontinuities in the CA1-subiculum of the hippocampus in freely-moving rats. *Neurosci.* 38:609-619, 1990.

Burgess,N., O'Keefe,J. and Recce,M. Using hippocampal `place cells' for navigation, exploiting phase coding. In: *Advances in Neural Information Processing Systems 5*, edited by S.J.Hanson, J.D.Cowan and C.L.Giles. Morgan Kaufmann, San Mateo, California, 929-936, 1993.

Buzsaki,G., Leung,L.W.S. and Vanderwolf,C.H. Cellular bases of hippocampal EEG in the behaving rat. *Brain Res.Rev.* 6:139-171,1983.

Buzsaki,G. Hippocampal sharp waves: their origin and significance. *Brain Res.* 398:242-252, 1986.

Callippi,C. and Recce,M. Classifying and filtering hippocampal spikes with back-propagation neural networks. In: *Proc.IJCNN*, Beijing, China, 1992

Chan,D. A topographical analysis of hippocampal field connectivity in the rat. Ph.D. thesis 1992.

Chan,D., Al Dulaimi,D. and O'Keefe,J. Patterns of connectivity in the hippocampal formation of the rat. *Soc.Neurosci.Abstr.* 18:323, 1992.

Christian,E.P. and Deadwyler,S.A. Behavioral functions and hippocampal cell types: evidence for two nonoverlapping populations in the rat. *J.Neurophysiol.* 55:331-348, 1986.

Christian,E.P. and Dudek,F.E. Electrophysiological evidence from glutamate microapplications for local excitatory circuits in the CA1 area of rat hippocampal slices. *J.Neurophysiol.* 59:110-123, 1988.

Claiborne,B.J., Amaral,D.G. and Cowan,W.M. A light and electron microscopic analysis of the mossy fibres of the rat dentate gyrus. *J.Comp.Neurol.* 246:435-458, 1986.

Cocatre-Zilgien,J.H. and Delcomyn,F. A slope-based approach to spike discrimination in digitized data. *J.Neurosci.Meth.* 33:241-249, 1990.
Cohen,N.J. and Eichenbaum,H. The theory that wouldn't die: a critical look at the spatial mapping theory of hippocampal function. *Hippocampus* 1:265-268, 1991.

Collingridge,G.L. and Bliss,T.V.P. NMDA receptors: their role in long-term potentiation. *TINS* 10:288-293, 1987.

Colom,L.V. and Bland,B.H. State-dependent spike train dynamics of hippocampal formation neurons: evidence for theta-on and theta-off cells. *Brain Res.* 422:277-286, 1987.

Crawford,I.L. and Connor,J.D. Localization and release of glutamic acid in relation to the hippocampal mossy fibre pathway. *Nature* 244:442-443, 1972.

Deadwyler,S.A., Biela,J., Rose,G., West,M. and Lynch,G. A microdrive for use with glass or metal microelectrodes in recording from freely-moving rats. *Electroenceph.Clin. Neurophysiol.* 47:752-754, 1980.

Dietz,V., Bischofberger,E., Wita,C. and Freund,H.J. Correlation between the discharges of two simultaneously recorded motor units and physiological tremor. *Electroenceph.Clin.Neurophysiol.* 40:97-105, 1976.

Dinning,G.J. and Sanderson,A.C. Real-time classification of multiunit neural signals using reduced feature sets. *IEEE Trans.* BME-28:804-811, 1981.

Dymond,A.M. Characteristics of the metal-tissue interface of stimulation electrodes. *IEEE Trans.* BME-23:274-280, 1976.

Ebner,T.J. and Bloedel,J.R. Correlation between activity of Purkinje cells and its modification by natural peripheral stimuli. *J.Neurophysiol.* 45:948-960, 1981.

Eichenbaum,H., Kuperstein,M., Fagan,A. and Nagode,J. Cue-sampling and goal-approach correlates of hippocampal unit activity in rats performing an odor discrimination task. *J.Neurosci.* 7:716-732, 1987.

Eichenbaum,H. and Cohen,N.J. Representation in the hippocampus: what do hippocampal neurons code? *TINS* 11:244-248, 1988.

Eichenbaum,H., Wiener,S.I., Shapiro,M.L. and Cohen,N.J. The organization of spatial coding in the hippocampus: a study of neural ensemble activity. *J.Neurosci.* 9:2764-2775, 1989.

Eichenbaum,H., Stewart,C. and Morris,R.G.M. Hippocampal representation in place learning. *J.Neurosci.* 10:3531-3542, 1990.

Eichenbaum,H., Otto,T. and Cohen,N.J. The hippocampus - what does it do? *Behav.Neural Biol.* 57:2-36, 1992.

Finch,D.M. and Babb,T.L. Neurophysiology of the caudally directed hippocampal efferent system in the rat: projections to the subicular complex. *Brain Res.* 197:11-26, 1980.

Finch,D.M. and Babb,T.L. Demonstration of caudally directed hippocampal efferents in the rat by intracellular injection of horseradish peroxidase. *Brain Res.* 214:405-410, 1981.

Finch,D.M., Derian,E.L. and Babb,T.L. Demonstration of axonal projections of neurons in the rat hippocampus and subiculum by intracellular injection of HRP. *Brain Res.* 271:201-216, 1983.

Fontani,G. and Vegni,V. Hippocampal electrical activity and behaviour in rabbits during adaptation to a novel semi-natural environment. *Eur.J.Neurosci.* 2:203-210, 1990.

Foster,T.C., Christian,E.P., Hampson,R.E., Campbell,K.A. and Deadwyler,S.A. Sequential dependencies regulate sensory evoked responses of single units in the rat hippocampus. *Brain Res.* 408:86-96, 1987.

Foster,T.C., Castro,C.A. and McNaughton,B.L. Spatial selectivity of rat hippocampal neurons is dependent on preparedness for movement. *Science* 244:1580-1582, 1989.

Fox,S.E. and Ranck,J.B. Localization and anatomical identification of theta and complex spike cells in dorsal hippocampal formation of rats. *Exp.Neurol.* 49:299-313, 1975.

Fox,S.E. and Ranck,J.B. Electrophysiological characteristics of hippocampal complex-spike cells and theta cells. *Exp.Brain Res.* 41:299-410, 1981.

Fox,S.E., Wolfson,S. and Ranck,J.B. Hippocampal theta rhythm and the firing of neurons in walking and urethane anesthetized rats. *Exp.Brain Res.* 62:495-508, 1986.

Frotscher,M., Leranth,C.S., Lubbers,K. and Oertel,W.H. Commissural afferents innervate glutamate decarboxylase immunoreactive non-pyramidal neurons in the guinea pig hippocampus. *Neurosci.Lett.* 46:137-143, 1984.

Frotscher,M. Mossy fibres form synapses with identified pyramidal basket cells in the CA3 region of the guinea pig hippocampus: a combined Golgi-electron microscope study. *J.Neurocytol.* 14:245-259, 1985.

Frotscher,M., Seress,L., Schwerdtfeger,W.K. and Buhl,E. The mossy cells of the fascia dentata: a comparative study of their fine structure and synaptic connections in rodents and primates. *J.Comp.Neurol.* 312:145-163, 1991.

Fuxe,K. Evidence for the existence of monoamine neurons in the central nervous system. IV. The distribution of monoamine nerve terminals in the central nervous system. *Acta Physiol.Scand.* 64:37-85, 1965.

Gaarskjaer,F.B. Organization of the mossy fibre system of the rat studied in extended hippocampi. I. Terminal area related to number of granule and pyramidal cells. *J.Comp.Neurol.* 178:49-72, 1978.

Gaarskjaer,F.B. The hippocampal mossy fibre system of the rat studied with retrograde tracing techniques. Correlation between topographic organization and neurogenetic gradients. *J.Comp.Neurol.* 203:717-735, 1981.

Gardner-Medwin,A.R. The recall of events through the learning of associations between their parts. *Proc.R.Soc.Lond.B* 194:375-402, 1976.

Georgopoulos,A.P., Kettner,R.E. and Schwartz,A.B. Primate motor cortex and free arm movements to visual targets in three-dimensional space. II. Coding of the direction of movement by a neuronal population. *J.Neurosci.* 8:2928-2932, 1988.

Germroth,P., Schwerdtfeger,W.K. and Buhl,E.H. Ultrastructure and aspects of functional organization of pyramidal and nonpyramidal entorhinal projection neurons contributing to the perforant path. *J.Comp.Neurol.* 305:215-231, 1991.

Gerstein,G.L., Bloom,M.J., Espinosa,I.E., Evanczuk,S. and Turner,M.R. Design of a laboratory for multineuron studies. *IEEE Trans.* SMC-13:668-675, 1983.

Gochin,P.M., Miller,E.K., Gross,C.G. and Gerstein,G.L. Functional interactions among neurons in inferior temporal cortex of the awake macaque. *Exp.Brain Res.* 84:505-516, 1991.

Golgi,C. *Sulla fina anatomia degli organi centrali sistema nervoso.* U.Hoepli, Milan, 1886.

Gray,C.M. and Singer,W. Stimulus-specific neuronal oscillations in orientation columns of cat visual cortex. *Proc.Natl.Acad.Sci.USA* 86:1698-1702, 1989.

Gray,J.A. and Ball,C.G. Frequency-specific relation between hippocampal theta rhythm, behavior and amobarbital action. *Science, N.Y.* 168:1246-1248, 1970.

Gray,J.A. Medial septal lesions, hippocampal theta rhythm and the control of vibrissal movement in the freely-moving rat. *Electroencephalogr.Clin.Neurophysiol.* 30:189-197, 1971.

Gray,J.A. *The Neuropsychology of Anxiety, an enquiry into the functions of the septo-hippocampal system.* Oxford University Press, Oxford, 1982.

Green,J.D. and Arduini,A. Hippocampal electrical activity in arousal. *J.Neurophysiol.* 17:533-557, 1954.

Green,J.D., Maxwell,D.S., Schindler,W.J. and Stumpf,C. Rabbit EEG "theta" rhythm: its anatomical source and relation to activity in single neurons. *J.Neurophysiol.* 23:403-420, 1960.

Green,J.D., Maxwell,D.S. and Petsche,H. Hippocampal electrical activity. III. Unitary events and genesis of slow waves. *Electroenceph.Clin.Neurophysiol.* 13:854-867, 1961.

Grinvald,A., Lieke,E., Frostig,R.D., Gilbert,C.D. and Wiesel,T.N. Functional architecture of cortex revealed by optical imaging of intrinsic signals. *Nature* 324:361-364, 1986.

Gustaffssn,B. and Wigström, H. Basic features of long-term potentiation in the hippocampus. *Seminars in Neuroscience* 2:321-333, 1990.

Haug,F.M.S. Heavy metals in the brain. *Adv.Anat.Embryol.Cell Biol.* 47:1-71, 1973.

Hebb,D.O. *The Organization of Behavior.* John Wiley, New York, 1949.

Heimer,L. Synaptic distribution of centripetal and centrifugal nerve fibers in the olfactory system of the rat: an experimental anatomical study. *J.Anat.* 103:413-432, 1968.

Hess,B.J.M., Blanks,R.H.I., Lannou,J. and Precht,W. Effects of kainic acid lesions of the nucleus reticularis tegmenti pontis on fast and slow phases of vestibulo-ocular and optokinetic reflexes in the pigmented rat. *Exp.Brain Res.* 74:63-79, 1989.

Hill,A.J. First occurrence of hippocampal spatial firing in a new environment. *Exp.Neurol.* 62:282-297, 1978.

Hill,A.J. and Best,P.J. Effects of deafness and blindness on the spatial correlates of hippocampal unit activity in the rat. *Exp.Neurol.* 74:204-217, 1981.

Hoppensteadt,F.C. *An Introduction to the Mathematics of Neurons.* Cambridge University Press, Cambridge, 1986.

Hubbard,J.I., Llinas,R. and Quastel,D.M.J. *Electrophysiological Analysis of Synaptic Transmission.* Camelot Press, London, 1969.

Hubel,D.H. and Wiesel,T.N. Functional architecture of macaque monkey visual cortex. *Proc.R.Soc.* 198:1-59, 1977.

Hull,C.L. The goal gradient hypothesis and maze learning. *Psychol.Rev.* 39:25-43, 1932.

Insausti,R., Amaral,D.G. and Cowan,W.M. The entorhinal cortex of the monkey. 2. Cortical afferents. *J.Comp.Neurol.*264:356-395, 1987[a].

Insausti,R., Amaral,D.G. and Cowan,W.M. The entorhinal cortex of the monkey. 3. Subcortical afferents. *J.Comp.Neurol.* 264:396-408, 1987[b].

Ishizuka,N., Weber,J. and Amaral,D.G. Organization of intrahippocampal projections originating from CA3 pyramidal cells in the rat. *J.Comp.Neurol.* 295:580-623, 1990.

Jansen,R.F. The reconstruction of individual spike trains from extracellular multineuron recordings using a neural network emulation program. *J.Neurosci.Meth.* 35:203-213, 1990.

Jarrard,L.E. On the role of the hippocampus in learning and memory in the rat. *Behav.Neural Biol.* 60:9-26, 1993.

Jung,M.W. and McNaughton,B.L. Spatial selectivity of unit activity in the hippocampal granular layer. *Hippocampus* 3:165-182, 1993.

Jung,R. and Kornmüller,A.E. Eine methodik der ableitung lokalisierter Potentialschwankungen aus subcorticalen Hirngebieten. *Arch.Psychiat.* 109:1-30, 1938.

Kandel,E.R. and Spencer,W.A. Electrophysiology of hippocampal neurons. II. After-potentials and repetitive firing. *J.Neurophysiol.* 24:243-259, 1961

Kjaerheim,A. and Blackstad,T.W. Special axo-dendritic synapses in the hippocampal cortex: electron and light microscopic studies on the layer of mossy fibres. *J.Comp.Neurol.* 117:133-159, 1961.

Klemm,W.R. Correlation of hippocampal theta rhythm, muscle activity and brain-stem reticular formation activity. *Commun.Behav.Biol.* 5:147-151, 1970.

Knowles,W.D. and Schwartzkroin,P.A. Local circuit synaptic interactions in hippocampal brain slices. *J.Neurosci.* 1:318-322, 1981.

Kohler,C. and Steinbusch,H. Identification of serotonin and non-serotonin-containing neurons of the midbrain raphe projecting to the entorhinal area and the hippocampal formation. A combined immunohistochemical and fluorescent retrograde tracing study in the rat brain. *Neuroscience* 7:951-975, 1982.

Kohler,C., Chan-Palay,V. and Wu,J-Y. Septal neurons containing glutamic acid decarboxylase immunoreactivity project to the hippocampal region in the rat brain. *Anat.Embryol.* 169:41-44, 1984.

Kohler,C. A projection from the deep layers of the entorhinal area to the hippocampal formation in the rat brain. *Neurosci.Lett.* 56:13-19, 1985[a].

Kohler,C. Intrinsic projections of the retrohippocampal region in the rat brain. 1. The subicular complex. *J.Comp.Neurol.* 236:504-522, 1985[b].

Kohonen,T. and Makisara,K. The self-organizing feature maps. *Physica Scripta* 39:168-172, 1989.

Kosel,R.C., van Hoesen,G.W. and West,J.R. Olfactory bulb projections to the parahippocampal area of the rat. *J.Comp.Neurol.* 198:467-482, 1981.

Kramis,R.C., Vanderwolf,C.H. and Bland,B.H. Two types of hippocampal slow activity in both the rabbit and the rat: relations to behaviour and effects of atropine, diethulether, urethane and pentobarbital. *Exp.Neurol.* 49:58-85, 1975.

Kruger,J. and Bach,M. Simultaneous recording with 30 microelectrodes in monkey visual cortex. *Exp.Brain Res.* 41:191-194, 1981.

Kubie,J.L. and Ranck,J.B. Sensory-behavioral correlates in individual hippocampus neurons in three situations: space and context. In: *Neurobiology of the Hippocampus*, edited by W.Seifert. Academic Press, London, 433-447, 1983.

Kubie,J.L. A driveable bundle of microwires for collecting single-unit data from freely-moving rats. *Physiol.Behav.* 32:115-118, 1984.

Kubie,J.L., Muller,R.U. and Bostock,E. Spatial firing properties of hippocampal theta cells. *J.Neurosci.* 10:1110-1123, 1990.

Kuperstein,M. and Eichenbaum,H. Unit activity, evoked potentials and slow waves in the rat hippocampus and olfactory bulb recorded with a 24-channel microelectrode. *Neuroscience* 15:703-712, 1985.

Laatsch,R.H. and Cowan,W.M. Electron microscopic studies of the dentate gyrus of the rat. I. Normal structure with special reference to synaptic organization. *J.Comp.Neurol.* 128:359-396, 1966.

Lacaille,J.C., Mueller,A.L., Kunkel,D.D. and Schwartzkroin,P.A. Local circuit interactions between oriens/alveus interneurons and CA1 pyramidal cells in hippocampal slices: electrophysiology and morphology. *J.Neurosci.* 7:1979-1993, 1987.

Larson,J. and Lynch,G. Theta pattern stimulation and the induction of LTP: the sequence in which synapses are stimulated determines the degree to which they potentiate. *Brain Res.* 489:49-58, 1989.

Lecas,J.C. and Dutrieux,G. Head movements and actographic recordings in free-moving animals, using computer analysis of video images. *J.Neurosci.Meth.* 9:357-365, 1983.

Leranth,C., Deller,T. and Buzsaki,G. Intraseptal connections redefined: lack of a lateral septum to medial septum path. *Brain Res.* 583:1-11, 1992.

Lewis,P.R. and Shute,C.C.D. The cholinergic limbic system: projections of hippocampal formation, medial cortex, nuclei of the ascending cholinergic reticular system, and the subfornical organ and supra-optic crest. *Brain Res.* 90:521-540, 1967.

Liang,J.J. and Clarson,V. A new approach to classification of brainwaves. *Patt.Recog.* 22:767-774, 1989.

Llinás,R.R. The intrinsic electrophysiological properties of mammalian neurons: insights into central nervous function. *Science* 242:1654-1664, 1988.

Lorente de Nó,R. Studies on the structure of the cerebral cortex. I. The area entorhinalis. *J.Psychol.Neurol.* 45.6:381-438, 1933.

Lorente de Nó,R. Studies on the structure of the cerebral cortex. II. Continuation of the study of the ammonic system. *J.Psychol.Neurol.(Leipzig)* 46:113-177, 1934.

MacQueen,J. Some methods of classification and analysis of multivariate observations. In L.M. LeCam and J. Neyman, editors, *Proc. 5th Berkeley Symposium on Math., Stat., and Prob.*, p. 281. U. California Press, Berkeley, CA, 1967.

McFarland,W.L., Teitelbaum,H. and Hedges,E.K. Relationship between hippocampal theta activity and running speed in the rat. *J.Comp.Physiol.Psychol.* 88:324-328, 1975.

McNaughton,B.L. and Nadel,L. Hebb-Marr networks and the neurobiological representation of action in space. In: *Neuroscience and Connectionist Theory*, edited by M.A.Gluck and D.E.Rumelhart. Lawrence Erlbaum Associates, Hillsdale NJ, 1-63, 1990.

Marr,D. Simple memory: a theory for archicortex. *Phil.Trans.R.Soc.* B262:23-81, 1971.

McNaughton,B.L., Barnes,C.A. and Andersen,P. Synaptic efficacy and EPSP summation in granule cells of rat fascia dentata studied in vitro. *J.Neurophysiol.* 46:952-966, 1981.

McNaughton,B.L., O'Keefe,J. and Barnes,C.A. The stereotrode: a new technique for simultaneous isolation of several single units in the central nervous system from multiple unit records. *J.Neurosci.Meth.* 8:391-397, 1983[a].

McNaughton,B.L., Barnes,C.A. and O'Keefe,J. The contributions of position, direction and velocity to single unit activity in the hippocampus of freely-moving rats. *Exp.Brain Res.* 52:41-49, 1983[b].

McNaughton,B.L. Neuronal mechanisms for spatial computation and information storage. In: *Neural Connections, Mental Computation*, edited by L.Nadel, L.A.Cooper, P.Culicover and R.M.Harnish. MIT Press,Cambridge, Mass., 285-350, 1989.

McNaughton,B.L., Barnes,C.A., Meltzer,J. and Sutherland,R.J. Hippocampal granule cells are necessary for normal spatial learning but not for spatially-selective pyramidal cell discharge. *Exp.Brain Res.* 76:485-496, 1989.

Mathews,D.A., Cotman,C. and Lynch,G. An electron microscopic study of lesion-induced synaptogenesis in the dentate gyrus of the adult rat. I.Magnitude and time course of degeneration. *Brain Res.* 115:1-21, 1976.

Meibach,R.C. and Siegel,A. Efferent connections of the septal area in the rat: an analysis utilizing retrograde and anterograde transport methods. *Brain Res.* 119:1-20, 1977.

Miller,V.M. and Best,P.J. Spatial correlates of hippocampal unit activity are altered by lesions of the fornix and entorhinal cortex. *Brain Res.* 194:311-323, 1980.

Milner,B. Visually-guided maze learning in man: Effects of bilateral hippocampal, bilateral frontal and unilateral cerebral lesions. *Neuropsychologia* 3:17-38, 1965.

Milner,T.A., Loy,R. and Amaral,D.G. An anatomical study of the development of the septo-hippocampal projection in the rat. *Dev.Brain Res.* 8:343-371, 1983.

Milner,T.A. and Amaral,D.G. Evidence for a ventral septal projection to the hippocampal formation of the rat. *Exp.Brain Res.* 55:579-585, 1984.

Mitchell,S.J. and Ranck,J.B. Firing patterns and behavioural correlates of neurones in entorhinal cortex of freely-moving rats. *Soc.Neurosci.Abstr.* 3:202, 1977.

Mizumori,S.J.Y., McNaughton,B.L. and Barnes,C.A. A comparison of supramammillary and medial septal influences on hippocampal field potentials and single-unit activity. *J.Neurophysiol.* 61:15-31, 1989[a].

Mizumori,S.J.Y., McNaughton,B.L., Barnes,C.A. and Fox,K.B. Preserved spatial coding in hippocampal CA1 pyramidal cells during reversible suppression of CA3c output: evidence for pattern completion in hippocampus. *J.Neurosci.* 9:3915-3928, 1989[b].

Monmaur,P. and Thomson,M.A. Topographic organization of septal cells innervating the dorsal hippocampal formation of the rat: special reference to both the CA1 and dentate theta generators. *Exp.Neurol.* 82:366-378, 1983.

Morris,R.G.M., Black,A.H. and O'Keefe,J. Hippocampal EEG during a ballistic movement. *Neurosci.Lett.* 3:102, 1976.

Morris,R.G.M., Garrud,P., Rawlins,J.N.P. and O'Keefe,J. Place navigation impaired in rats with hippocampal lesions. *Nature* 297 (5868):681-683, 1982.

Morris,R.G.M. and Hagan,J.J. Hippocampal electrical activity and ballistic movement. In: *Neurobiology of the Hippocampus*, edited by W.Seifert. Academic Press, London, 321-331, 1983.

Muller,R.U. and Kubie,J.L. The effects of changes in the environment on the spatial firing of hippocampal complex-spike cells. *J.Neurosci.* 7:1951-1968, 1987.

Muller,R.U., Kubie,J.L. and Ranck,J.B. Spatial firing patterns of hippocampal complex-spike cells in a fixed environment. *J.Neurosci.* 7:1935-1950, 1987.

Muller,R.U. and Kubie,J.L. The firing of hippocampal place cells predicts the future position of freely moving rats. *J.Neurosci.* 9:4101-4110, 1989.

Muller,R.U., Kubie,J.L. and Saypoff,R. The hippocampus as a cognitive graph (Abridged version). *Hippocampus* 1:243-246, 1991.

Novak,J.L. and Wheeler,B.C. Multisite hippocampal slice recording and stimulation using a 32 element microelectrode array. *J.Neurosci.Meth.* 23:149-159, 1988.

O'Keefe,J. and Dostrovsky,J. The hippocampus as a spatial map: preliminary evidence from unit activity in freely moving rats. *Brain Res.* 34:171-175, 1971.

O'Keefe,J. Place units in the hippocampus of the freely moving rat. *Exp.Neurol.* 51:78-109, 1976.

O'Keefe,J. and Conway,D.H. Hippocampal place units in the freely moving rat: why they fire where they fire. *Exp.Brain Res.* 31:573-590, 1978.

O'Keefe,J. and Nadel,L. *The Hippocampus as a Cognitive Map.* Clarendon Press, Oxford, 1978.

O'Keefe,J. A review of the hippocampal place cells. *Prog.Neurobiol.* 13:419-439, 1979.

O'Keefe,J. and Conway,D.H. On the trail of the hippocampal engram. *Physiol.Psychol.* 8:229-238, 1980.

O'Keefe,J. Spatial memory within and without the hippocampal system. In: *Neurobiology of the Hippocampus*, edited by W.Seifert. Academic Press, London, 375-403, 1983.

O'Keefe,J. Is consciousness the gateway to the hippocampal cognitive map? A speculative essay on the neural basis of mind. In: *Brain and Mind*, edited by D.A.Oakley. Methuen, London, 59-98, 1985.

O'Keefe,J. and Speakman,A. Single unit activity in the rat hippocampus during a spatial memory task. *Exp.Brain Res.* 68:1-27, 1987.

O'Keefe,J. Computations the hippocampus might perform. In: *Neural Connections, Mental Computation*, edited by L.Nadel, L.A.Cooper, P.Culicover and R.M.Harnish. MIT Press, Cambridge, Mass., 225-284, 1989.

O'Keefe,J. The hippocampal cognitive map and navigational strategies. In: *Brain and Space,* edited by J.Paillard. Oxford University Press, Oxford, 273-295, 1991.

Olmstead,C.E., Best,P.J. and Mays,L.E. Neural activity in the dorsal hippocampus during paradoxical sleep, slow wave sleep and waking. *Brain Res.* 60:381-391, 1973.

Olton,D.S., Collison,C., and Werz,M.A. Spatial memory and radial arm maze performance in rats. *Learn.Motiv.* 8:289-314, 1977.

Olton,D.S., Branch,M. and Best,P.J. Spatial correlates of hippocampal unit activity. *Exp.Neurol.* 58:387-409, 1978.

Olton,D.S., Becker,J.T. and Handelman,G.E. Hippocampus, space and memory, *Behav.Brain Sci.* 2:315-365, 1979.

Olton,D.S., Wible,C.G., Pang,K. and Sakurai,Y. Hippocampal cells have mnemonic correlates as well as spatial ones. *Psychobiology* 17:228-229, 1989.

Ono,T., Nakamura,K., Fukuda,M. and Tamura,R. Place recognition responses of neurons in monkey hippocampus. *Neurosci.Lett.* 121:194-198, 1991.

Ottersen,O.P. and Storm-Mathisen,J. Different neuronal localization of aspartate-like and glutamate-like immunoreactivities in the hippocampus of rat, guinea-pig and Senegalese baboon (Papio papio), with a note on the distribution of gamma-aminobutyrate. *Neuroscience* 16:589-606, 1985.

Otto,T., Eichenbaum,H., Wiener,S.I. and Wible,C.G. Learning-related patterns of CA1 spike trains parallel stimulation parameters optimal for inducing hippocampal long-term potentiation. *Hippocampus* 1:181-192, 1991.

Otto,T. and Eichenbaum,H. Neuronal activity in the hippocampus during delayed non-match to sample performance in rats: evidence for hippocampal processing in recognition memory. *Hippocampus* 2:323-334, 1992.

Pavlides,C., Greenstein,Y.J., Grudman,M. and Winson,J. Long-term potentiation in the dentate gyrus is induced preferentially on the positive phase of theta-rhythm. *Brain Res.* 439:383-387, 1988.

Pavlides,C. and Winson,J. Influences of hippocampal place cell firing in the awake state on the activity of these cells during subsequent sleep episodes. *J.Neurosci.* 9:2907-2918, 1989.

Petsche,H., Stumpf,C. and Gogolak,G. The significance of the rabbit's septum as a relay station between the midbrain and the hippocampus. I. The control of hippocampal arousal activity by the septum cells. *Electroenceph.Clin.Neurophysiol.* 14:202-211, 1962.

Phillipson,O.T. and Griffiths,A.C. The topographic order of inputs to the nucleus accumbans in the rat. *Neuroscience* 16:275-296, 1985.

Pigott,S. and Milner,B. Memory for different aspects of complex visual scenes after unilateral temporal- or frontal lobe resection. *Neuropsychologia* 31:1-15, 1993.

Quirk,G.J., Muller,R.U. and Kubie,J.L. The firing of hippocampal place cells in the dark depends on the rat's recent experience. *J.Neurosci.* 10:2008-2017, 1990.

Quirk,G.J., Muller,R.U., Kubie,J.L. and Ranck,J.B. The positional firing properties of medial entorhinal neurons: description and comparison with hippocampal place cells. *J.Neurosci.* 12:1945-1963, 1992.

Raisman,G., Cowan,W.M. and Powell,T.P.S. An experimental analysis of the efferent projection of the hippocampus. *Brain* 89:83-108, 1966.

Rall,W. Membrane potental transients and membrane time constant of motoneurons. *Exp. Neurol.*, 2: 503-532, 1960.

Ramón y Cajal,S. *Histologie de systeme nerveux de l'homme et des certebres*. Maloine, Paris, 1911.

Ranck,J.B. Studies on single neurons in dorsal hippocampal formation and septum in unrestrained rats. *Exp.Neurol.* 41:461-555, 1973.

Rawlins,J.N.P. Associations across time: the hippocampus as a temporary memory store. *Behav.Brain Sci.* 8:479-496, 1985.

Recce,M.L. and O'Keefe,J. The tetrode: a new technique for multi-unit extracellular recording. *Soc.Neurosci.Abstr.* 15:1250, 1989.

Recce,M., Speakman,A. and O'Keefe,J. Place fields of single hippocampal cells are smaller and more spatially localised than you thought. *Soc.Neurosci.Abstr.* 17:484, 1991.

Rector,D. and Harper,R. Imaging of hippocampal neural activity in freely behaving animals. *Behav.Brain Res.* 42:143-149, 1991.

Robinson,D.A. The electrical properties of metal microelectrodes. *Proc.IEEE* 56:1065-1071, 1968.

Robinson,T.E. Hippocampal rhythmic slow activity (RSA; theta): a critical analysis of selected studies and discussion of possible species-differences. *Brain Res.Rev.* 2:69-101, 1980.

Rose,G. Physiological and behavioral characteristics of dentate granule cells. In: *Neurobiology of the Hippocampus*, edited by W.Seifert. Academic Press, London, 449-472, 1983.

Rose,G., Diamond,D. and Lynch,G.S. Dentate granule cells in the rat hippocampal formation have the behavioral characteristics of theta neurons. *Brain Res.* 266:29-37, 1983.

Routtenberg,A. Hippocampal correlates of consummatory and observed behavior. *Physiol.Behav.* 3:533-535, 1968.

Sandler,R. and Smith,A.D. Coexistence of GABA and glutamate in mossy fiber terminals of the primate hippocampus: an ultrastructural study. *J.Comp.Neurol.* 303:177-192, 1991.

Saper,C.B. Organization of cerebral cortical afferent systems in the rat. II. Magnocellular basal nucleus. *J.Comp.Neurol.* 222:313-342, 1984.

Sarna,M.F., Gochin,P., Kaltenbach,J., Salganicoff,M. and Gerstein,G.L. Unsupervised waveform classification for multi-neuron recordings: a real-time, software-based system. II. Performance comparison tpo other sorters. *J.Neurosci.Meth.* 25:189-196, 1988.

Schmidt,E.M. Instruments for sorting neuroelectric data: a review. *J.Neurosci.Meth.* 12:1-24, 1984.

Schmidt,E.M. Computer separation of multi-unit neuroelectric data: a review. *J.Neurosci.Meth.* 12:95-111, 1984.

Schwartzkroin,P.A. and Kunkel,D.D. Morphology of identified interneurons in the CA1 regions of guinea pig hippocampus. *J.Comp.Neurol.* 232:205-218, 1985.

Schwerdtfeger,W.K. and Buhl,E. Various types of non-pyramidal hippocampal neurons project to the septum and contralateral hippocampus. *Brain Res.* 386:146-154, 1986.

Scoville,W.B. and Milner,B. Loss of recent memory after bilateral hippocampal lesions. *J.Neurol.Neurosurg.Psychiat.* 20:11-21, 1957.

Segal,M. and Olds,J. The behavior of units in the hippocampal circuit during learning. *J.Neurophysiol.* 35:680-690, 1972.

Segal,M. and Olds,J. Activity of units in the hippocampal circuit of the rat during differential classical conditioning. *J.Comp.Physiol.Psychol.* 82: 195-204, 1973.

Segal,M. A potent inhibitory monosynaptic hypothalamo-hippocampal connection. *Brain Res.* 162:137-141, 1979.

Sharp,P.E., Kubie,J.L. and Muller,R.U. Firing properties of hippocampal neurons in a visually symmetrical environment: contributions of multiple sensory cues and mnemonic processes. *J.Neurosci.* 10:3093-3105, 1990.

Sinclair,B.R., Seto,M.G. and Bland,B.H. Theta-cells in CA1 and dentate layers of hippocampal formation: relations to slow-wave activity and motor behavior in the freely-moving rabbit. *J.Neurophysiol.* 48:1214-1225, 1982.

Skaggs,W.E., McNaughton,B.L., Gothard,K.M. and Markus,E.J. An information-theoretic approach to deciphering the hippocampal code. In: *Advances in Neural Information Processing Systems 5*, edited by S.J.Hanson, J.D.Cowan and C.L.Giles. Morgan Kaufmann,San Mateo, California, 1030-1037, 1993.

Speakman,A. and O'Keefe,J. Hippocampal complex spike cells do not change their place fields if the goal is moved within a cue controlled environment. *Eur.J.Neurosci.* 2:544-555, 1990.

Stanton,P.K. and Sejnowski,T.J. Associative long-term depression in the hippocampus induced by hebbian covariance. *Nature* 339:215-218, 1989.

Stengaard-Pedersen,K., Fredens,K. and Larsson,L.I. Comparative localization of enkephalin and cholecystokinin immunoreactivities and heavy metals in the hippocampus. *Brain Res.* 273:81-96, 1983.

Steward,O. and Scoville,S.A. Cells of origin of entorhinal cortical afferents to the hippocampus and fascia dentata of the rat. *J.Comp.Neurol.* 169:347-370, 1976.

Stewart,M. and Fox,S.E. Firing relations of lateral septal neurons to the hippocampal theta rhythm in urethane anesthetized rats. *Exp.Brain Res.* 79:92-96, 1990.

Storm-Mathisen,J., Leknes,A.K., Bore,A.T., Vaaland,J.L., Edminson,P., Haug,F.M.S. *et al.* First visualisation of glutamate and GABA in neurones by immunocytochemistry. *Nature* 301:517-520, 1983.

Struble,R.G., Desmond,N.L. and Levy,W.B. Anatomical evidence for interlamellar inhibition in the fascia dentata. *Brain Res.* 152:580-585, 1978.

Sutherland,R.J. and Rudy,J.W. Configural association theory: the role of the hippocampal formation in learning, memory and amnesia. *Psychobiology* 17:129-144, 1989.

Suzuki,S.S. & Smith,G.K. Single-cell activity and synchronous bursting in the rat hippocampus during waking behavior and sleep. *Exp.Neurol.* 89:71-89, 1985[a].

Suzuki,S.S. & Smith,G.K. Burst characteristics of hippocampal complex spike cells in the awake rat. *Exp.Neurol.* 89:90-95, 1985[b].

Swanson,L.W. and Cowan,W.M. Autoradiographic studies of the development and connections of the septal area in the rat. In: *The Septal Nuclei: Advances in Behavioral Biology, Vol.20*, edited by J.F.DeFrance. Plenum Press, New York, 37-64, 1976.

Swanson,L.W. and Cowan,W.M. An autoradiographic study of the organization of the efferent connections of the hippocampal formation in the rat. *J.Comp.Neurol.* 172:49-84, 1977.

Swanson,L.W. and Cowan,W.M. The connections of the septal region in the rat. *J.Comp.Neurol.* 186:621-656, 1979.

Swanson,L.W., Sawchenko,P.E. and Cowan,W.M. Evidence for collateral projections by neurons in Ammon's horn, the dentate gyrus, and th subiculum: a multiple retrograde labelling studies in the rat. *J.Neurosci.* 1:548-559, 1981.

Swanson,L.W. The hippocampus and the concept of the limbic system. In: *The Neurobiology of the Hippocampus*, edited by W.Seifert. Academic Press, London, 3-19, 1983.

Tam,D.C., Ebner,T.J. and Knox,C.K. Conditional cross-interval correlation analyses with applications to simultaneously recorded cerebellar Purkinje neurons. *J.Neurosci.Meth.* 23:23-33, 1988.

Tamamaki,N., Abe,K. and Nojyo,Y. Columnar organization in the subiculum formed by axon branches originating from single CA1 pyramidal neurons in the rat hippocampus. *Brain Res.* 412:156-160, 1987.

Tamamaki,N. and Nojyo,Y. Disposition of the slab-like modules formed by axon branches originating from single CA1 pyramidal neurons in the rat hippocampus. *J.Comp.Neurol.* 291:509-519, 1990.

Tamamaki,N. and Nojyo,Y. Crossing fiber arrays in the rat hippocampus as demonstrated by three-dimensional reconstruction. *J.Comp.Neurol.* 303:435-442, 1991.

Taube,J.S., Muller,R.U. and Ranck,J.B. Head-direction cells recorded from the postsubiculum in freely moving rats. I. Description and quantitative analysis. *J.Neurosci.* 10:420-435, 1990[a].

Taube,J.S., Muller,R.U. and Ranck,J.B. Head-direction cells recorded from the postsubiculum in freely moving rats. II. Effects of environmental manipulations. *J.Neurosci.* 10:436-447, 1990[b].

Teitelbaum,H., McFarland,W.L. and Mattsson,J.L. Classical conditioning of hippocampal theta patterns in the rat. *J.Comp.Physiol.Psychol.* 91:674-681, 1977.

Thakor,N.V. Adaptive filtering of evoked potentials. *IEEE Trans.* BME-34:6-12, 1987.

Thompson,L.T. and Best,P.J. Place cells and silent cells in the hippocampus of freely-behaving rats. *J.Neurosci.* 9:2382-2390, 1989.

Thompson,L.T. and Best,P.J. Long-term stability of the place-field activity of single units recorded from the dorsal hippocampus of freely behaving rats. *Brain Res.* 509:299-308, 1990.

Tolman,E.C. *Purposive Behaviour in Animals and Men.* Century, New York, 1932.

Tolman,E.C. Cognitive maps in rats and men. *Psychol.Rev.* 55:189-208, 1948.
Traub,R.D., Miles,R. and Wong,R.K.S. Model of the origin of rhythmic population oscillations in the hippocampal slice. *Science* 243:1319-1325, 1989.

Treves,A. and Rolls,E.T. Computational constraints suggest the need for two distinct input systems to the hippocampal CA3 network. *Hippocampus* 2:189-200, 1992.

Van Groen,T. and Wyss,J.M. Extrinsic projections from area CA1 of the rat hippocampus: olfactory, cortical, subcortical and bilateral hippocampal formation projections. *J.Comp.Neurol.* 302:515-528, 1990.

Vanderwolf,C.H. Hippocampal electrical activity and voluntary movement in the rat. *Electroencephalogr.Clin.Neurophysiol.* 26:407-418, 1969.

Vanderwolf,C.H. Neocortical and hippocampal activation in relation to behavior: effects of atropine, eserine, phenothiazines and amphetamine. *J.Comp.Physiol.Psychol.* 88:306-323, 1975.

Von der Malsburg,C. and Bienenstock,E. Statistical coding and short-term synaptic plasticity: a scheme for knowledge representation in the brain. In: *Disordered Systems and Biological Organization*, edited by E.Bienenstock, F.Fogelman and G.Weisbuch. Springer, Berlin, 247-272, 1986.

Werbos,P. *Beyond regression: new tools for prediction and analysis in the behavioral sciences.* PhD thesis, Harvard University, 1974.

Whishaw,I.Q. and Vanderwolf,C.H. Hippocampal EEG and behavior: effects of variation in body temperature and relation of EEG to vibrissae movement, swimming and shivering. *Physiol.Behav.* 6:391-397, 1971.

Whishaw,I.Q. and Vanderwolf,C.H. Hippocampal EEG and behavior: changes in amplitude and frequency of RSA (theta rhythm) associated with spontaneous and learned movement patterns in rats and cats. *Behav.Biol.* 8:461-484, 1973.

Wible,C.G., Findling,R.L., Shapiro,M., Lang,E.J., Crane,S. and Olton,D.S. Mnemonic correlates of unit activity in the hippocampus. *Brain Res.* 399:97-110, 1986.

Wiener,S.I., Paul,C.A. and Eichenbaum,H. Spatial and behavioral correlates of hippocampal neuronal activity. *J.Neurosci.* 9:2737-2763, 1989.

Willshaw,D.J. and Buckingham,J.T. An assessment of Marr's theory of the hippocampus as a temporary memory store. *Phil.Trans.R.Soc.* B 329:205-215, 1990.

Wilson,M.A. and McNaughton,B.L. Dynamics of the hippocampal ensemble code for space. *Science* 261:1055-1058, 1993.

Witter,M.P. and Groenewegen,H.J. Connections of the parahippocampal cortex in the cat IV subcortical efferents.*J.Comp.Neurol.* 252:51-77, 1986.

Witter,M.P., Groenewegen,H.J., Lopes da Silva,F.H. and Lohman,A.H.M. Functional organization of the extrinsic and intrinsic circuitry of the parahippocampal region. *Prog.Neurobiol.* 33:161-253, 1989.

Wyss,J.M., Swanson,L.W. and Cowan,W.M. A study of subcortical afferents to the hippocampal formation in the rat. *Neurosci.* 4:463-476, 1979.

Wyss,J.M. An autoradiographic study of the efferent connections of the entorhinal cortex in the rat. *J.Comp.Neurol.* 199:495-512, 1981.

Yang,X. and Shamma,S.A. A totally automated system for the detection and classification of neural spikes. *IEEE Trans.* BME-35:806-816, 1988.

Zola-Morgan,S., Squire,L.R. and Amaral,D.G. Lesions of the hippocampal formation but not lesions of the fornix or the mammillary nuclei produce long-lasting memory impairment in monkeys. *J.Neurosci.* 9:898-913, 1989.